



Universiteit
Leiden
The Netherlands

Supporting the Silicon Anode Industry

Connecting the Environmental Footprint of a Silicon Anode to the Ideal
Production Location

Dietlind Ahrens

Leiden Student ID s3602788

Delft Student ID 5894336

Thesis Committee José Mogollón
 Robert Istrate

*Thesis submitted in partial fulfillment of the requirements for the degree of Master
of Science in Industrial Ecology at Delft Institute of Technology and Leiden
University*

To be defended publicly on
March 27, 2025

Executive Summary

With the upcoming market introduction of silicon anodes in lithium-ion batteries (LIBs), there is a growing concern about their sustainability. However, due to their novelty, existing life cycle assessments (LCA) on the environmental impacts of silicon anodes rely exclusively on laboratory data about their production process and performance. Moreover, as there are no established manufacturing sites yet, literature assumes predetermined locations despite the significant influence of the location choice on the environmental performance of the anode. Therefore, this study adapts the Suitability–Feasibility–Acceptability (SFA) framework to identify the optimal production location for silicon anode manufacturers on a global scale, considering the general nature and interests of scale-up businesses in the clean energy technology sector. Based on the outcome, this study conducted an LCA using the PEF impact categories to compare the life cycle environmental impacts of a pure hydro-generated amorphous silicon thin film anode, prepared via plasma enhanced chemical vapour deposition (PECVD), to the current market standard of natural and synthetic graphite anodes in a lithium cobalt oxide (LCO) battery for consumer electronics. The life cycle inventory data of the silicon anode's production process was provided by an up-scaling silicon anode manufacturer.

The results of the location study suggest that Europe is the optimal production location for silicon anode manufacturers because of its favourable energy mix. Nevertheless, due to the high electricity consumption of the PECVD process, the findings of the subsequent LCA indicate that a LIB with a silicon anode produced in Europe performs significantly worse than its graphite-based counterparts from China in almost all impact categories, regardless of its higher energy density. Among the graphite-based alternatives, the LIB with a synthetic graphite anode is associated with higher emissions, owing to its energy-intensive graphitisation step. Unlike the emissions of the silicon anode, which are primarily caused by the electricity consumption, the impacts of both graphite anodes are more attributed to copper production given the higher content of primary copper in their current collectors. On the basis of the whole lifecycle, the impacts of the three battery types converge, with electricity being the main contributor in all three product systems. Nevertheless, the ranking in terms of environmental performance remains identical, even in different battery performance and production efficiency scenarios. Moreover, the results prove to be robust with respect to the allocation method and the electricity consumption during the silicon anode production process.

Although the outcomes indicate that graphite anodes are preferable in LIBs, silicon anodes should not be dismissed as a viable alternative, given their early development stage. Since their potential improvements in performance and production efficiencies are uncertain at this point, research around silicon anodes should continue. Furthermore, future studies should regularly update the life cycle inventory data of the production process of silicon anodes and their precursor materials, to critically monitor the development. Finally, based on the results of the scenario analysis, the author encourages silicon anode manufacturers to rather improve several of the anode's production and performance parameters than to focus on one parameter individually.

Contents

1. Introduction	5
2. Methods	9
2.1. Adapted Suitability-Feasibility-Acceptability Framework	9
2.1.1. Necessary Requirements	12
2.1.2. Sufficient Requirements	13
2.2. Life Cycle Assessment	13
2.2.1. Goal and Scope	14
2.2.2. Life Cycle Inventory Analysis	16
2.2.2.1. System Boundaries	16
2.2.2.2. Flowchart	17
2.2.2.3. Data Collection and Relating Data to Unit Processes	21
2.2.2.4. Multi-functionality and Allocation	24
2.2.2.5. Scenario Development	25
2.2.3. Impact Assessment Method and Interpretation	26
3. Results	27
3.1. Location Study	27
3.1.1. Suitability and Feasibility	27
3.1.2. Acceptability	30
3.2. Comparative Life Cycle Analysis	32
3.2.1. Contribution Analysis	35
3.2.2. Economic Flow Analysis	38
3.2.3. Scenarios	40
4. Discussion	43
5. Conclusions	48
List of Figures	50
List of Tables	52
Bibliography	53
Appendix	61
A. Method	61
A.1. Adapted Suitability-Feasibility-Acceptability Framework	61
A.2. Life Cycle Assessment	61
A.2.1. Multi-functionality and Allocation	62
A.2.2. Scenario Development	63
B. Results	64
B.1. Location Study	64

B.2. Comparative Analysis	69
B.2.1. Economic Flow Analysis	75
B.2.2. Scenarios	75
C. Discussion	82
C.1. Sensitivity Analysis	83
C.2. Consistency Check	86
D. Supplementary Material	87

1. Introduction

To mitigate climate change, 197 countries worldwide signed the Paris Agreement in 2015, committing to the target of limiting “the increase in the global average temperature to well below 2°C” compared to pre-industrial levels [1]. In order to achieve this target, countries have to reduce their greenhouse gas (GHG) emissions by decarbonising their transportation and energy sectors, as they are the two largest contributors, accounting for around two-thirds of all GHG emissions [2, 3]. Since decarbonisation implies a shift from emission-intensive, fossil-fuel based technologies to carbon-neutral ones, the most promising solution is the electrification of the transportation and energy sector [4]. In particular, this involves replacing combustion vehicles by electric vehicles (EV) [5, 6] and substituting fossil-fuel based energy sources like coal, natural gas and crude oil by renewable ones like wind and solar power [7–9]. However, as wind and solar do not provide uninterrupted and continuous flows of energy, such a shift comes with a need for energy storage solutions [9–12]. Consequently, the World Economic Forum and Global Battery Alliance [13] predict that by 2030 battery technologies could reduce the emissions in the transport and energy sector by 30 %. Thus, batteries play a critical role in mitigating climate change. As a result, the International Energy Agency (IEA) [14] predicts that the global battery supply has to increase 14-fold to 1200 GW by 2030.

The first battery was invented by Alessandro Volta in 1800 [15]. The so-called Voltaic pile consisted of a stack of zinc and silver disks that were separated by a cloth soaked in a sodium chloride solution [15]. After this discovery it took another 59 years until Gaston Planté invented the first secondary, meaning rechargeable, battery, namely the lead-acid battery [16], which still forms the basis of many of today’s commercial batteries [17]. However, due to their considerable size and weight, lead-acid batteries were ill-suited for portable, electronic devices, which require batteries of light weight, high energy density and long operational life [9, 17]. The solution came with lithium-ion batteries (LIBs), as the high theoretical specific gravimetric capacity (3860 mAh g^{-1}), low electrochemical reduction potential (-3.045 V), and low density (0.534 g cm^{-3}) of lithium, enable LIBs to have a high volumetric and gravimetric energy capacity as well as high power densities [18–21]. Together with their long service life, memoryless effect, eco-friendly nature, scalability, and versatility in design, this has led to the widespread adoption of LIBs, ranging from small electronic appliances in consumer electronics like laptops and cameras to large high-power devices in grid storage and transportation [22–25]. However, independent of their broad acceptance, rapid developments in the electronics sector and the expanded range of applications for batteries have resulted in increased requirements for LIBs and thus a need to further improve them [9, 26]. For instance, as a consequence of the increased use of batteries in the transportation sector, there is a rising request for LIBs with a higher energy density, since this significantly determines how far an EV can drive on a single charge [27, 28]. While most current middle-class vehicles only achieve driving ranges of 200–400 km with a single charge due to their limited energy capacity, the goal is to achieve driving ranges of 500 km [27, 29, 30]. Furthermore, the energy density remains a key factor for batteries in consumer electronics, given the limited amount of space and weight allocated to the battery [31]. Hence, there is a persisting demand for the development of cheaper LIBs, with a higher cycle life and thus longer lifespan, faster charging rate and, most importantly, higher energy density [9, 20, 32, 33].

The energy density of a LIB primarily depends on the choice of active material, meaning the type of anode and cathode material [21, 34]. To achieve a high energy density on cell level, both components must have a high specific energy, as otherwise the overall capacity will always be reduced [34]. But

while there are numerous different cathode materials for LIBs on the market, offering varying characteristics including different levels of energy density, the majority of LIBs (98 %) have a graphite anode with a theoretical capacity of 372 mAhg^{-1} [24, 35]. However, as graphite anodes are approaching their theoretical limit thanks to technological advancements, it becomes increasingly important to develop new, alternative anode materials with higher energy densities for next-generation LIBs [21, 23, 35–38]. One of the most promising alternatives to graphite are silicon anodes with a theoretical capacity of 4200 mAhg^{-1} , exceeding that of graphite by more than tenfold [9, 35, 39, 40]. In addition to possessing one of the highest gravimetric and volumetric capacities [35], silicon anodes have a relatively low discharge potential (0.4 V vs. Li^+/Li), which prevents the formation of lithium dendrites, increasing the safety of the battery and allowing for fast charging [23]. Furthermore, silicon is the second most abundant element in the Earth’s crust, inexpensive, environmentally friendly, and non-toxic [35]. However, the high energy density of silicon anodes is associated with a large volume expansion of up to 400% and a huge stress generation during the charging process, causing the silicon particles to pulverise and disconnect from the current collector, i.e. the copper foil [20, 35]. The repeated fracturing of the silicon leads to electrical isolation and, due to the re-exposed silicon surface, a continuous solid electrolyte interface (SEI) formation [40]. Both processes create a synergy of accelerated capacity loss, reduced electrochemical reactivity, and low coulombic efficiency (CE) [20, 35, 40]. Thus, the exceptional energy capacity of silicon anodes comes with the challenge of a significantly deteriorating electrochemical performance [40].

To circumvent this challenge, the battery industry currently uses silicon/graphite composites [41], where the graphite acts as a matrix that minimizes the volume expansion of the silicon [20, 42]. However, since these anodes consist of at most 20 wt% silicon and thus yield lower energy capacities than pure silicon anodes¹ [42], research on alternative solutions with higher levels of silicon content is progressing. The most favourable and effective solutions comprise nano-sized silicon with porous structures and/or shape preserving shells including zero dimensional (0D) nanoparticles, one dimensional (1D) nanotubes and nanowires, and two-dimensional (2D) thin films [20, 23, 40, 43]. While the nano-size suppresses the pulverisation of the silicon particles, the hollow structure allows the silicon to expand inwards, resulting in an enhanced structural integrity and cycling stability [44, 45]. As a consequence of these recent advancements in pure silicon anodes, Cui [46] predicts that “silicon-based batteries are now on the verge of large-scale commercial success”.

With the anticipated market introduction of pure silicon anodes, there is an expected increase in large-scale manufacturing plants of pure silicon anodes, accompanied by growing concerns about their sustainability. Due to the large, irreversible upfront investments associated with the construction of large-scale production facilities, the location choice of these plants is highly relevant to companies [47]. Moreover, as the location choice influences for instance the transport routes and electricity mix associated with the production, it has a significant impact on the environmental footprint of the silicon anode [48–50], which in turn can determine the location choice considering the increasing number of green subsidies [51]. Nevertheless, despite the relevance of the location selection on the environmental footprint and vice versa, literature about the location choice in the context of batteries focuses on battery recycling centres [52–54] and swapping stations [55, 56]. To this date, only a few studies have investigated different production locations for LIBs: In 2013, Brodd & Helou [57] compared the production cost of LIBs for consumer electronics in the USA and China. Since this analysis only incorporated the cost dimension of the site selection, Duffner *et al.* [47] adapted their framework and included the knowledge level dimension to account for the quality of the finished product. The authors applied their two-dimensional framework to analyse the trade-offs between knowledge and cost when selecting a location for an EV LIB factory in the EU. Finally, Asaba *et al.* [58] extended their framework by the environmental impact of energy production as a third dimension. Similarly to Duffner *et al.* [47], their analysis revealed that there is no single best production location,

¹In accordance with the industry-specific terminology, pure describes all anodes with a silicon content of more than 80 %.

but rather that it depends on the specific requirements of the battery manufacturer. Still, although their framework considers the environmental production impact, its sole focus on the electricity mix of the chosen location overlooks other crucial factors such as transportation distances. Furthermore, as the aforementioned studies analyse the production of conventional LIBs utilising graphite anodes, their results cannot be transferred to the specific characteristics and environmental impacts associated with silicon-based LIB production. Hence, despite the expected commercialisation of silicon-based LIBs, there is a lack of research about the optimal location for silicon anode manufacturing facilities.

This research gap is particularly significant as most existing studies on the environmental impact of silicon-based LIBs assume a predetermined production location primarily in the USA and the EU, as visible in Figure 1.1. An exception forms Philippot *et al.* [59], who examined the impact of location choice on the environmental footprint of a LIB with a silicon-rich anode, and found that it is especially sensitive to the carbon intensity of the electricity mix used during the manufacturing and charging process in the use phase. But regardless of the production location, the outcomes of the life cycle assessments on silicon-based anodes seem to be consistent: After substituting the graphite anode by a lithium-based one, Lastoskie & Dai [60] discovered that anodes with higher specific energy can reduce the environmental impact of a battery. Yet, several studies found contradictory results when using a silicon-based anode instead [61–65]. Nonetheless, these findings are still consistent, as the assessment of Wu & Kong [66] indicates that the environmental impact of a LIB with a graphite anode is higher than that of a LIB with a lithium-metal anode, but smaller than the one of a silicon-based LIB. However, as depicted in Figure 1.1, all aforementioned studies base their assessment of the environmental footprint of graphite anodes on industry primary data, whereas their life cycle inventories (LCI) of silicon anodes rely on laboratory data. Accardo *et al.* [67] attempt to resolve this discrepancy by scaling the LCI data of silicon anodes up to industrial scale. But their results, suggesting that silicon-based LIBs still perform worse environmentally, must be interpreted with caution, as their underlying data remains on laboratory scale.

Therefore, the early development stage of silicon anodes presents two key research gaps in existing environmental assessments: First, despite the lack of established manufacturing sites for silicon anodes, there are no rigorous analyses regarding suitable production locations, a factor that significantly influences the environmental footprint. Second, while LCAs for silicon anodes predominantly rely on laboratory-scale data, graphite anodes benefit from industry primary data, necessitating further analysis to ensure comparability and accuracy. Hence, to address these research gaps, this study seeks to explore the following research question:

Depending on the optimal production location, what are the life-cycle environmental impacts of a lithium-ion battery with a pure silicon anode, and how does it compare to the market standard of synthetic and natural graphite-based lithium-ion batteries?

To answer the research question, this study adapts the Suitability-Feasibility-Acceptability (SFA) Framework as outlined in Chapter 2 to first exclude countries that do not fulfil basic requirements for a stable production process using a quantitative data analysis and to then determine the most favourable location depending on the regional environmental footprint of the silicon anode using the LCA methodology. Based on these results, summarised in Chapter 3, this study compares the life-cycle environmental impacts of the silicon anode with those of the market standard, namely synthetic and natural graphite, and identifies hot spots in all three product systems. Chapter 4 puts the results of this study in context with the existing literature, taking into account the limitations of the analysis regarding both the modelling assumptions and the quality of the data. Moreover, it tests the robustness of the comparative analysis' results by conducting a sensitivity analysis with respect to the allocation and electricity assumptions. Finally, the study ends with answering the research question and providing some recommendations to future research, politics, and the silicon anode industry in Chapter 5.

1. Introduction

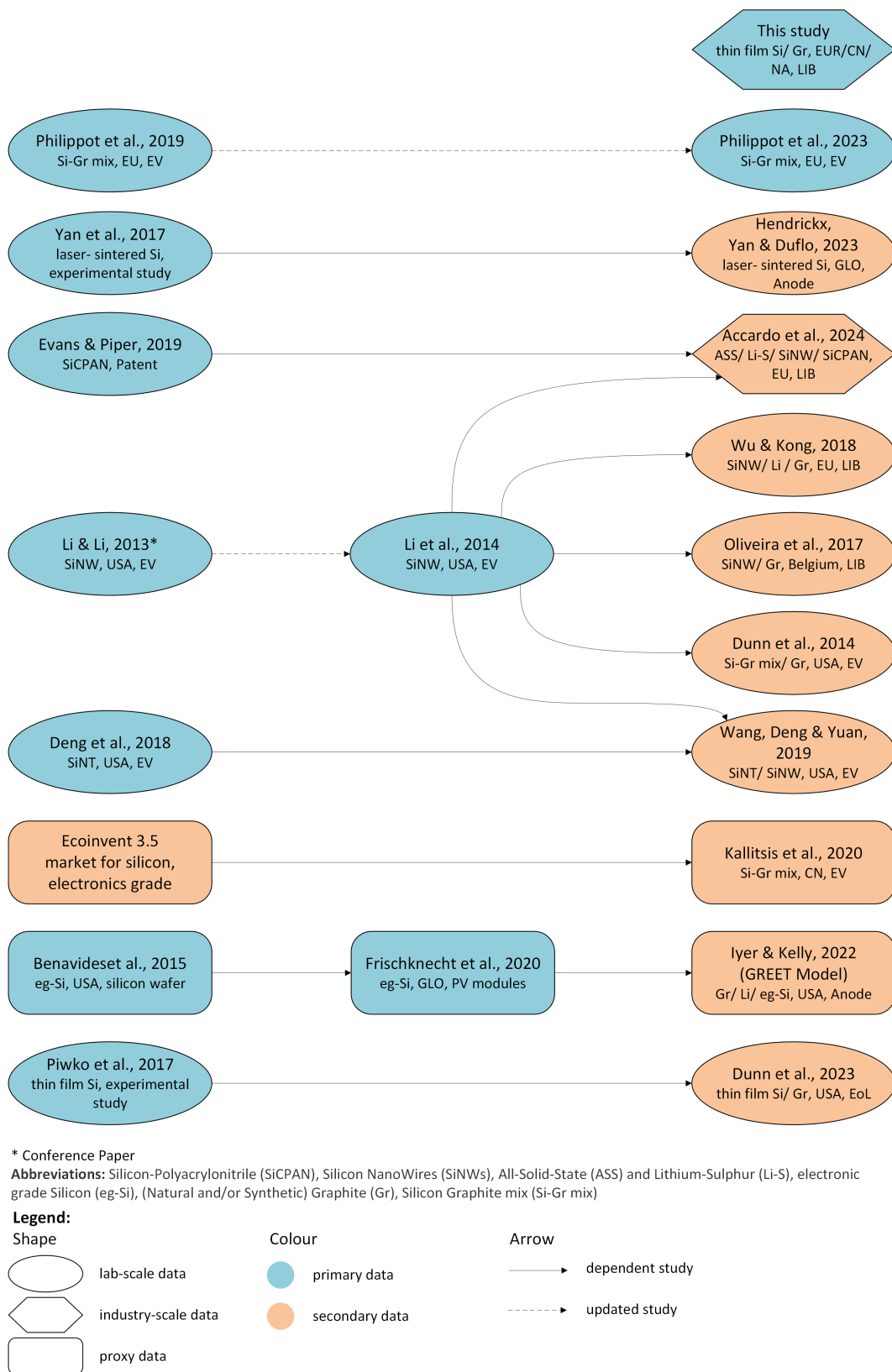


Figure 1.1.: Data network of LCI data for silicon anodes, their sources and their further usage in different publications

Sources in order of appearance: Philippot *et al.* [33], Philippot *et al.* [59], Yan *et al.* [68], Hendrickx *et al.* [63], Evans & Piper [69], Accardo *et al.* [67], Li *et al.* [70], Li *et al.* [62], Wu & Kong [66], Oliveira *et al.* [71], Dunn *et al.* [72], Deng *et al.* [65], Wang *et al.* [73], Wernet *et al.* [74], Kallitsis *et al.* [64], Benavides *et al.* [75], Frischknecht *et al.* [76], Iyer & Kelly [77], Piwko *et al.* [78], and Dunn *et al.* [61].

2. Methods

The main objective of this study is to quantify the environmental impacts of pure silicon anodes produced on industrial-scale, taking into account the choice of production location, and compare them to the ones of graphite anodes as a benchmark. The silicon anode under consideration is a pure hydrogenated amorphous silicon thin film anode that is produced via Plasma-Enhanced Chemical Vapor Deposition (PECVD) [79]. Its amorphous nature reduces the stress caused by the volume expansion during the charging and discharging process as it leads to a higher surface/volume ratio, increasing the silicon surface that is in contact with the electrolyte. Furthermore, during the PECVD process, the silicon in form of silane (SiH_4) is directly deposited on the copper foil, eliminating the need for any binder and thus lowering the amount of input factors. Moreover, as a roll-to-roll method, the PECVD process limits the number of production steps and thus eases the control over the properties of the anode, since it only requires the adjustment of the deposition parameters [80, 81].

Adhering to the main objective, this study consists of three consecutive parts: the search for a suitable production location for pure silicon anodes, the calculation of its environmental footprint, and an LCA comparing it to synthetic and natural graphite anodes. Thus, the main research question can be divided into the following three sub-research questions:

1. *What is a suitable production location for a pure silicon anode manufacturer?*
2. *Depending on the optimal location, what are the life-cycle environmental impacts of a lithium-ion battery with a pure, amorphous silicon anode and how are they influenced by different production and battery performance parameters?*
3. *How does a silicon-based lithium-ion battery compare to the market standard of a lithium-ion battery with a synthetic or natural graphite anode?*

To answer the first sub-research question, this study adapts the SFA framework, as outlined in Section 2.1. The framework is used to identify a suitable production location for silicon anode manufacturers, because, unlike commonly used Multiple Criteria Decision Making (MCDM) methods [82], it does not involve any weighting or normalisation of the selection criteria [83], suiting the broader scope of this analysis better. Furthermore, the LCA methodology is integrated into the SFA framework to account for the increased influence of the environmental production footprint on the location choice. Given the outcome of this location study, this analysis follows the existing literature and addresses the second and third research question by conducting a comparative LCA, explained in Section 2.2.

2.1. Adapted Suitability-Feasibility-Acceptability Framework

The suitability-feasibility-acceptability, short SFA, framework was proposed by Johnson *et al.* [84] to evaluate different strategic options. As the name suggests, the framework consists of three key evaluation dimensions: suitability, feasibility, and acceptability. Suitability addresses whether a strategy exploits the opportunities and avoids the threats of the external environment, considering the company's capabilities. The feasibility dimension assesses whether a strategy could work in practice, taking into account the availability of labour, input material, and financial capital. The acceptability criteria analyse whether the outcome of a strategy would meet the expectations of stakeholders by evaluating the expected risk and return of a strategy as well as the likely reaction of stakeholders.

2. Methods

Based on these three dimensions, the original framework is intended to assist the decision-making of one specific company. However, since this study applies the SFA framework to the production site selection of various silicon anode producers, it has to be adapted to fit the strategy selection of an entire industry segment. As a result, both the strategic options and criteria are kept more general, implementing the framework similar to Hashemkhani Zolfani *et al.* [83]. Furthermore, while the original framework selects one strategy based on all three dimensions equally, this adaptation differentiates between the suitability and feasibility criteria as necessary requirements and the acceptability dimension as sufficient. The resulting two-step process, visualised by Figure 2.1, allows to first exclude options that are inadequate because they do not fulfil the basic requirements necessary for a practicable and profitable strategy and then, based on the outcome, select the option that would have the highest chance of success considering the expectations of stakeholders and funding possibilities.

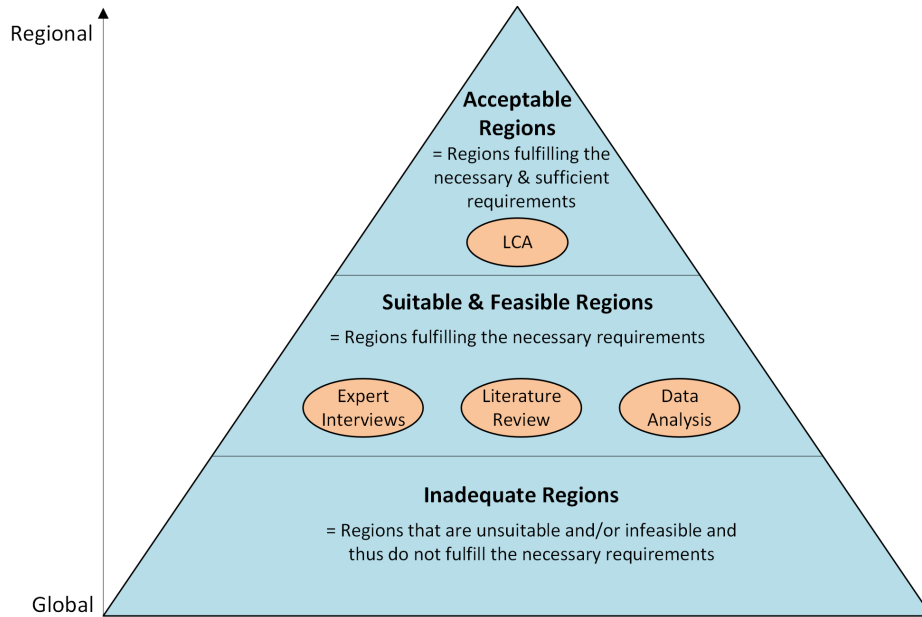


Figure 2.1.: Research Flow Diagram of the Adapted SFA Framework

After explaining the general framework, the set of strategic options, i.e. possible production locations, needs to be defined. Since there are no established manufacturing sites for silicon anodes yet, this study takes a broad approach and starts from the global scale. As Figure 2.2 shows, the world is divided into nine regions: North America (NAC), Latin America & Caribbean (LCN), Europe (EUR), Middle East & North Africa (MEA), Sub-Saharan Africa (SSF), Central Asia (CAS), East Asia (EAS), South Asia (SAS), and Oceania & Pacific (OCE). Conducting the location study on a regional instead of a country-level simplifies the analysis and accounts for possible spill-over effects. For instance, the political instability of one country can impact its neighbouring countries, while the proximity to raw material suppliers might be similar across national borders. The partitioning of the world is based on the one of the World Bank Group [85] with the further subdivision of East Asia & Pacific and Europe & Central Asia to allow for a slightly more detailed comparison. A list of all countries excluded from the analysis due to a lack of data can be found in Appendix A.1.

Table 2.1 provides an overview of the decision criteria and their affiliation to the three dimensions. Since silicon anodes are not commercialised yet, the majority of silicon anode producers are start-ups without an established business model or revenue stream but with a disruptive innovation [86]. It is therefore necessary for silicon anode producers to protect their intellectual property and ensure a stable production given the limited resources they have if they want to grow and become profitable. Hence, a suitable location is characterised by a certain degree of political stability and legal protection



Figure 2.2.: World Map Partitioned into Regions

of company-owned knowledge. Moreover, due to the limited internal resources, the project is only feasible if the input materials are available and the regulatory landscape facilitates a factory setup. If any of these criteria are not met, a location is considered inadequate. Within the set of suitable and feasible options, a strategy fulfils the sufficient requirement if it is acceptable to the stakeholders. Beyond profitability, stakeholders in the battery industry are presumably concerned about the reputation, and thus public acceptance, of a company, its access to capital, and its environmental impact, specifically its carbon footprint [87]. Because of the rising environmental awareness and the related increase in green investments and subsidies like the EU Innovation Fund and the US Bipartisan Infrastructure Law [88–91], all three interests are likely influenced by the silicon anode’s environmental impact. Thus, out of all adequate options, the proposed framework selects the location resulting in the best environmental impact as the optimal manufacturing site for silicon anode producers.

Table 2.1.: The SFA Strategy Framework by Related Criteria

Requirement	Dimension	Definition	Criteria	Indicator
Necessary	Suitability	Addresses the key opportunities and threats an organisation faces, the external environment.	Stable production, Security of company-internal knowledge	Global Peace Index, Political Stability, Intellectual Property Rights Protection
	Feasibility	Concerns the internal capability of the company; whether a strategy would work in practice.	Input supply security, ease of factory setup	Ease of Doing Business Score, Trade Barrier Index, Availability of Silane Supply
Sufficient	Acceptability	Regards the expectations of stakeholders; risk, return and stakeholder reactions.	Public acceptance, chances of success for subsidies and investments	Environmental Footprint

2.1.1. Necessary Requirements

According to the proposed framework, the first step of the strategy selection entails the exclusion of options that do not meet the necessary requirements. A strategy meets the necessary requirements if it fulfils the suitability and feasibility criteria to at least a certain level, which in this study is set as the global average due to a lack of a natural or recommended threshold value. The average was chosen as it is a common statistical measure, minimising the bias in the threshold selection. Hence, the first step of the location study is to exclude those regions that are underperforming in the suitability and feasibility criteria compared to the global average. To measure the regional performances, the criteria are translated into quantitative indicators. For instance, to assess the prospect of a stable production at a certain location, this analysis includes both the *political stability* and *global peace index* (cf. Fig. 2.1), since the former evaluates the subjective expectation of internal conflict whereas the latter assesses objective measures of internal and external peacefulness. Another example is the input supply security measured by the regional *silane supply* and the *trade barrier index*, indicating the ease of importing necessary input materials.

Table 2.2.: Quantitative Indicators from Publicly Available Data Sets

The last column (#NA) provides information about the number of countries for which no indicator value was available.

Indicator	Abbr.	Defintion	Source	Year	Scale	#NA
Ease of doing business score	EDB	Depicts an economy's performance with respect to a measure of regulatory best practice across 10 topics, like permits, taxation and electricity availability.	World Bank [92]	2019	0–100	28
Political stability	PS	Assesses the perceptions of the likelihood of political instability and/or politically-motivated violence, incl. terrorism	World Bank [93]	2022	-2.5–2.5	12
Intellectual property rights protection	IP	Measures the status of property rights in the world's nations, incl. the legal & political environment and physical & intellectual property rights.	Property Rights Alliance [94]	2022/23	1–9	89
Trade barrier index	TBI	Indicates the most direct and indirect trade barriers imposed by 88 countries affecting 76 % of the world's people and 96 % of world GDP	Tholos Foundation [95]	2023	10–1	130
Global peace index	GPI	Measures the absence of violence or fear of violence and the level of peacefulness, incl. extent of ongoing domestic & international conflict, level of societal safety & security, and the degree of militarisation	Institute for Economics & Peace [96]	2023	5–1	56

While most of these indicators are publicly available data sets, no such data exist for the *availability of silane supply*. Therefore, extensive research was conducted in English using publicly available

online resources and search engines, coupled with insights from industry experts, to identify possible silane producers and their locations. The remaining quantitative indicators are presented in Table 2.2, summarising their characteristics, data sources, and representativeness. For the regional comparison, these indicators were processed in Python, using the `wbgapi` package for the World Bank data and `pandas` to read-in and analyse the data. Based on the country codes as the common identifier, the indicator data sets were merged into one single DataFrame. After cleaning the merged DataFrame, the global and regional averages per indicator were calculated. The results were plotted with `seaborn`.

2.1.2. Sufficient Requirements

A strategy satisfies the sufficient requirements if it fulfils the necessary requirements and performs best in the criteria of the acceptability dimension. Thus, in contrast to the first step, the second step of the framework selects the single-best strategy out of the remaining pool of suitable and feasible options. In terms of the location study, this means that the second step encompasses the selection of the suitable and feasible location with the best environmental footprint of the silicon anode, as explained previously. Due to the particular focus of the public awareness and stakeholders' interest on carbon emissions, special attention is given to its impact category during the comparison. Therefore, the climate change impact category serves as the final selection criterion in the case that different regions result in overall similar environmental performances of the silicon-based LIB. For every adequate region, the environmental impact of the silicon anode was calculated using the LCA methodology. The region leading to the best environmental performance of the anode is considered the most suitable production location. Although the focus lies on the environmental impact of the anode's production process, the whole life cycle of the LIB is assessed to account for the influence of different transport distances and production processes of input materials depending on their origin on the environmental performance of the LIB. The following section further explains the details of the LCA analysis.

2.2. Life Cycle Assessment

This study applies the LCA methodology for the second step of the location study and for the comparative analysis of silicon- vs. graphite-based LIBs to calculate the life cycle environmental impacts of the different product systems. Although graphite anodes nowadays consist of a natural and synthetic graphite mix, this study evaluates the two types separately to understand the differences among them and with regard to the silicon anode. Additionally, the exact ratio of synthetic to natural graphite is unknown, with synthetic graphite ranging at 50 to 80 % [97–99]. The assessment conforms with the ISO 14040 [100] and ISO 14044 [101] standards, as the most commonly used frameworks for conventional LCAs [67], and thus, follows the four-step approach visualised by Figure 2.3.

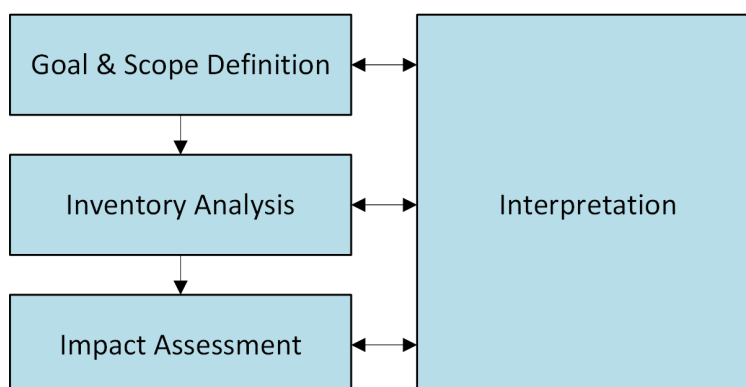


Figure 2.3.: LCA Framework According to the ISO 14040 [100] and ISO 14044 [101] Standards

2.2.1. Goal and Scope

The first objective of this analysis is to identify the optimal production location for silicon anodes based on their environmental footprint. The second objective is to compare the environmental impacts of a LIB with a silicon anode produced at the optimal location with the impacts of LIBs with natural and synthetic graphite anodes produced in China as benchmarks and determine if one battery is environmentally less impactful than the others. Moreover, the comparative analysis aims to investigate the effect of different production and battery performance parameters on the results of the comparison and attempts to identify hot-spots in all three product systems. To achieve these goals, a holistic LCA was conducted in cooperation with an upscaling silicon anode manufacturer, who provided the data of the silicon anode production process. Since the study intends to support the decision-making process of silicon anode manufacturers and inform the public about likely future production locations of batteries and anodes, along with their environmental impact compared to the status quo, the target audience encompasses private and public market players in the battery industry.

To ensure a fair comparison regarding both the different production locations and types of anodes, the complete life cycles of the three battery systems are analysed, including the extraction of resources, production of anode and cathode materials, battery cell assembly, use, and EOL phase. Table 2.3 summarises the geographical scope of the analysis and Figure 2.4 visualises it for the case of the comparative LCA, where the silicon anode is produced in Europe (cf. Chapter 3), by mapping the battery life cycle stages to their respective locations. While both graphite anodes are produced in China, the silicon anode is produced in Europe, China or North America, depending on the objective of the analysis (Table 2.3). However, in all three battery systems, the production of the remaining battery parts and their assembly takes place in China (Fig. 2.4), which is and is predicted to stay the largest battery manufacturer globally [102]. For the use phase, one-third of the batteries are shipped to Europe and two-thirds to North America (Table 2.3), based on the forecast of the silicon anode manufacturer regarding the largest sales markets for silicon-based LIBs. Following Cusenza *et al.* [103], the batteries are collected and transported to Europe at their EOL, where they are recycled in a combined pyro- and hydro-metallurgical process. This recycling process corresponds to the one of Umicore [104], one of the leading recycling companies at industrial scale in Europe [105], which has the second-highest recycling capacity for LIBs globally [106].

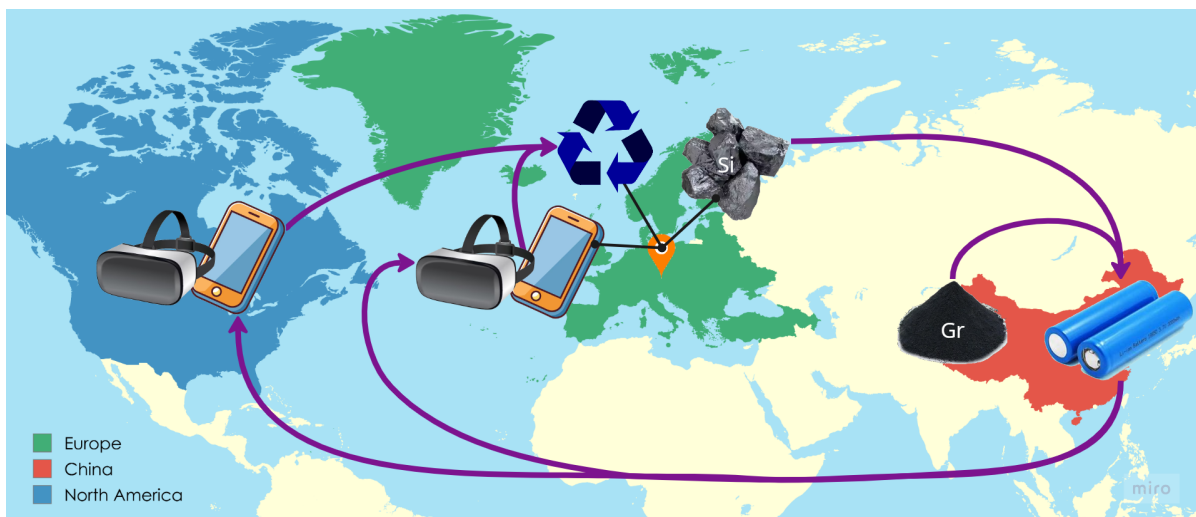


Figure 2.4.: Connecting the Life Cycle Stages of the Three Battery Systems to the Geographical Scope of the Comparative LCA. The icon for graphite (Gr) represents both types, synthetic and natural graphite. The silane gas and silicon (Si) anode are produced in Europe, which is the optimal production location for silicon anode manufacturers according to the outcome of the location study. The purple arrows indicate the transport of products.

2. Methods

During their service lives, the LIBs are assumed to be used in a consumer electronics (CE) device, like a mobile phone or wearable (Fig. 2.4). This application was chosen based on the characteristics of silicon anodes: While silicon anodes offer a high energy density, they also suffer from volume expansion issues at their current development stage, limiting the cycle life of silicon-based LIBs. This makes LIBs with a silicon anode a strong candidate for CE, as opposed to applications like transportation where a high cycle life is demanded [26, 107–110]. Furthermore, based on the application, the cathode material is set to Lithium Cobalt Oxide (LCO, LiCoO_2) since its high volumetric energy density led to its widespread use in CE and, additionally, complements the performance of silicon anodes [11, 23, 24, 34, 36]. Thus, attributed to application and cathode material, the LIB referenced in this study is a 18650 cylindrical battery cell similar to the one in Figure A.1. However, while the scope includes the battery cell, it excludes the CE device, adhering to the goal of this study.

Table 2.3 summarises the technical properties of the three product systems in more detail. The technological level of the two graphite-based LIBs corresponds to the current global standard of LIBs in the CE market, whereas the silicon-based LIB is considered an emerging technology, given the early development stage of its anode. Therefore, the study uses the most recent data available in literature, mainly from 2014 to 2022, coupled with primary industry data for the silicon anode production process, which was collected during the second half of 2024 and extrapolated to industrial scale based on the information of the silicon anode manufacturer. It should be noted that, due to the difference in technological maturity, the production data of the silicon anode is on the level of an industrial-scale demonstration plant¹, whereas the corresponding data for both graphite anodes is on the level of a mass-producing commercial plant. To accurately assess the environmental impacts of the three LIBs over their whole life cycle at a fixed point in time, this study conducted a detailed, ex-ante, cradle-to-grave, attributional LCA (ALCA).

Table 2.3.: Technical Properties and Geographical Coverage of the Reference Batteries

Characteristic	LIB with Si Anode	LIB with NG Anode	LIB with SG Anode
Voltage	3.45 V	3.5 V	3.5 V
Life Cycles	800	1,000	1,000
Gravimetric capacity of anode	1,500 mAh/g Si	372 mAh/g NG	372 mAh/g SG
Efficiency loss during charging	10 %	5 %	5 %
Cathode material	LCO	LCO	LCO
Battery cell type	18650 battery	18650 battery	18650 battery
Lifetime specific energy of battery cell	140 Wh/kg	120 kWh/kg	120 kWh/kg
Production location of Anode	Europe, North America, China	China	China
Production location of LIB	China	China	China
Use phase	$\frac{1}{3}$ Europe, $\frac{2}{3}$ North America	$\frac{1}{3}$ Europe, $\frac{2}{3}$ North America	$\frac{1}{3}$ Europe, $\frac{2}{3}$ North America
EOL phase	Recycling in Europe	Recycling in Europe	Recycling in Europe

In accordance with the goal and scope, the function of this study is defined as the storage and delivery of energy. Ergo, the functional unit (FU) of this analysis is *the delivery of 1 kWh stored energy over the lifetime* of a battery. As Chapter 3 will show, the first step of the location study results in the following alternatives: Europe, North America, and China. Among these, the second step of the location

¹According to Hellsmark *et al.* [111], the silicon anode plant can best be defined as an industrial-scale verification and validation demonstration plant, as it demonstrates an industrial production capacity, while verifying a new anode technology along the battery value chain.

study identifies Europe as the optimal location for silicon anode producers (Chapter 3). Thus, considering the three alternative anode systems, namely silicon, natural graphite, and synthetic graphite, we obtain the following six reference flows:

1. Location study:

- a) The delivery of 1 kWh stored energy over the lifetime of a LIB with a Chinese cathode and a silicon anode produced in Europe.
- b) The delivery of 1 kWh stored energy over the lifetime of a LIB with a Chinese cathode and a silicon anode produced in North America.
- c) The delivery of 1 kWh stored energy over the lifetime of a LIB with a Chinese cathode and a silicon anode produced in China.

2. Comparative analysis:

- a) The delivery of 1 kWh stored energy over the lifetime of an LCO LIB with a silicon anode produced in Europe.
- b) The delivery of 1 kWh stored energy over the lifetime of an LCO LIB with a synthetic graphite anode produced in China.
- c) The delivery of 1 kWh stored energy over the lifetime of an LCO LIB with a natural graphite anode produced in China.

2.2.2. Life Cycle Inventory Analysis

Based on the goal and scope, this section defines the different product systems by setting the system boundaries and describing the life-cycle stages. Moreover, it explains how this analysis deals with the problem of multifunctionality and outlines the impact assessment method used.

2.2.2.1. System Boundaries

To distinguish between the product systems and the environment, all human-controlled processes are defined as unit processes and belong to the economic system. For instance, the wastewater occurring during the collection and discharging of the used LIBs is treated by humans and thus an economic flow, while the steam released to the environment during both recycling steps is an elementary flow. Consequently, all agricultural and waste treatment processes are part of the economy. Furthermore, this study assumes that the recovered materials from the LIB recycling can be reused in a different product as they have a lower quality than the original virgin material, so-called downcycling [112]. To still account for the avoided virgin material production of the other product, the substitution approach is used, and the production process is included in the system boundaries. Hence, this study follows the PEFCR guidelines [113] and differentiates between generated and avoided emissions by giving credit to the recycling of the battery cells.

Adhering to the goal, the CE device is beyond the scope of this analysis and thus cut off, assuming that the three battery cells are used in the same device and applied identically during their service lives. Furthermore, this analysis does not consider any cutting losses, occurring during the battery cell assembly, and only accounts for the machinery and equipment, excluding any facilities. In the battery product system with a silicon anode, the abatement system of the PECVD process is included, but the associated filter systems are deemed negligible and thus cut off. Similarly, the subsequent laser ablation process is excluded. Because they are beyond the scope of the analysis or considered negligible, none of these cut-offs were modelled. Consequently, they do not appear in the flowcharts representing the models.

2.2.2.2. Flowchart

This section contains the flowcharts visualising the life cycles of a LIB with an LCO cathode and a silicon (Fig. 2.5), natural graphite (Fig. 2.6), and synthetic graphite (Fig. 2.7) anode. The flowchart of the silicon-based LIB shows Europe as the production location of the anode since that is the outcome of the location study (see Chapter 3) and thus the flowchart depicts the base case of the silicon anode battery system in the comparative analysis. Nevertheless, this flowchart is representative for all alternative product systems of the location study. For the sake of readability, the environmental flows have been omitted and processes with a star do not show all their non-functional flows. The full list of the flows is given by the unit process tables in the Supplementary Material.

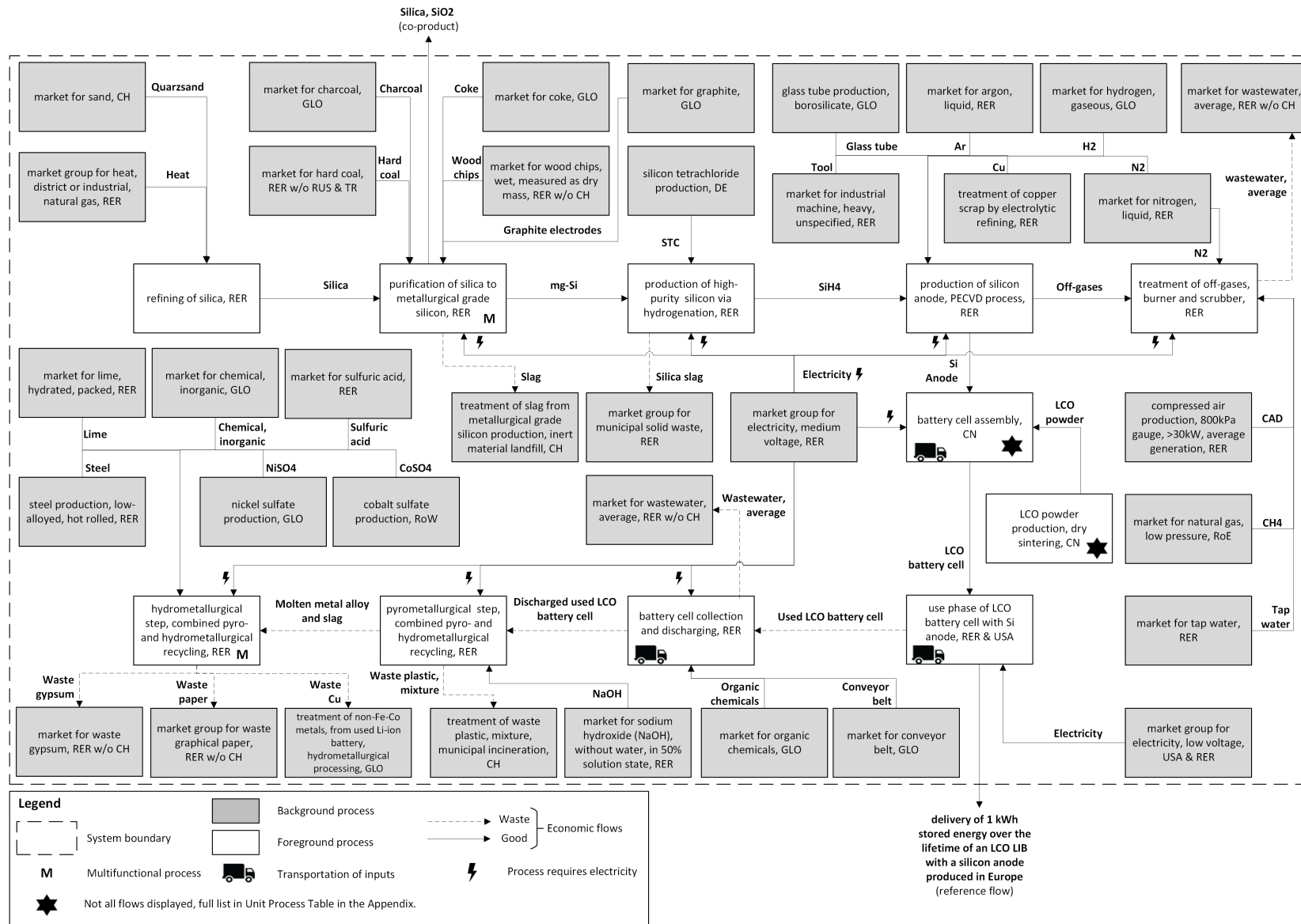


Figure 2.5.: Flowchart LCO Battery with Silicon Anode

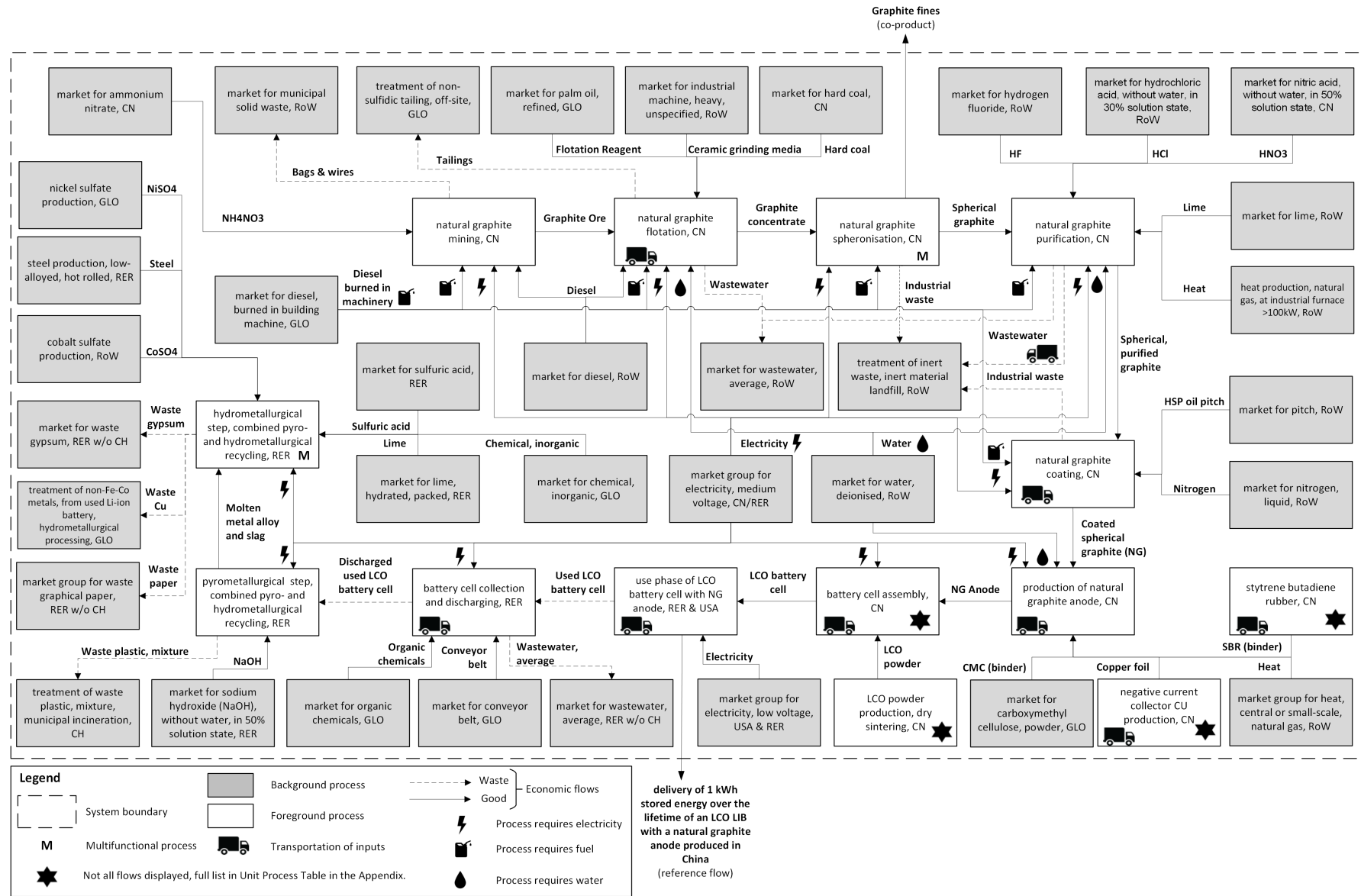


Figure 2.6.: Flowchart LCO Battery with Natural Graphite Anode

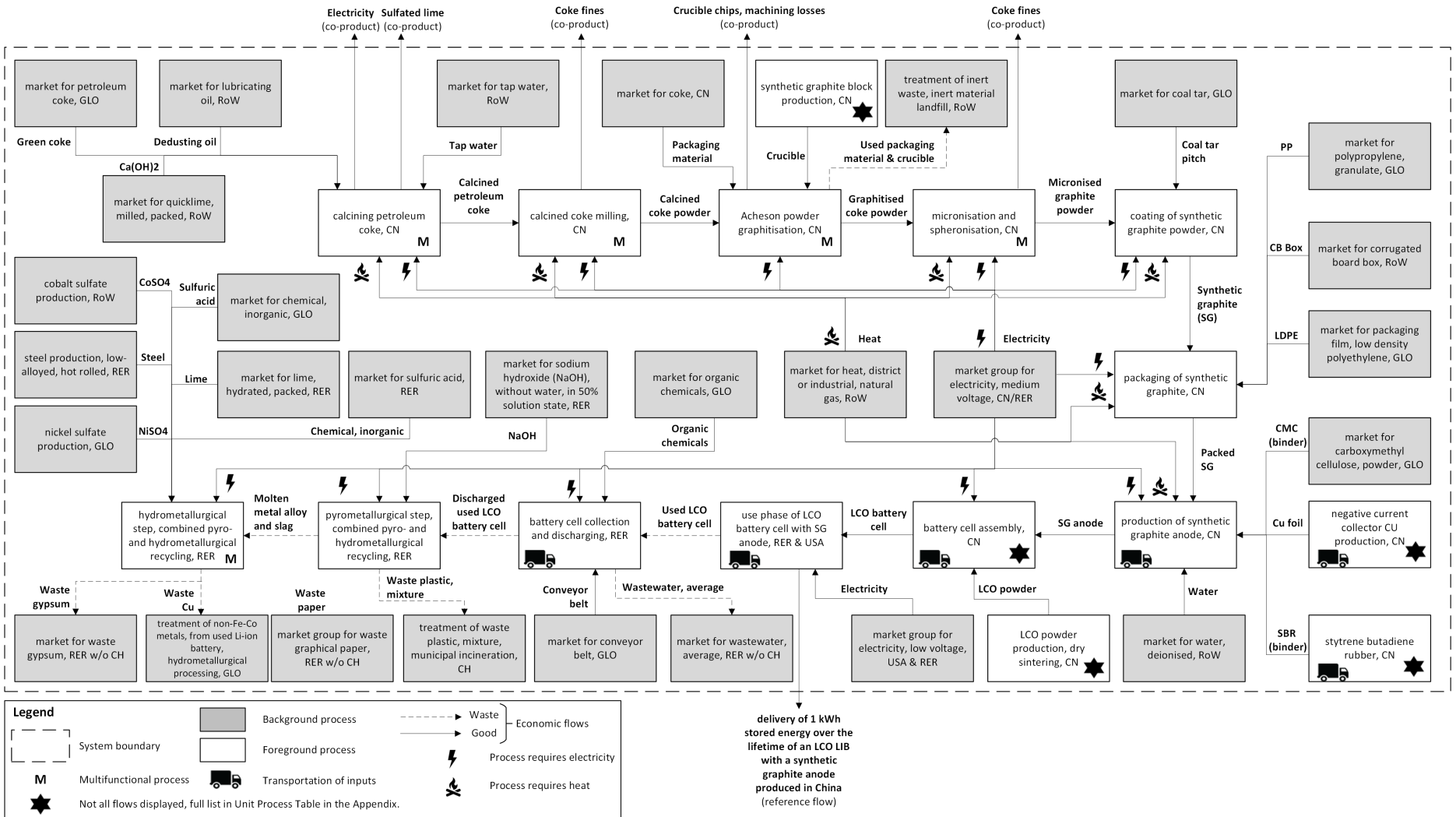


Figure 2.7.: Flowchart LCO Battery with Synthetic Graphite Anode

2.2.2.3. Data Collection and Relating Data to Unit Processes

All relevant background data was taken from the Ecoinvent v3.9.1 database with a cut-off system [74]. The foreground system consists of primary data for the silicon anode production process and secondary data from literature for the remaining processes. When no data for a specific location was available, approximations, based on comparable countries and regions, were used. The following describes the life-cycle stages in more depth and connects them to their respective data source. Furthermore, a detailed composition of the three anode-battery systems can be found in Table A.1 in the appendix. An extensive list of the unit processes, their calculations, and the parameter of the silicon anode production are provided in the Supplementary Material “Unit_Process_Tables”. In Chapter 4, the data is scrutinised regarding its accuracy and consistency.

Silicon Anode Production According to the silicon anode manufacturer, the hydrogenated, amorphous silicon anode is produced using Plasma-Enhanced Chemical Vapour Deposition (PECVD). During the PECVD process, the plasma causes the silicon in the form of monosilane gas (SiH_4 , silicon tetrahydride) to deposit on the copper substrate. The reaction takes place in an inert atmosphere of nitrogen and argon gas and is set off by a small amount of hydrogen gas. To create the plasma, a significant amount of electricity is required. Throughout the chemical reaction, a mix of off-gases is produced containing the nitrogen and argon gas, but also any silane that did not deposit in the PECVD process and the hydrogen released during the deposition of the silicon on the copper foil. Due to the reactivity of silane and hydrogen, this off-gas mix is treated in a subsequent burner and scrubber process, where the two gases are combusted by adding natural gas and the depositions are washed away with tap water. After passing several filter systems, the obtained gas mix of steam, air, carbon oxides, argon, and nitrogen oxides is released to the atmosphere. Since the exact composition and amount of these emissions is unknown, they were calculated using mass balance assuming that all the bound and unbound hydrogen and natural gas, approximated by methane (CH_4), react with oxygen to steam and carbon oxides, represented by carbon dioxide (CO_2) for simplification. Furthermore, based on a study by Ariemma *et al.* [114], 0.002 % of the remaining oxygen is assumed to react during the combustion process with the nitrogen gas and form nitrogen oxides, approximated by nitrogen dioxide (NO_2). The argon gas does not react during any of the processes and is released as such to the atmosphere.

Owing to the production process, the anode does not require any binders and, thus, consists only of the copper foil as the current collector and the hydrogenated silicon as the active material. Because of its advantageous characteristics for the PECVD method, the copper foil is composed of 100 % recycled material, which was assumed to be produced via an electrolytic refining process taken from Ecoinvent. Although Ecoinvent also provides a production process for monosilane gas, called “silicon tetrahydride production, silicon hydrochlorination”, this study modelled it itself to increase the detail and accuracy of the analysis. According to Phylipsen & Alsema [115], the first step to produce silane entails the refining of quartz sand with heat from natural gas. Besides dust, the extraction process causes no significant direct emissions. The obtained silica is then purified to metallurgical grade silicon (mg-Si) using carbon in the form of coal and wood chips as the reducing agent [116]. Following Phylipsen & Alsema [115], the efficiency of the purification process was increased to 85 % to account for technological advancements since the publication of the original study by Hagedorn & Hellriegel [116] in 1992. Finally, the mg-Si is converted to silane via hydrogenation, a process developed by the Union Carbide Corporation [115]. During the hydrogenation, the mg-Si particles are fluidised in a Fluidised Bed Reactor (FBR) using heated, high-pressure silicon tetrachloride (STC, SiCl_4) and hydrogen to form trichlorosilane (TCS, HCl_3Si). In the subsequent quench condenser and three distillation columns, the TCS is purified to monosilane gas [117]. Along the process, hydrogen and several chlorosilanes are recycled, resulting in a process yield of 98 %. Independent of the anode’s production location, the silane and silicon anode were assumed to be produced in co-location, i.e. at the same site or sites close to each other, based on information provided by the silicon anode manufacturer.

Natural Graphite Anode Production As it is the most recent study providing industry primary data, the whole production process of battery-grade natural graphite was sourced from Engels *et al.* [118]. However, while Engels *et al.* [118] model the production process of a particular Chinese factory in the Heilongjiang province in China, this study generalised the data by using the general Chinese electricity mix and Ecoinvent's market processes for the input materials instead of the factory-specific transport routes. According to Engels *et al.* [118], the graphite ore is extracted via open pit mining, using ammonium nitrate (NH_4NO_3) as explosives, and then transported in bulldozers to the co-located flotation facility. At the flotation facility, the ore is first crushed and milled before the graphite is extracted from it using pine oil as the flotation reagent and diesel as a dust collector. Due to data availability, this study approximated the pine oil by refined palm oil. Depending on the ore's graphite content, the flotation process has a yield of ca. 10 %, the other 90 % are non-sulfidic tailings and treated as such. After drying the extracted carbon matter using hard coal, the graphite concentrate is carefully micronised and spheronised to obtain spherical graphite. As a consequence of its strict requirements, including a high purity level, small size, and smooth surface, the efficiency of this process is only 40 %. The other 60 % are sold as low-value graphite fines. To increase the carbon content in the spherical graphite to more than 95 %, the remaining impurities are removed in a purification process based on chemical leaching using hydrogen fluoride (HF), hydrochloric acid (HCl), and nitric acid (HNO_3). Consequently, the acidic wastewater needs to be neutralised before undergoing further treatment. This is done using quicklime as an alkaline reagent, which is afterwards landfilled. In the last step, the spherical, purified graphite particles are coated with high softening point (HSP) pitch to seal their surfaces and carbonised in an electrical furnace to remove any volatile matter [118].

To produce the natural graphite anode, the battery-grade natural graphite is pasted and then baked onto a copper foil, necessitating a binder to glue the graphite slurry to the copper substrate. Thus, following the study by Peters *et al.* [119], the graphite anode consists of natural graphite as the active material, a copper foil, composed of 15 % primary and 85 % secondary material [64, 120] as the current collector, and a mix of styrene butadiene rubber (SBR) and carboxymethyl cellulose powder (CMC) as the electrode binder. Since the Ecoinvent database does not include SBR, its production process was based on data by Peters *et al.* [121].

Synthetic Graphite Anode Production To model the production of synthetic graphite, this analysis mainly followed the study by Carrère *et al.* [98], since it is the latest on this topic and provides industrial data for the Acheson powder route, the current industrial standard [98]. The raw material for synthetic graphite anodes is calcined petroleum coke, also called needle coke. Thus, prior to the graphite production, raw petroleum coke, known as green coke, is calcined to increase its carbon content by removing moisture and volatile matter. The data for the calcination process was taken from Edwards *et al.* [122], stating that the coke is calcined using thermal energy from natural gas. Furthermore, during the calcination process, a flue gas containing carbon monoxide (CO), carbon dioxide (CO_2), sulphur dioxide (SO_2), steam (H_2O), and coke fines is produced. The flue gas is treated by first combusting the coke fines and CO to additional CO_2 and SO_2 in a pyroscrubber and then neutralising the SO_2 with hydrated lime ($\text{CA}(\text{OH})_2$). The authors suggest that the heat created during the combustion is recovered and sold as electricity, whereas the sulphated lime is used for bricks [122]. At the graphite producer, the needle coke is milled with a yield of 80 % and afterwards graphitised in an electric Acheson furnace at 3,000 °C for a few weeks [98]. For this electricity intensive process, the coke powder is packed into graphite crucibles and covered with packaging material made out of coke to increase the thermal conductivity [98]. This study approximated the crucible production with the baking and graphitisation step of synthetic graphite from Surovtseva *et al.* [123]. After the graphitisation, the synthetic graphite powder is micronised to obtain smaller-sized particles with a smooth surface [98]. Similarly to the natural graphite production, the last step entails coating the spherical graphite powder, but with coal tar pitch instead of HSP pitch [98]. Afterwards, the finished

and packed synthetic graphite is sent to the anode manufacturer [98].

Since natural and synthetic graphite can be used interchangeably in battery anodes, the production process of the two anodes was modelled identically using the respective type of graphite. Thus, the composition of the anodes are the same, including the copper foil and electrode binders (see above).

Battery Cell Assembly During the battery cell assembly, the anodes are placed in a cylindrical 18650 battery cell with a plastic and steel casing. The cathode consists of LCO as the positive active material and aluminium as the positive current collector. As reported by Dunn *et al.* [124], LCO is produced with a solid-state technique, also called dry sintering, in which a mix of cobalt oxide (Co_3O_4) and lithium carbonate (Li_2CO_3) is calcined. The cathode is separated from the anode by a low-density polyethylene (LDPE) film. The lithium-ions transfer between the two electrodes through a lithium hexafluorophosphate (LiPF_6) and ethylene carbonate (EC) electrolyte mix. For the production and assembly of the battery cells, this study adapts data from Lastoskie & Dai [60] by replacing the anode. In case of the graphite anodes, this was done by simply exchanging the copper and graphite of the original process with the anodes modelled in this analysis while keeping the amount of active material, i.e. graphite, constant. For the silicon-based LIB on the other hand, the graphite anode was replaced based on its specific capacity instead of its mass, to account for the higher energy density of silicon. Thus, this study first derived the energy capacity of the reference battery's anode, given the gravimetric energy density of graphite (see Table 2.3), and then calculated the corresponding amount of silicon anode needed to achieve that capacity. The size of the battery was not adapted despite the smaller volume of the silicon anode due to a lack of data. Furthermore, for the scenarios where the silicon anode is not produced in China, a transport process was added to include the additional shipping.

Use phase According to the anode manufacturer, the largest sales markets for silicon-based LIBs are expected to be in Europe and North America. However, since the exact distribution is unclear, the shares were approximated by the average number of internet-enabled devices and connections per capita in both regions [125], given that phones and computers generate the highest revenue on the CE market [126]. Accordingly, after their production in China, two-thirds of the batteries are assumed to be shipped to North America and one-third to Europe [125].

During their service life, the LIBs with a natural and synthetic graphite anode are assumed to perform identical, even though natural graphite usually provides a higher capacity whereas synthetic graphite has a greater longevity [32]. However, because the exact effect is unclear and the application and treatment of the battery have a greater influence on its performance, this difference is ignored. Therefore, both LIBs with a graphite anode deliver 120 kWh/kg battery over their lifetime of 1,000 cycles [60]. Although the silicon-based LIB has a shorter lifetime of 800 cycles, due to the volume expansion issues of its anode, it can deliver 140 kWh/kg battery because of the higher density of silicon. Thus, the lifetime energy capacities of the LIBs reflect their differences in cycle life, energy density, and capacity loss over lifetime. Furthermore, during the charging process of the graphite-based LIBs 5 % of the energy is lost, while the LIB with a silicon anode incurs a 10 % loss.

End-of-Life Management Once the batteries reach 80 % of their initial capacity, they enter their EOL and are collected and recycled in Europe [127]. The recycling activity consists of a combined pyro- and hydrometallurgical process, adapted from Cusenza *et al.* [103] and consistent with the PEFCR guidelines [113]. First, the LIBs are melted in a pyrometallurgical treatment to transform the metal oxides into their metallic form [103]. In the subsequent hydrometallurgical step, the obtained black mass is leached with chemicals to recover valuable materials. However, this recycling technique prevents the recovery of any graphite, plastics, aluminium, and lithium contained in the LIBs since

they are either burned, evaporated, or disposed of as part of the slag in the pyrometallurgical process. During the chemical leaching, 90 % of the nickel and cobalt are extracted as sulfate compounds and 95 % of the copper is recovered as part of the non-ferrous metals [103]. The absolute amounts of recovered materials were adapted based on the composition of the battery cells and the recovery rates. It should be noted that for silicon-based batteries, no empirical data regarding their recycling efficiencies exists. Furthermore, in the two graphite-based battery systems, no carbon emissions are modelled during the pyrometallurgical step albeit graphite is burned due to a limited data availability.

Transportation In all three product systems, transport was modelled as receiver input. For the production processes, the transport distances and modes were directly adopted from the respective data sources. Since the manufacturing of the silicon anode is co-located with the silane production, none of the production steps of the silicon anode involve transportation of the intermediate products. In case of the use and EOL phase, this study adapted data from Notteboom *et al.* [128] to account for the shipping of the batteries between China, North America, and Europe. Moreover, this model includes the intraregional transportation by lorry of both the finished batteries and battery wastes. Consequently, after the battery assembly in China, the finished LIBs are transported to the port of Shanghai, which is the largest port in China by cargo throughput [129]. Due to a lack of data, the transport distance was estimated with Google Maps using Beijing as the start location, given that it is the capital of China and located in the east of the country between Heilongjiang and Shandong, where the graphite production takes place according to Engels *et al.* [118]. Subsequently to their shipping, the batteries are distributed to the consumers in North America and Europe by lorry, which was approximated with freight transport data from the USA [130] and EU [131], respectively. Finally, the used batteries are collected and, if applicable, shipped from North America to Europe, where they are transported to a recycling facility based on intercontinental transport data of waste in the EU [131].

2.2.2.4. Multi-functionality and Allocation

Some processes have more than one purpose, like a recycling process that treats waste and turns it into a good, or a manufacturing process with a by-product. Since these processes fulfil more functions than the one of interest, their economic flows and environmental interventions have to be partitioned between the system under study and the other system or systems.

This study solved the problem of multifunctionality with the substitution and allocation method as suggested by the ISO standards [100, 101]. Therefore, the substitution approach was applied to the hydrometallurgical recycling step in all three battery product systems to give credit for the avoided virgin material production of the corresponding recycled resources. Furthermore, during the production process of the three negative active materials, several co-products occur that cannot be used in the subsequent production processes of the anodes due to their inadequate particle size and surface structure, but are still well-suited for the use in other products. These by-products encompass the silica during the production of mg-Si, the graphite fines from the spheronisation of natural graphite, and the coke fines created during the milling and micronisation of synthetic graphite. The environmental and economic flows were partitioned between these by-products and the anode systems using economic allocation to account for the differences in quantity and material properties of the products. In an equal manner, this study solved the multifunctionality of the graphitisation process of needle coke during the synthetic graphite anode production. In the same product system, a physical allocation based on the energy content was chosen for the calcination of green coke, since the price of the co-produced electricity was regarded as too volatile for an economic allocation. More details on the allocations and their derivation can be found in Appendix A.2.1 and the Supplementary Material.

2.2.2.5. Scenario Development

This study evaluates four scenarios to assess how different production efficiencies and battery performances affect the environmental impact of the silicon-based LIB. Two production efficiency scenarios analyse varying levels of silane utilisation and the reuse of hydrogen during the production process of the anode, and the two battery performance scenarios concern the effect of the mass loading (ML) of the silicon anode and the cycle life of the LIB. Table A.2 in the appendix summarises the parameters of the scenarios. The two battery performance scenarios were selected considering the results of Peters *et al.* [132], who found that the modelling assumptions regarding a battery's cycle life and energy density, which is influenced by the mass loading of its anode [133], significantly affect the environmental life cycle performance of the battery. The two production scenarios are based on information provided by the silicon anode manufacturer and thus limited to the manufacturing process of the silicon anode itself, i.e. the PECVD process and its subsequent off-gas treatment, including the production of silane and the other input materials. Therefore, the functional unit of the underlying LCA model is adjusted accordingly to "the production of 1 kWh of activated anode material". The following describes in more detail how the respective processes were modified for the scenarios.

Hydrogen Reuse Scenario At the beginning of the PECVD process, a small amount of hydrogen is needed to start the deposition process. At the same time, hydrogen is released from the silane when the silicon deposits onto the copper substrate. In the base case scenario, this hydrogen is part of the off-gas mix and hence treated in the burner and scrubber process. For the reuse scenario, this study assumes that the hydrogen necessary to start the PECVD process can be extracted from the off-gas mix before the treatment. Thus, the hydrogen used in the PECVD is substituted by a share of the hydrogen contained in the off-gas mix and the emissions of the burner and scrubber are adapted accordingly. However, it should be noted that due to a lack of data and for the sake of simplicity, the hydrogen is filtered out of the off-gas mix without further treatment. Moreover, the amount of natural gas, with which the off-gases are burned off, is kept constant despite the lower level of hydrogen and thus reduced reactivity of the gas mix.

Silane Utilisation Scenario The silane utilisation factor describes the share of silane that deposits on the copper foil during the PECVD process. In other words, it depicts the share of silane that does not deposit on the equipment or is part of the off-gas mix. The silane utilisation scenario investigates how the production efficiency changes from an environmental point of view when this factor is set to values between 15 % and 30 %, while keeping all other production parameters and the properties of the anode constant. Consequently, the underlying model is adapted by adjusting the deposition time in accordance with the utilisation factor, since a lower silane utilisation translates into a longer deposition time, and vice versa, if the produced anode is to remain the same.

Mass Loading Scenario In the context of batteries, mass loading (ML) refers to the thickness of the active material on the current collector. Hence, in this case, it defines the thickness of the silicon layer on the copper foil. Since it determines the specific energy density of the anode, it is an important factor for the performance of the battery [134]. Therefore, this study analyses its impact on the environmental performance of the anode by varying it between 1.5 mg/cm² and 2.5 mg/cm². Because a higher ML leads to both a higher energy density but also a greater volume expansion and thus shorter cycle life of the anode, its overall effect on the performance of the battery is uncertain. Therefore, the ML scenario follows the production efficiency scenarios and limits the impact assessment to the manufacturing of the silicon anode. The PECVD process was adapted accordingly by exploiting that the ML of the anode is controlled by the deposition time, as a higher ML implies a thicker layer of silicon and thus a longer deposition process and, consequently, a higher amount of input gases, provided

that the efficiency of the PECVD process stays the same. Furthermore, the performance of the anode was adjusted, given the changed amount of silicon per kilogramme of anode material.

Cycle Life Scenario The cycle life of a battery defines the number of charging and discharging cycles before the battery reaches 80 % of its initial capacity and thus its EOL. For this scenario, the cycle life of the silicon-based LIB was changed to values between 500 and 1,500 cycles. In the model, only the amount of battery required to fulfil the FU during the use phase was changed, since the production processes of the anode and LIB were kept the same. Depending on the cycle life, the respective battery quantity was calculated based on the average amount of energy the LIB can deliver per cycle, as specified by the anode manufacturer. As opposed to the others, this scenario considers the whole life cycle of the silicon-based LIB.

2.2.3. Impact Assessment Method and Interpretation

Following the EU recommendations and the guidelines of the PEF CR [113], this study uses the PEF impact categories to calculate the environmental impacts of the different product systems. The PEF family encompasses 24 impact categories constituting the EF impact assessment method [135]. In addition to global warming, the categories assess human health, resource depletion, and ecosystem quality. The impacts were calculated using the openLCA software from GreenDelta [136].

In Chapter 4, the outcomes of a consistency check and two sensitivity analyses are discussed. The consistency check was performed to verify whether the assumptions and data underlying the different models are consistent between each other and with the goal and scope. With the sensitivity analyses, the robustness of the comparative results between the batteries with the three alternative anodes are tested. Since electricity is the main contributor to the climate change impact of the LIB with a silicon anode (cf. Section 3.2.1), one sensitivity analysis assesses its influence on the overall results by altering the electricity required during the production of the silicon anode by $\pm 15\%$. The other sensitivity analysis evaluates the impact of the allocation method and compares the base case, as described in Section 2.2.2.4, to a conservative allocation method, allocating all burdens to the final output product.

3. Results

This chapter first presents the outcomes of the location study following the two-step approach of the adapted SFA framework. Afterwards, the results of the comparative LCA are discussed and the contribution of different processes and emissions are analysed.

3.1. Location Study

Adhering to the two-step approach, Section 3.1.1 outlines the findings of the first step of the location study entailing the exclusion of regions that are underperforming in any of the necessary, i.e. suitability and feasibility, criteria. Based on these findings, Section 3.1.2 identifies the optimal location by selecting the suitable and feasible region associated with the lowest environmental footprint of the silicon-based LIB focussing especially on climate change, which corresponds to the second step of the location study.

3.1.1. Suitability and Feasibility

Figure 3.1 displays the results of the indicators from publicly available data sets (see Table 2.2). The diagonal of the pair plot visualises the performance of each region per indicator by showing the univariate distribution of the respective countries. The upper and lower triangular matrices are symmetrical, since they both consist of scatter plots depicting the pairwise relationship between the indicators. In the scatter plots, the countries are coloured according to their region. Furthermore, it should be noted that in case of the *ease of doing business*, *political stability*, and *IP protection* indicators a higher value points at a better performance of the country or region, whereas for the *TBI* and *GPI* a lower value is preferable.

Although this analysis is mainly interested in the distribution of the countries per indicator, the pairwise relationships in the scatter plots provide valuable insights. For instance, all indicators seem to be correlated in such a way that a better performance in one indicator is associated with a better performance in all the other indicators. Moreover, the *IP protection* indicator appears to have the strongest correlation with all other indicators, while the *TBI* seems to be least correlated with the others. Based on these findings, it can be expected that countries and thus regions that score better in one indicator, also tend to perform better in the others and vice versa. This conclusion is supported by the univariate distributions, indicating for example that on average, the European region scores in all indicators better than the global average, whereas Sub-Saharan Africa performs worse.

Since it proves to be difficult to visually identify from the univariate distributions in Figure 3.1 which regions score worse than the respective global average in at least one of the indicators, Table 3.1 summarises the results. The table provides the global and regional averages per indicator, with the regional averages being divided into four categories depending on their performance. The averages are expressed in terms of the arithmetic mean. For every indicator, the categories are defined based on the relative distance between the global and regional average with respect to the global standard deviation (σ). As a consequence, the regional averages are either coloured dark green, indicating that the regional average is more than one standard deviation better than the global average, light green, meaning the regional average outperforms the global one but not by more than one standard deviation,

3. Results

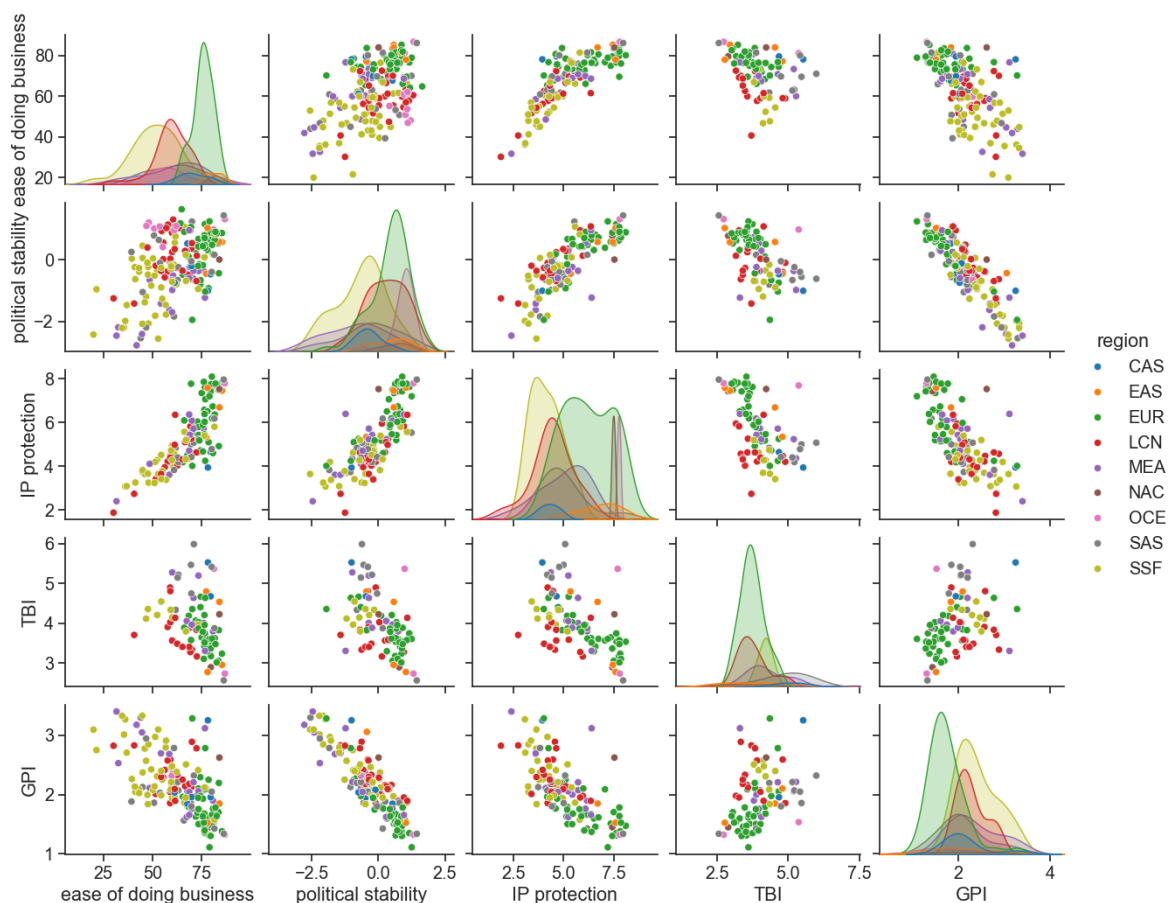


Figure 3.1.: The Ease of Doing Business, Political Stability, IP Protection, Trade Barrier Index, and Global Peace Index for All Countries and the Respective Distribution per Region

yellow, implying the regional average is within one standard deviation worse than the global indicator average, or red, meaning the region scores on average more than one standard deviation worse than the global average.

Table 3.1.: Average Performance of Each Region per Quantitative Indicator

Darkgreen = Outperforms indicator mean by more than one standard deviation (σ); Green = Outperforms indicator mean within one σ ; Yellow = Within one σ worse than indicator mean; Red = More than one σ worse than indicator mean.

Index	Mean ($\pm \sigma$)	CAS	EAS	EUR	LCN	MEA	NAC	OCE	SAS	SSF
EDB	62.959 (± 13.839)	70.744	81.150	75.601	59.511	60.726	81.819	60.720	61.906	51.846
PS	-0.035 (± 0.999)	-0.353	0.405	0.424	0.281	-0.867	0.604	0.898	-0.289	-0.662
IP	5.224 (± 1.42)	4.288	6.764	6.163	4.420	5.006	7.473	7.740	4.991	4.141
TBI	3.976 (± 0.703)	5.105	3.770	3.732	3.773	4.240	3.565	4.055	4.754	4.188
GPI	2.147 (± 0.51)	2.167	2.132	1.756	2.288	2.349	2.035	1.725	2.103	2.409

3. Results

As visible in Table 3.1, the regions that consistently perform better than the global average in all indicators are Europe, North America, and East Asia. While the European region performs only slightly better than the global average in every indicator, East Asia and North America are the only regions that outperform the global average significantly in two indicators, namely the *ease of doing business* and *IP protection* indicator. Contrarily, all other regions score worse than the global average in at least two indicators. However, only Central and South Asia perform significantly worse compared to the global average in one indicator, the TBI, whereas the remaining regions underperform moderately. Nevertheless, they all do not fulfil the necessary requirements. Furthermore, this result remains the same when the median instead of the mean is used to express the average (see Appendix B.1), as a measure of central tendency that is less sensitive to outliers. It is noteworthy, however, that South and Central Asia, the Middle East & North Africa, and Oceania & the Pacific strictly perform better in at least one indicator. This is especially striking in the case of Oceania & the Pacific, since they substantially outperform the global average and all other regions in *political stability*, *IP protection*, and *GPI*. Still, as the region scores slightly below the average in the other two indicators, it is not a feasible option and thus does not fulfil the necessary requirements. Hence, independent of the choice of measure for the average, the result persists and only Europe, East Asia, and North America outperform the global averages in all indicators.



Figure 3.2.: Silane Producer Map

The map does not contain any silane suppliers that are bound by exclusive supply agreements.

The result is further supported by the availability of silane supply. Figure 3.2 shows a world map with the locations of global silane gas producers. A complete list of all companies displayed can be found in Table B.2 in the appendix, providing more information on their product lines, maturity, and production capacities. In the map, the location pins of the silane producers are either coloured blue, in case of a planned production facility, or green for already existing factories. If it was not possible to find the location of a company's production facility, the headquarter of the company was used as a proxy, marked with a red location pin. While there might be disparities, the information of companies with a known production site indicates that production close to the headquarter is likely. Furthermore, the map only displays silane gas suppliers whose production capacity is at least partially available to a potential anode manufacturer. Thus, the map excludes Wacker and Hemlock Semiconductor Corporation (HSC), Koch Modular, and Schmid Silicon Group, since they only produce

3. Results

silane gas for themselves or are bound by exclusive supply agreements. Moreover, Praxair is included in Table B.2 for completeness but not in the map, as it is now part of Linde AG. The total number of silane producers included in the map is 34. With almost 80 %, the majority of them are located in East Asia, especially in China. This concentration can be explained by the national plan of the Chinese government, which, among others, aimed at increasing the country's silane production capacity. As a consequence, China has many, relatively young silane producers with a considerable production volume (see Table B.2). Apart from China, the map indicates that the only two other regions producing silane gas are Europe and North America. Although North America, more specifically the USA, has just two silane companies, one of them, REC Silicon, is the world's largest silane gas producer with a capacity of 30,000 Mt/year (cf. Table B.2). On the other hand, three out of the five silane suppliers located in Europe are not producing at the moment, but rather plan to start production in the future. Nonetheless, given that all other regions do not produce any silane gas, East Asia, Europe, and North America are the only regions with available silane supply. Therefore, combined with the previous results of the other indicators, these three are the only regions that fulfil the necessary requirements and are thus suitable and feasible locations for a silicon anode manufacturer.

3.1.2. Acceptability

To determine the optimal location, Figure 3.3 displays the life cycle environmental impacts of a silicon-based LIB produced in East Asia (yellow), North America (dark green), or Europe (turquoise), normalised to the largest impact per category. Due to data availability, East Asia is approximated by China, where the majority of the region's silane suppliers are located. Table B.3 in the appendix provides all absolute characterisation results.

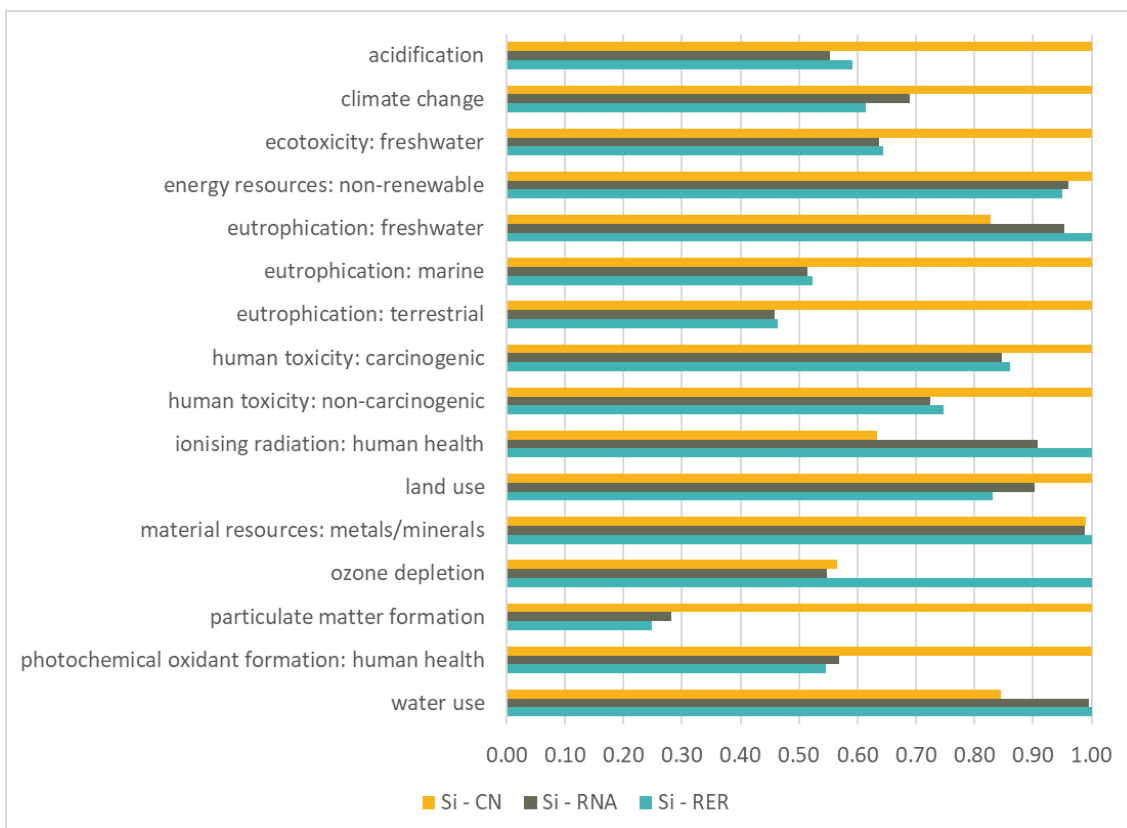


Figure 3.3.: Regional Environmental Footprint of a LIB with a Silicon Anode

Values are scaled relative to the largest impact per category. East Asia is approximated by China. Impacts are per 1 kWh delivered energy over the full life cycle of the batteries.

3. Results

As visible in Figure 3.3, a LIB with a silicon anode manufactured in China is in the majority of categories associated with the highest environmental impact. Production facilities in Europe and North America, on the other hand, seem to perform similarly from an environmental perspective. While there is a noticeable difference between the three alternatives in most impact categories, the depletion of material resources is almost the same, since the silicon anode produced is identical. The differences in the other categories can be explained mainly by the variations in the regional electricity mixes, as Figure 3.4 illustrates using the impact category of climate change as an example. The figure visualises the relationship between the greenhouse gas emissions occurring during the life cycle of the silicon-based LIB and the electricity grid, depending on the choice of location. Since only the electricity mix differs between the European locations, while all other factors like transportation distances and origin of input materials are kept constant, a clear linear correlation can be identified between the climate change impact of the LIB and electricity grid. Moreover, since the LIBs with the anode produced in China and North America are almost on the same line, it can be concluded that the other factors are only of minor importance. Hence, most of the variations in the climate change impacts between the three alternative production locations originate from the differences in their regional energy mixes.

In Ecoinvent v3.9, the electricity mixes are modelled based on their composition in 2020, shown by Figure B.1. It should be noted that in this figure, China is part of Asia Pacific. When linking the characterisation results (Fig. 3.3) to the regional compositions of energy sources (Fig. B.1), it becomes evident that the relatively low impact of the silicon-based LIB produced in China on ionising radiation and water use is caused by the comparably low share of nuclear power in the Chinese grid mix, since nuclear energy requires a significant amount of cooling water and generates radioactive waste. Moreover, the small share of natural gas in China's electricity grid, results in the relatively low impact of the LIB on ozone depletion compared to Europe. Yet, the country's dependence on coal leads to the poor performance of the Chinese LIB in most of the other impact categories, including climate change and particulate matter (PM) formation. Hence, China and thus East Asia can be excluded as it is a suitable and feasible but not acceptable location for a silicon anode manufacturer.

The comparison between Europe and North America as anode production locations proves to be more difficult due to the overall similar environmental performance of the two LIBs (Fig 3.3). Nevertheless, given the particular interest of public and private stakeholders in climate change, Europe is considered the more acceptable location, since a LIB with an anode manufactured in Europe causes 0.802 kg CO₂-eq./kWh over its whole lifetime, whereas the North American equivalent produces 0.9 kg CO₂-eq./kWh (see Table B.3). Again, this outcome can be explained by the composition of the two electricity mixes, as they are similar, but the European grid mix has a higher share of renewable energy sources (cf. Fig. B.1). Therefore, among the three suitable and feasible regions, Europe is the most acceptable production location for a silicon anode manufacturer, since it results in a comparably good overall environmental performance and specifically low climate change impact of the whole LIB.

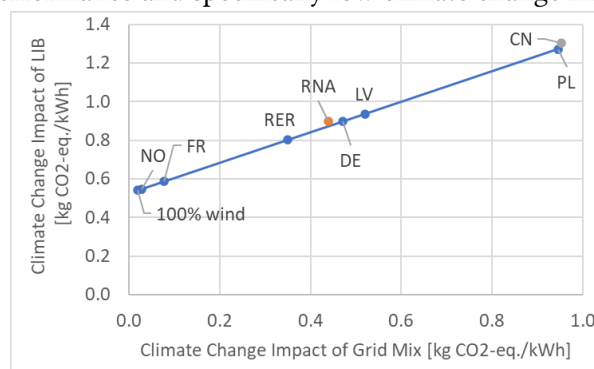


Figure 3.4.: Correlation Between the Carbon Footprint of a Region's Electricity Grid Mix and the Production Footprint of a Silicon Anode. 100 % wind energy is sourced from Switzerland (CH).

3.2. Comparative Life Cycle Analysis

Based on the results of the location study, Europe was identified as the optimal production location for a silicon anode manufacturer. Therefore, to compare the environmental performance of the three battery systems with different anode types, the silane and silicon anode are assumed to be produced in co-location in Europe. Afterwards, the finished silicon anode is shipped to China, where the battery assembly takes place. The benchmark batteries with a natural and synthetic graphite anode on the other hand are fully produced in China, as described in Section 2.2.2. Figure 3.5 visualises the relative life cycle environmental impacts associated with the delivery of 1 kWh of stored energy for all three battery systems, normalised to the largest impact. The corresponding absolute values are given in Table B.4 in the appendix.

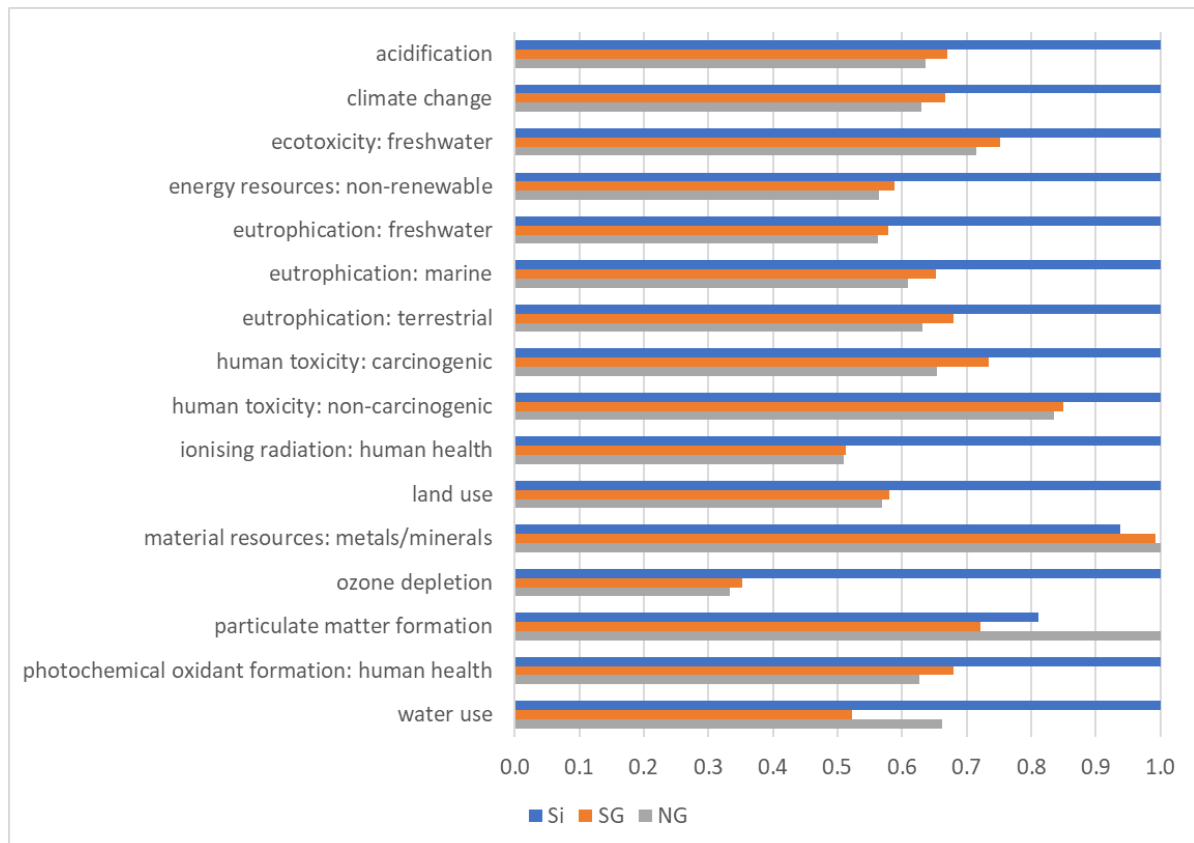


Figure 3.5.: Relative Cradle-to-Grave Impact of the PEF Impact Categories for 1 kWh Delivered Energy of LIBs with a Silicon (Si), Natural Graphite (NG), and Synthetic Graphite (SG) Anode
Values are scaled relative to the largest impact per category.

In all but two of the impact categories, the silicon-based LIB has significantly higher environmental impacts than the two graphite-based LIBs. The biggest relative difference is in ozone depletion, indicating higher chlorofluorocarbon (CFC) emissions during the lifetime of a silicon-based battery. Since CFCs are, among others, emitted during the production of natural gas, this difference can be explained by the higher share of natural gas as an energy source in the European grid mix compared to the Chinese one (Fig. B.1) and, in addition, an overall higher electricity consumption in the life cycle of the LIB with a silicon anode. The two categories in which the silicon-based battery outperforms the graphite-based ones are material resources: metals/minerals and particulate matter (PM) formation (Fig. 3.5). In the category of material resources, the three product systems have almost the same impact, as the three batteries are nearly identical. Nevertheless, the higher energy density of the silicon anode and its greater share of recycled copper in the negative current collector result

3. Results

in a lower consumption of material resources as opposed to the two graphite anodes. In case of PM formation, the silicon-based product system performs better than the one of natural graphite, due to the dust created during the mining of the graphite ore, but worse than the synthetic graphite system, because of the silica dust released during the purification of silica to mg-Si. Thus, in this category, the LIB with a synthetic graphite anode has the lowest impact. Besides PM formation, this is only the case in water use, where the larger water consumption of the other two alternatives is caused by the flotation and purification of the natural graphite and the greater usage of nuclear energy during the production of the silicon anode, given the European electricity mix (Fig. B.1). In all other categories, the LIB with a natural graphite anode marginally outperforms its synthetic graphite counterpart (Fig. 3.5), owing to the large amount of electricity consumed by the electric Acheson furnace during the graphitisation of needle coke to produce synthetic graphite. Hence, in the majority of the impact categories, the LIB with a natural graphite anode is associated with the lowest emissions, closely followed by the LIB with a synthetic graphite anode, whereas the LIB with a silicon anode is associated with the highest impacts.

While the similar performance of the two graphite-based LIBs is plausible given that the two batteries are identical except for the negative active material, the considerably higher environmental impacts of the silicon-based LIB in almost all categories despite its higher energy capacity are less intuitive. Since the lower cycle life and voltage of the LIB with a silicon anode are compensated by the significantly higher gravimetric energy capacity of its anode, the fulfilment of the functional unit to deliver 1 kWh of stored energy during the use phase requires only 7.17 g silicon-based LIB compared to 8.33 g graphite-based LIB. Thus, one would rather expect that the silicon-based LIB performs better than the graphite-based alternatives. However, as the results suggest otherwise, it seems that there is a notable difference between the production processes of the anodes, since all other processes, i.e. the battery production, use, and EOL phase, are comparable. Therefore, the relative environmental impacts associated with the production of 1 kWh activated anode material for all three anode types are displayed in Figure 3.6. Table B.5 provides the corresponding absolute results.

According to Figure 3.6, the production process of the silicon anode results in the highest environmental impacts compared to the production of the two graphite alternatives in most impact categories. Among the graphite anodes, natural graphite causes fewer emissions during its production as opposed to synthetic graphite in the majority of cases. Thus, the trend identified in the comparison of the cradle-to-grave battery product systems remains the same. However, the relative differences in the environmental impacts between the three alternatives increase when limiting the scope to the production processes of the anodes, supporting the hypothesis that the variations in the environmental footprints of the three battery types originate from the differences in the environmental impacts of the anode production processes. The greatest change in the relative results occurs in ionising radiation: human health, where the impact of the graphite-based product systems increases from almost 0 % compared to the ionising radiation caused by the silicon anode (Fig. 3.6) to ca. 50 % when considering the whole life cycle of the battery (Fig. 3.5). This change can be explained by the different locations and associated electricity mixes assumed for the life cycle stages of the product systems, since the Chinese electricity grid mainly depends on hard coal, whereas the European and North American electricity grids rely more on nuclear energy (cf. Fig. B.1), causing a higher ionising radiation impact. Therefore, in contrast to the silicon anode produced in Europe, the production processes of the two graphite anodes in China emit relatively low ionising radiation, but as the use and EOL phase in all product systems take place in Europe and North America, the relative differences decrease when comparing the entire life cycle of the batteries. Thus, the overall ranking of the three battery systems persists, but the relative differences between their impacts diminish.

The same change, even if less pronounced, can be observed in all other impact categories. When extending the scope from the anode production to the battery assembly, the performance rankings of the three alternatives stay the same in each impact category (see Table B.7). However, the relative

3. Results

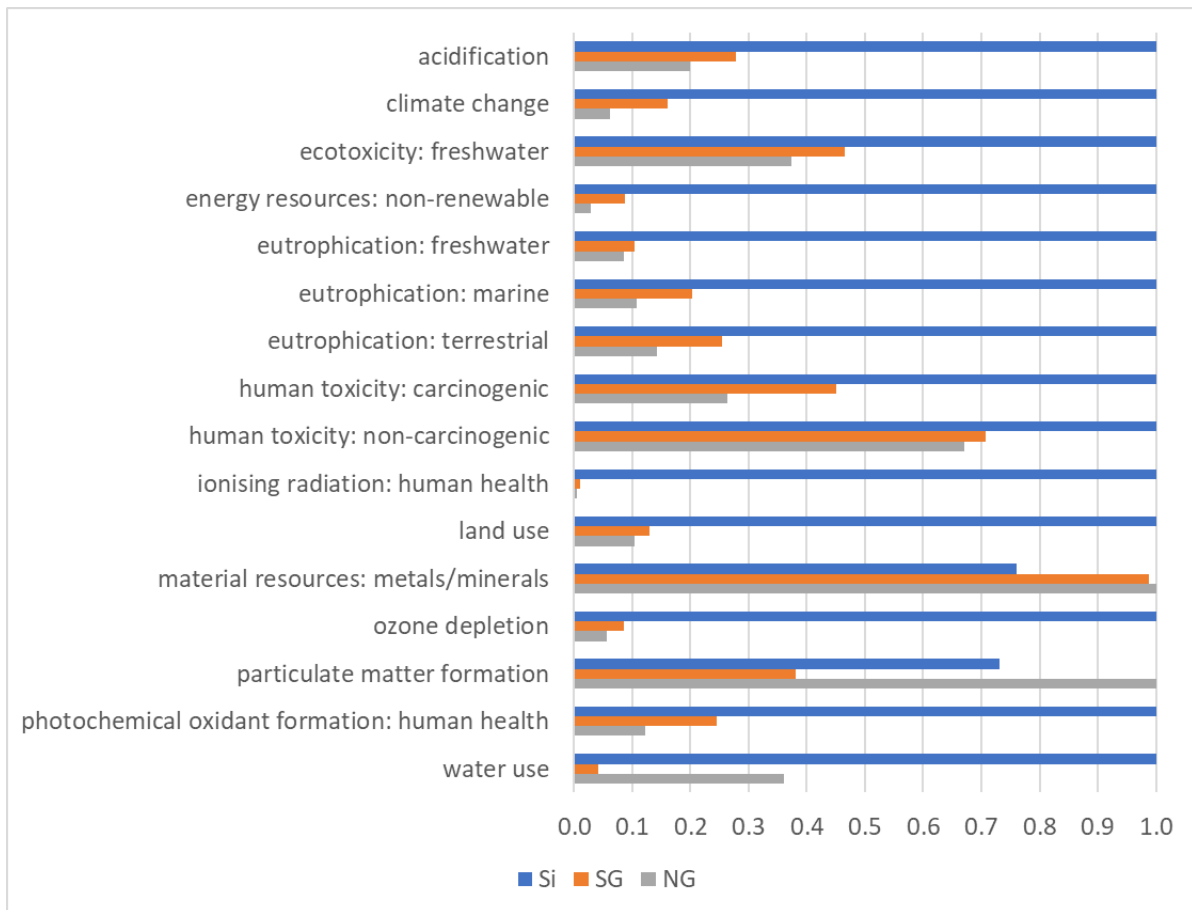


Figure 3.6.: Relative Cradle-to-Gate Impact of the PEF Impact Categories for 1 kWh Activated Silicon (Si), Natural Graphite (NG), and Synthetic Graphite (SG) Anode
Values are scaled relative to the largest impact per category.

differences are smaller, as, apart from the anode, the batteries are identical and thus the relative contribution of the anode to the overall environmental impacts decreases. Moreover, due to the higher energy density of the silicon anode, the battery only requires 1.84 g of silicon anode per kWh of battery cell as opposed to 2.12 g of graphite anode per kWh. Hence, the higher energy density of the silicon anode additionally reduces the differences in the environmental performances of the graphite and silicon systems. It should be noted that, therefore, the relative differences between the graphite-based and silicon-based product systems are greater when comparing the environmental impacts per kg instead of per kWh of activated anode material or battery cell (cf. Table B.6 and B.8). Given the similarity of the use and EOL phases across the three product systems, most relative differences are further reduced when considering the whole life cycle of the battery, while the rankings still remain identical (Fig. 3.5). However, contrarily to the battery assembly, the environmental gains arising from the higher energy density of the LIB with a silicon anode, are partially diminished by the credits awarded for recycling. On the one hand, a smaller amount of the silicon-based LIB is sufficient to fulfil the functional unit as compared to the graphite-based battery cells. On the other hand, the consequently lower material consumption in the silicon product system results in less recycled material and thus fewer credits at the EOL. In the cases of ozone depletion and water use, the gains from recycling seem to even outweigh the gains from the higher energy density, as the relative differences in the two categories between the graphite-based and silicon-based LIB are larger when considering the whole life cycle in contrast to the battery cell production (Table B.4 and B.7). Hence, the overall trend of a battery with a natural graphite anode, followed by a synthetic graphite anode, being envi-

ronmentally less impactful than a battery with a silicon anode persists independent of the functional unit (kg vs. kWh) and scope (cradle-to-grave vs. cradle-to-gate LIB vs. cradle-to-gate anode) of the comparison due to the differences in the anode production processes.

3.2.1. Contribution Analysis

To identify the main factors contributing to the environmental impacts of the three battery types, the study includes two contribution analyses on the processes and interventions, one on the level of the whole life cycle of the batteries and one focussing on the anode production processes due to their relevance on the overall impact results. In the resulting four contribution analyses, the study only considers flows and processes contributing more than 1% to the overall environmental impact per category. For presentation purposes, the two process contribution analyses involved the assignment of the economic flows to process categories following the ISIC classification in Ecoinvent [74]. Moreover, the PEF impact categories were divided into four groups, namely climate change, ecosystem quality, resource depletion, and human health. Figure 3.7 and Figure 3.8 summarise the outcomes of the contribution analyses for the battery life cycle and anode production systems, respectively. The detailed results for the grouped PEF impact categories can be found in the Supplementary Material “Multifunctionality_and_Contribution-Analysis”.

Independent of the anode type, the primary contributor to climate change during the anode manufacturing process and entire life cycle of the LIBs is the production of electricity (Fig. 3.8 and 3.7). Consequently, carbon dioxide is with around 90% the dominant emission in this category due to the dependence of the Chinese, European, and North American electricity grids on fossil energy sources (cf. Fig. B.1). Since the Chinese grid relies more on hard coal whereas the European grid depends more on natural gas, the mining of coal and lignite contributes more to the climate change emissions of the manufacturing process of the graphite anodes while the extraction of crude petroleum and natural gas is more relevant for the silicon anode production (Fig. 3.8). This difference is still visible when the entire life cycle of the batteries is taken into account (Fig. 3.7), indicating the relevance of the anode manufacturing processes to the total environmental life cycle impacts. Nevertheless, by extending the scope to the whole life cycle, the processes contributing to climate change in the three product systems converge, as processes specific to the anode types, like the manufacturing of graphite for the crucible production in the synthetic graphite anode system, become less significant. This effect is less present in the silicon anode product system, since the process sources its electricity from a grid similar to the ones in the use and EOL phase.

The group of ecosystem quality encompasses acidification, freshwater ecotoxicity, as well as freshwater, marine, and terrestrial eutrophication. Similar to the climate change category, the contribution results of the economic processes and environmental flows converge in this group when the scope is extended to the whole life cycle of the product systems. For instance, on the anode production level (Fig. 3.8), the acidification of the silicon anode is mainly caused by the consumed electricity, as opposed to the natural graphite anode, where it primarily stems from the manufacturing of basic metals due to the high content of primary copper (85%) in the negative current collector. The acidification of the synthetic graphite anode is driven by a mix of these two contributors, since the anode has the same primary copper content as the natural graphite anode, but requires more electricity due to the energy-intensive graphitisation step in the electric Acheson furnace. However, as in the case of climate change, electricity becomes the main contributor to acidification in all three product systems on the cradle-to-grave battery level (Fig. 3.7). The process and interventions contributing to freshwater ecotoxicity align likewise. The freshwater ecotoxicity impacts of the anode production processes originate mostly from the waste treatment process of the sulfidic tailings from copper mining, releasing hydrogen sulfide emissions, and the iron ion emissions from coal and lignite mining operations. While the production of the graphite anode creates more hydrogen sulfide emis-

3. Results

sions due to the higher share of primary copper, and the iron ion emissions are more predominant in the silicon anode production process, since the coal is used for both electricity generation and as a reducing agent during the purification of silica to mg-Si (Fig. 3.8), the contributions of the processes and environmental flows align with the increased importance of electricity on the battery level (Fig. 3.7). Another environmental flow contributing especially to the freshwater ecotoxicity associated with the production of the synthetic graphite anode is chloride, which occurs during the treatment of the water discharge from petroleum and natural gas extraction (Fig. 3.8). Thus, contrarily to the other product systems, where chloride is mainly produced during the electricity generation, the production of the synthetic graphite anode causes additional chloride emissions, as the raw material of synthetic graphite is petroleum coke. Besides freshwater ecotoxicity, the waste treatment processes of the tailings from the copper and coal mining activities are the main contributors to freshwater eutrophication in all three product systems independent of the scope. However, despite the lower rate of primary copper in the silicon anode, the characterisation results of its product system are significantly higher than the ones of the graphite-based systems (see Table B.5), indicating a substantially higher electricity consumption during the production of the silicon anode.

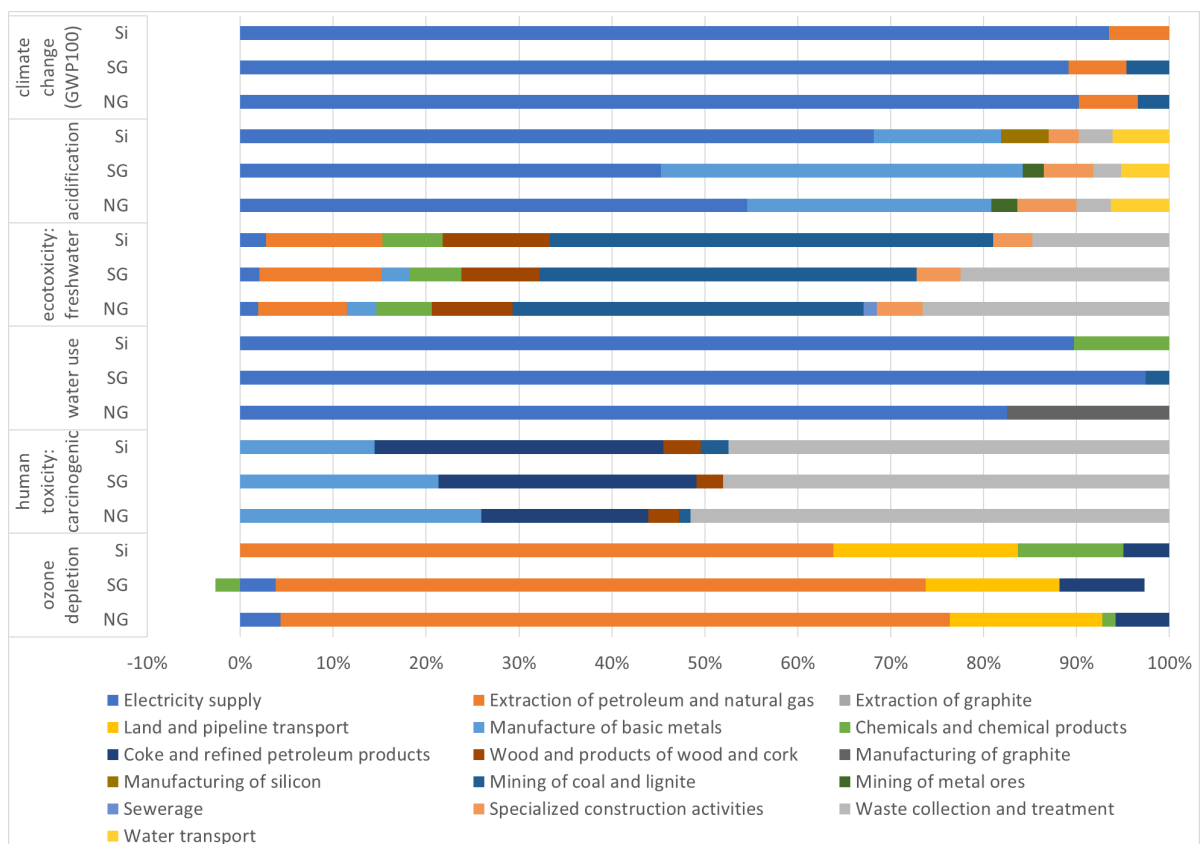


Figure 3.7.: Categorized Process Contributions to Cradle-to-grave Environmental Impacts of All Three Battery Product Systems; Only includes processes contributing >1%.

In the cluster of resource depletion are non-renewable energy resources, material resources, and water use. Independent of the scope, the material resources are dominated by the extraction of copper in all product systems. However, it is not the copper itself and instead tellurium, a by-product of copper mining, that contributes the most to the impacts on material resources. Furthermore, despite its large environmental impacts, cobalt production is not a significant contributor to this category, since the majority of the impacts associated with cobalt production are offset due to the battery recycling at the EOL. For non-renewable energy resources and water use, large impacts arise from the electricity production in all product systems except for the natural graphite anode production, where 92% of the

3. Results

water is used for the flotation and purification of natural graphite (Fig. 3.8). In all other cases, both scopes and product systems, the water is predominantly used for energy generation, i.e. hydropower, and for cooling in nuclear energy production. The impacts in non-renewable energy resources are primarily driven by the extraction of fossil fuels, like coal and natural gas, and the mining of uranium for nuclear power generation. Due to the electricity mixes of the anode production locations, the former is more present in the graphite-based systems, whereas the latter predominates in the silicon one.

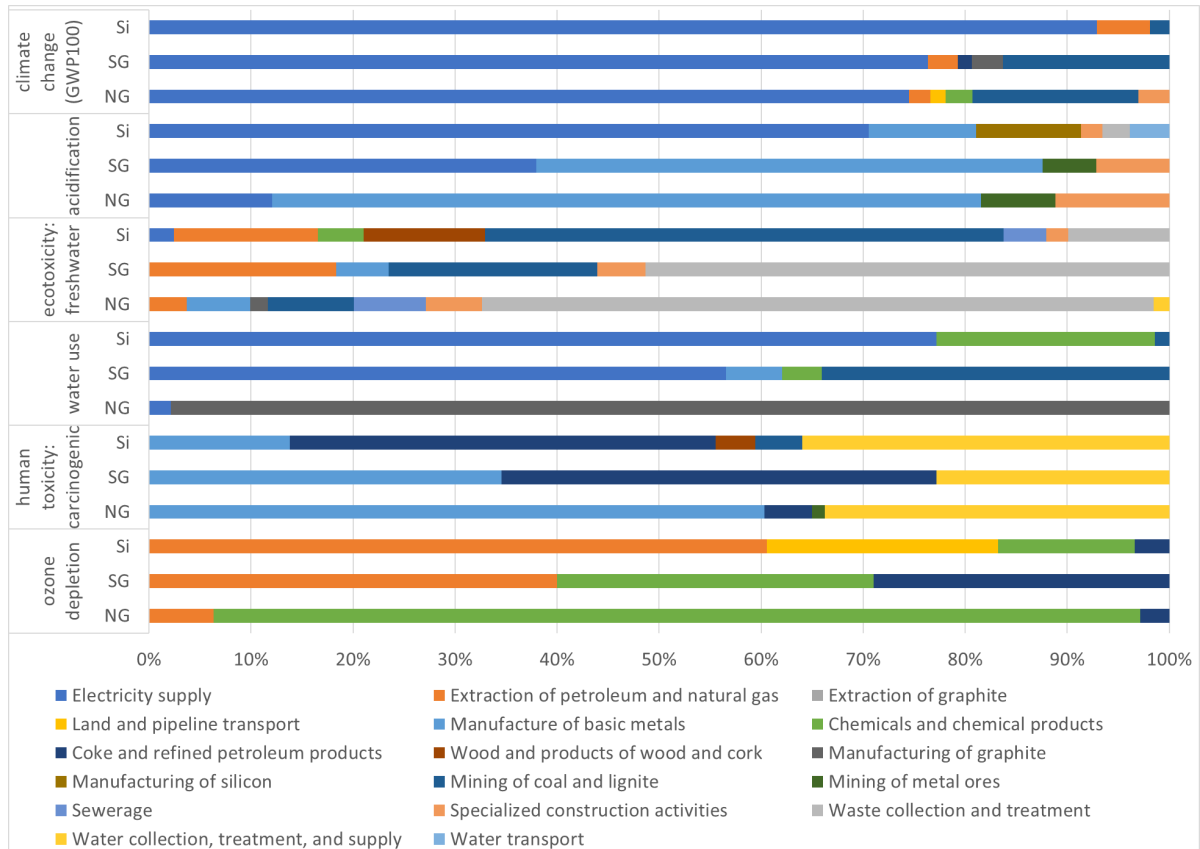


Figure 3.8.: Categorized Process Contributions to Cradle-to-gate Environmental Impacts of All Three Anode Product Systems; Only includes processes contributing >1 %.

The human health cluster consists of carcinogenic and non-carcinogenic human toxicity, ionising radiation, ozone depletion, PM formation, and photochemical oxidant formation. Similar to the other groups, the life cycle environmental impacts in this cluster are mainly caused by the required electricity in the three product systems, since the emissions released during its production and raw material extraction are the main contributors. For the silicon-based system, this still holds when the scope is limited to the anode production process (Fig. 3.8). However, for the product system of natural graphite, the copper production becomes relatively more important, as visible in carcinogenic human toxicity and ozone depletion. While the production, including the extraction and waste treatment, of natural gas and coal emits benzo(a)pyrene and chromium VI, which are more prevalent in the silicon anode production process, the copper foil production causes arsenic ion emissions and, due to the sodium hydroxide required in the process, creates tetrachloromethane (R10), which contributes in a greater share to the impacts of the natural graphite anode production. As in the case of acidification, the contributors in the synthetic graphite system are a more equal mix of these processes and emissions (Fig. 3.8), given the increased electricity consumption during the graphitisation step and identical share of primary copper in the current collector as in the natural graphite anode. Furthermore, the ozone depletion of the synthetic graphite product system is the only impact category where

3. Results

the effects of the substitution method are observable in the process contribution results, since the impacts are partially negative when the whole life cycle of the battery, including the recycling at the EOL, is considered (Fig. 3.7). The credited emissions originate mainly from the cobalt production for the cathode and consist especially of tetrachloromethane. They only outweigh the ozone depletion impacts of the process in the synthetic graphite system, because the purification of natural graphite causes additional tetrachloromethane emissions by using sodium hydroxide. Moreover, the silicon-based system requires less battery, and thus cobalt, to fulfil the functional unit, resulting in fewer emissions offset at the EOL.

Overall, the processes and flows contributing to the life cycle environmental impacts of the three battery types are comparable, with electricity production and its associated emissions being the main contributors. After electricity, copper mining and production seem to be significant sources of environmental impacts. Cobalt production on the other hand is not an important driver in any impact category, since its impacts are mostly offset by the credits given for the battery recycling at the EOL. When comparing the production processes of the anodes, the differences in the types and contributions of the processes and flows causing the environmental impacts increase. While electricity remains the main contributor in the silicon anode system, copper becomes more important in the natural graphite one due to the higher share of primary copper in the anode. In the synthetic graphite system, the contributions of electricity and copper are more balanced, since the anode contains the same amount of primary copper as its natural graphite counterpart, but requires a larger amount of electricity during its production because of the energy-intensive graphitisation step. As electricity is the main contributor in the silicon anode system, the significantly higher environmental impacts of its production process in the majority of categories point to a considerably higher electricity consumption as compared to the graphite-based systems.

3.2.2. Economic Flow Analysis

With an economic flow analysis, the contribution of individual life cycle stages are identified. In contrast to the previous contribution analyses, the economic flow analysis considers all the different processes and corresponding environmental flows belonging to one life cycle stage, instead of analysing the contribution of each process and intervention over the entire life cycle. In this study, an economic flow analysis for the climate change impact category was conducted based on the increased interest of public and private stakeholders in the topic of global warming. Moreover, since the electricity consumption and its associated emissions are the main contributors to the environmental, and specifically climate change, impacts of the three product systems, this analysis provides insights about the hotspots in the batteries' life cycles and their components. The absolute contribution results are illustrated by Figure 3.9, which is divided into three parts to increase the level of detail regarding the production processes. Each part consists of three columns, one per battery type. Accordingly, the first three columns show the complete life cycle, whereas the second and third part zoom into the production of the batteries and anodes, respectively. Figure B.2 in the appendix visualises the relative contributions to climate change of the life cycle stages and battery components for the three batteries.

As the use phases in the three product systems are almost identical, their climate change impacts are nearly the same. The slightly higher impacts in the silicon-based system can be explained by the difference in charging losses, since the battery loses 10 % of the electricity as opposed to 5 % like the graphite-based ones. Hence, the charging of the battery cell with a silicon anode requires more electricity. On the other hand, the higher energy density of its anode reduces the amount of battery needed to deliver the same amount of energy as the batteries with a graphite anode. However, this difference does not affect the climate change impacts associated with the use phase, but the battery production and the recycling step at the EOL. As visible in Figure 3.9, the EOL phases in all three

3. Results

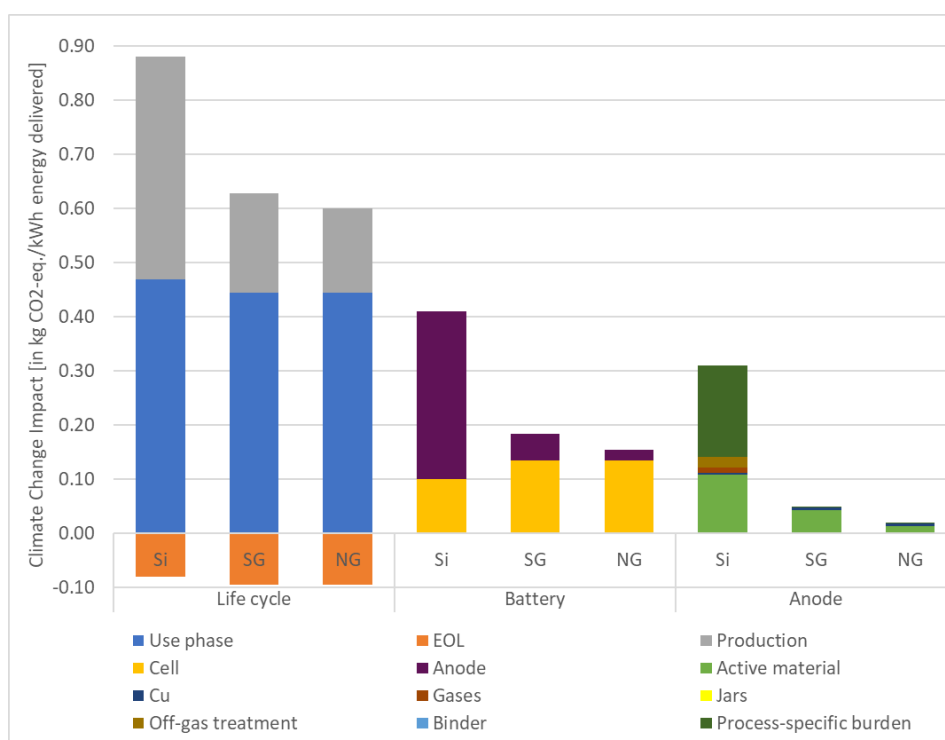


Figure 3.9.: Absolute Contribution of Life Cycle Stages to Climate Change Impacts

product systems have net negative emissions, indicating that the credits awarded for the recycling of the batteries exceed the climate change impacts linked to the process. Because of the lower amount of battery consumed during the use phase and thus recycled at the EOL, the negative emissions of the silicon-based product system are lower as compared to the graphite-based ones.

The life cycle stage that differs the most in climate change impacts between the product systems is the production phase (Fig. 3.9). Although the higher energy density of the silicon anode results in a lower amount of battery consumed, the impacts of the silicon-based battery production are with 0.41 kg CO₂-eq./kWh more than twice the size of the graphite-based alternatives. Since the battery components are apart from the anodes identical, the benefits from the reduced battery production are more than offset by the emissions from the production of the silicon anode, which at 0.31 kg CO₂-eq./kWh are ca. six times higher than the impacts of the synthetic graphite anode production (0.05 kg CO₂-eq./kWh) and almost 16-fold those of the natural graphite anode production (0.02 kg CO₂-eq./kWh). The main contributor in the production process of the silicon anode is the PECVD process, causing 0.17 kg CO₂-eq./kWh due to the large amount of electricity required for the plasma generation. Thus, the PECVD process alone constitutes 55 % of the anode's production footprint. It is followed by the silane production and the off-gas treatment, accounting for 35 % and 6 % of the anode production footprint, respectively (cf. Fig. B.2). In contrast to the silicon-based product system, the main contributor to the climate change impacts of both graphite-based LIBs is the battery cell apart from the anode, causing 0.14 kg CO₂-eq./kWh in both product systems (Fig. 3.9). Because the two batteries are identical except for their negative active material, their associated environmental impacts are the same in all life cycle stages other than the production of synthetic and natural graphite. In the climate change category, the impacts of the synthetic graphite are at 0.044 kg CO₂-eq./kWh approximately 2.6 times higher than that of natural graphite due to the energy-intensive graphitisation step.

Altogether, the outcomes of the economic flow analysis align with the characterisation and contribution results, since they identify the anode production process as the main reason for the differences in environmental performance between the three product systems. Moreover, they highlight the

3. Results

significantly higher electricity consumption during the production process of the silicon anode. Nevertheless, in addition to the previous analyses, the economic flow analysis reveals that the underlying reason for the higher electricity consumption during the silicon anode production is primarily caused by the PECVD process and the silane production.

3.2.3. Scenarios

To evaluate how different production efficiencies and battery performances affect the environmental performance of the LIB with a silicon anode, this study analyses four scenarios regarding the anode production process and characteristics of the silicon-based battery. Appendix B.2.2 provides the data corresponding to the results presented in this chapter. In the hydrogen reuse scenario, a part of the hydrogen that is released from the silane during the deposition of the silicon on the copper foil in the PECVD process is reused to start off the reaction. However, since the required amount of hydrogen is relatively small, its reuse decreases the impacts of the silicon anode production only marginally across all categories. The highest reduction is observable in freshwater ecotoxicity with just 0.9 % (cf. Table B.12). As a consequence, the environmental benefits from reusing the hydrogen are insignificant in comparison to the environmental impacts of the anode production processes. Hence, the relative environmental performances of the three anodes and thus batteries are not affected by the reuse of hydrogen in any impact category.

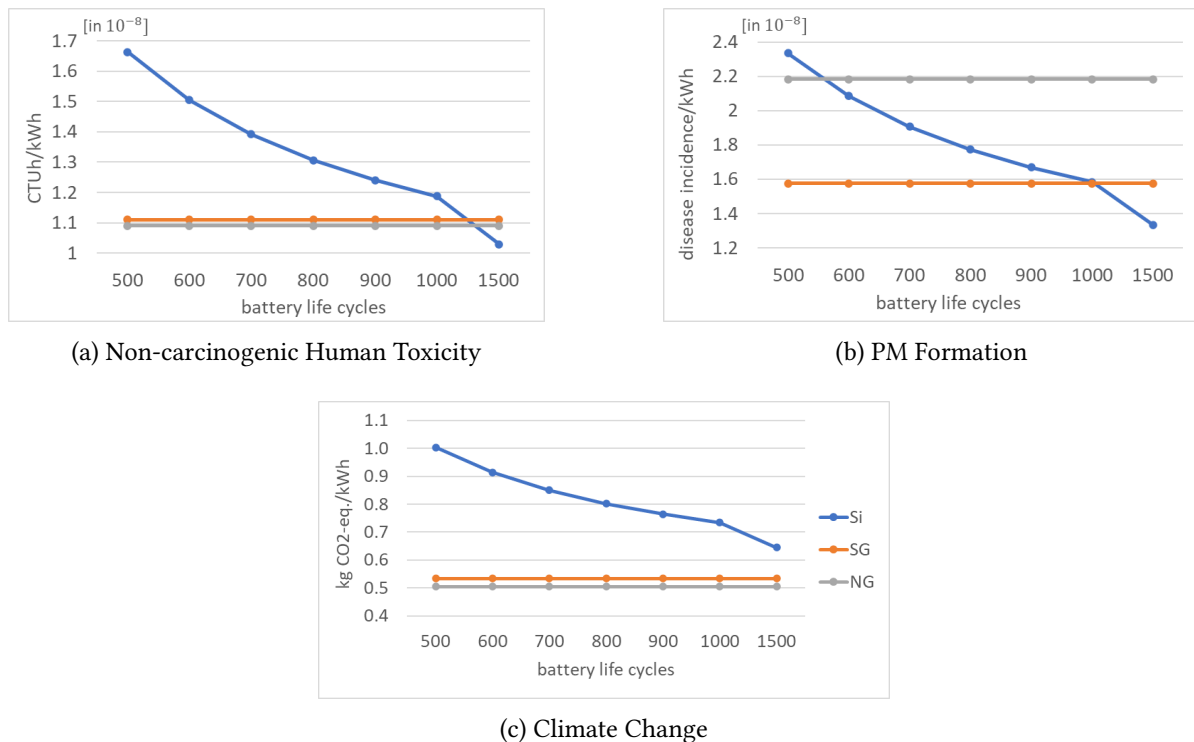


Figure 3.10.: Environmental Impacts of 1 kWh Delivered Energy by a Battery Containing a Silicon Anode (blue) with Changing Cycle Life for Three Categories; For reference, the environmental impacts of 1 kWh energy delivered by LIBs with natural (grey) and synthetic (orange) graphite anodes with a fixed cycle life of 1,000 cycles are included.

The life cycle scenario analyses the effect of different battery lifetimes between 500 and 1500 cycles on the environmental impacts caused by the silicon-based LIB over its entire life cycle, as a longer lifetime implies that a lower quantity of the battery is required to deliver the same amount of energy. Based on the results, three groups of impact categories can be derived, which are illustrated in Figure 3.10 using representative examples. To the first group belong those categories where the silicon-based battery

3. Results

already outperforms at least one of the graphite-based LIBs in the base case scenario at 800 cycles. Thus, the group contains PM formation, shown in Figure 3.10b, and material resources. The results of the life cycle scenario reveal that in the category of material resources, the silicon-based LIB breaks even with both graphite-based alternatives at ca. 700 cycles (Fig. B.4c). For PM formation, the break-even points of the battery with a silicon anode are at around 550 cycles with natural graphite and 1000 cycles with synthetic graphite (Fig. 3.10b). The second group includes the categories in which the silicon-based LIB only breaks even with at least one of the other two batteries at lifetimes between 801 and 1500 cycles. Hence, in these categories, the silicon-based battery performs worse than the graphite ones in the base case scenario. The group only consists of carcinogenic and non-carcinogenic human toxicity, with the latter being displayed in Figure 3.10a. In both categories, the break-even points are at lifetimes close to 1500 cycles. However, in case of carcinogenic human toxicity, the silicon-based LIB only breaks even with the LIB containing a synthetic graphite anode, but not with the one with a natural graphite anode (Fig. B.3h). Finally, the third group encompasses all categories in which the silicon-based product system does not break even with any of the graphite-based batteries, not even at 1500 cycles. The group is represented by climate change in Figure 3.10c and includes the majority of the impact categories (see Fig. B.3 and B.4). Thus, even with a lifetime of 1500 cycles, the product system of the silicon anode performs worse than the two graphite-based alternatives in most impact categories. Nevertheless, its impacts decrease with an increasing lifetime in all categories, even though they decrease at a diminishing rate. Furthermore, the difference in the performance of the silicon-based LIB between the groups can be explained by the contributing processes. While the necessary amount of battery and thus the copper quantity decrease with an increasing lifetime, the electricity consumption during the use phase, which is higher in the silicon-based product system, remains constant. Therefore, the effects of a longer battery lifetime are more pronounced in the first and second group, since material resources and human toxicity are primarily driven by the production of copper, whereas the main contributor of the impact categories in the third group is electricity.

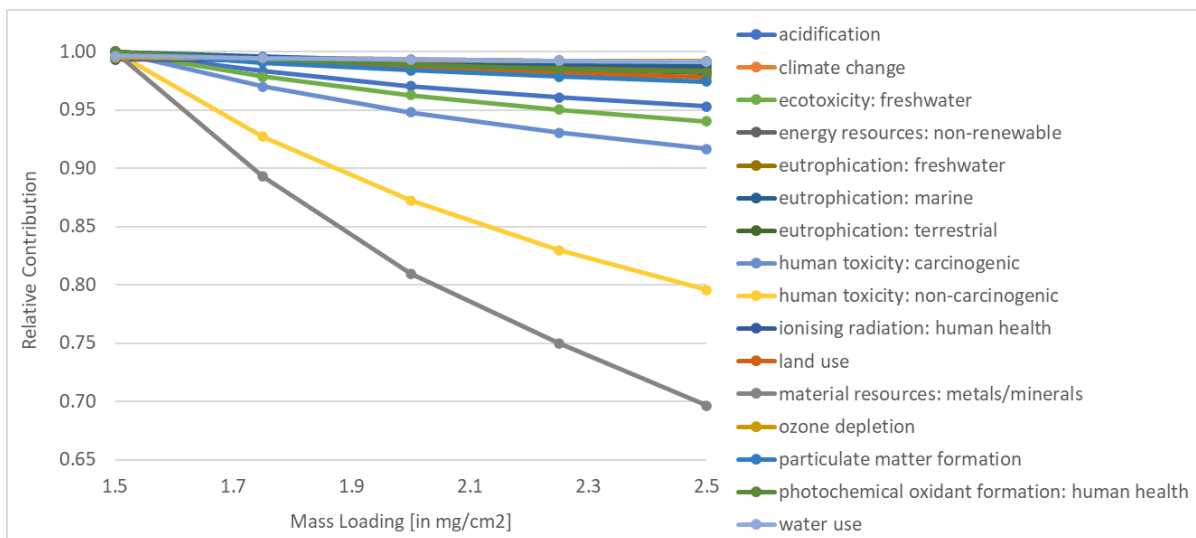


Figure 3.11.: Relative Environmental Impacts of 1 kWh Activated Silicon Anode with Changing Mass Loading; Values are scaled relative to the largest impact per category.

The third and fourth scenario assess the influence of the silicon anode's mass loading (ML) (Fig. 3.11) and the utilisation of silane during the PECVD process (Fig. 3.12) on the environmental production footprint of the silicon anode. In both scenarios, the environmental impacts decrease in all categories at a diminishing rate when the parameter increases, similar to the life cycle scenario. Moreover, the impacts of the categories decrease at different rates. Since ML defines the thickness of the active material on the current collector, i.e. the silicon on the copper foil, a higher ML implies that for 1 kWh

3. Results

of activated silicon anode less copper foil is required, whereas the amount of silicon stays the same. Consequently, the impacts that are driven more by copper production decrease at higher rates, with material resources and non-carcinogenic human toxicity showing the greatest change of ca. 30.4 % and 25.7 %, respectively, when comparing silicon anodes with ML of 1.5 mg/cm² and 2.5 mg/cm². On the other hand, impacts that are primarily influenced by the electricity consumption of the production process, especially the PECVD, decrease at lower rates. Hence, the smallest changes in impacts at 0.5 % are observable in climate change and water use (Fig. 3.11). In contrast to mass loading, silicon utilisation increases the production efficiency of the silicon anode, while keeping the composition of the anode, including the copper foil, constant. More specifically, a higher utilisation of silicon increases the efficiency of the PECVD process, lowering both the amount of necessary inputs, like silane, electricity, and emissions, i.e. off-gases. Accordingly, the impacts in categories, such as climate change, water use, ozone depletion, and ionising radiation, decrease by almost 50 %, whereas material resources and non-carcinogenic human toxicity show only a reduction in impacts of 19.7 % and 33.0 %, respectively, when the silane utilisation is increased from 15 % to 30 % (Fig. 3.12). Therefore, ML and silane utilisation have complementary effects, as the impact categories that are less reduced by increasing one parameter see a greater reduction when the other parameter is increased. Still, even with the highest ML and silane utilisation, the environmental impacts of the silicon anode remain higher than those of the graphite anodes (cf. Table B.9 and B.10). Hence, in most scenarios, including the reuse of hydrogen and battery lifetime, the silicon-based product system performs environmentally worse than the graphite alternatives, even with best case assumptions. However, each production efficiency and battery performance parameter was analysed individually. Based on the decreasing impacts at diminishing rates in the life cycle, ML, and silane utilisation scenario and the complementary effects of ML and silane utilisation, the improvement of more than one parameter seems promising.

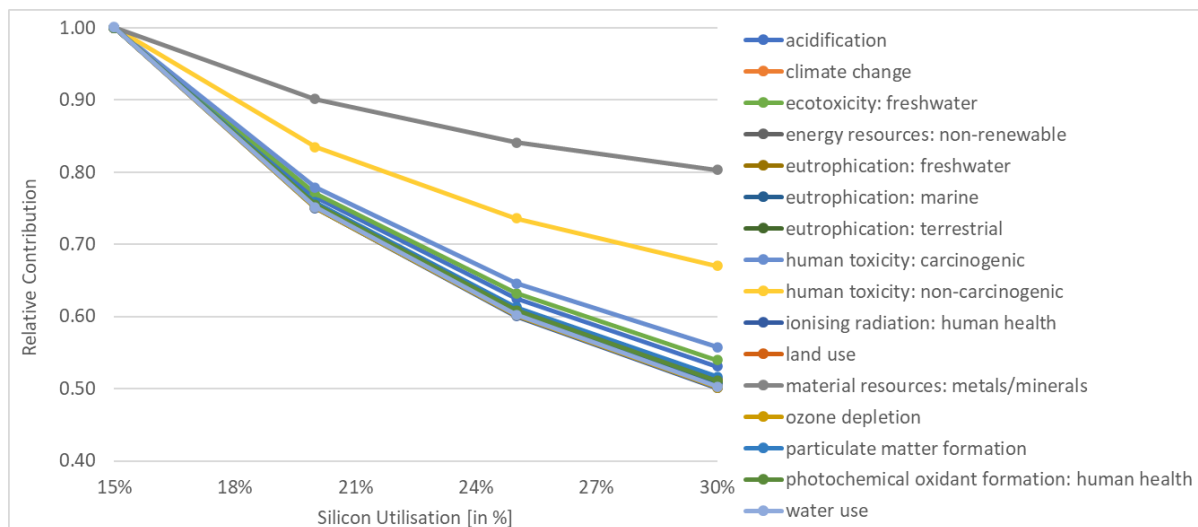


Figure 3.12.: Relative Environmental Impacts of 1 kWh Activated Silicon Anode with Changing Silane Utilisation; Values are scaled relative to the largest impact per category.

4. Discussion

With the upcoming market entry of silicon anodes in LIBs, there is a growing concern about their sustainability. However, due to their novelty, existing literature on the environmental impacts of silicon anodes relies exclusively on laboratory data about their production process and performance. Moreover, since silicon anodes are not commercialised yet, there are no established manufacturing sites. Yet, despite their significant influence on the environmental performance, there are no rigorous analyses regarding suitable production locations, and instead literature assumes predetermined locations. Therefore, this study first performed a location search, which identified Europe as the optimal production location for a pure silicon anode manufacturer. Subsequently, an LCA was conducted to compare the life cycle environmental impacts of a pure hydrogenated amorphous silicon thin film anode with the current market standard of natural and synthetic graphite anodes in a LIB with an LCO cathode. The findings of the LCA indicate that, due to the differences in the anode production processes, batteries with a natural graphite anode, followed by those with a synthetic graphite anode, are environmentally less impactful than batteries with a silicon anode, independent of the functional unit (kg vs. kWh) and scope (cradle-to-gate vs. cradle-to-grave) of the analysis. Thus, despite its higher energy density, the LIB with a silicon anode performs environmentally worse than its graphite-based counterparts in almost all impact categories.

This result is in line with most previous studies [62–64, 66, 67], who found that the emissions occurring during the production of the silicon anode exceed the environmental benefits owing to its higher energy density. Moreover, like Li *et al.* [62], Hendrickx *et al.* [63], and Wu & Kong [66], this analysis found that the main contributor in the graphite-based product systems is the copper production, whereas the impacts of the silicon anode are primarily caused by the electricity consumed during the preparation of the anode and its silicon precursor. However, contrarily to existing literature, the differences in the impacts between the product systems of the silicon and the graphite anodes seem to be greater. In this study, the production of 1 kg silicon anode causes 168.98 kg CO₂-eq./kg, while the production processes of the natural and synthetic graphite anodes emit 8.78 kg CO₂-eq./kg and 22.54 kg CO₂-eq./kg, respectively. Considering the differences in allocation and that these emissions account for the whole anode including the current collector, the impacts of the graphite anodes are similar to the results of Carrère *et al.* [98] and Engels *et al.* [118], who derived impacts of 9.62 kg CO₂-eq./kg and 42.2 kg CO₂-eq./kg for the production of natural and synthetic graphite, respectively. Yet, according to the results of Hendrickx *et al.* [63], who compared a sintered silicon anode with a graphite anode, the climate change impacts of the three anodes are significantly lower, suggesting that the production of a graphite anode causes 5.82 kg CO₂-eq./kg and the one of a silicon anode causes 47.6 kg CO₂-eq./kg. Although the study by Wu & Kong [66], who analysed a silicon nanowire anode, derived impacts that are more comparable with the ones of this study, the differences in the impacts of the anodes remain smaller, since the study found that the silicon and graphite anodes have a production footprint of approximately 130 kg CO₂-eq./kg and 10 kg CO₂-eq./kg, respectively. This difference is still visible on the battery level, as the same study indicates that the production of 1 kWh NMC battery with a silicon nanowire anode emits 222.13 kg CO₂-eq./kWh and the one with a graphite anode produces 168.68 kg CO₂-eq./kWh, as opposed to 382.05 kg CO₂-eq./kWh and 146.89 kg CO₂-eq./kWh or 123.58 kg CO₂-eq./kWh in this study for the silicon, synthetic graphite, and natural graphite anode product systems, respectively.

Contrarily to the aforementioned studies, Deng *et al.* [65] found that the impacts of an NMC LIB with

a silicon nanotube anode are comparable with the ones of a graphite-based LIB. Nevertheless, this result is still in line with the study of Wu & Kong [66], as an analysis by Wang *et al.* [73] discovered that the production impacts of an NMC battery with a silicon nanowire anode are higher than the ones of an NMC battery with a silicon nanotube anode. Likewise, the findings of Accardo *et al.* [67] imply that, from an environmental perspective, an NMC battery with a silicon nanowire anode performs significantly worse than the graphite benchmark, whereas one with a micro-structured silicon anode (SiCPAN) has impacts similar to the benchmark. Furthermore, a study by Kallitsis *et al.* [64], who compared different types of NMC LIBs with graphite and silicon-graphite composite anodes, shows that batteries containing silicon in their anodes are only associated with higher environmental impacts when compared on a per battery pack basis. When the batteries are instead compared on a kWh basis, the results are reversed. Thus, while the majority of studies suggest that batteries with a silicon anode cause higher environmental emissions than the current market standard, some studies find contradicting results indicating that the two battery types have comparable environmental impacts.

The contradicting results between the existing literature and the present study can be explained by the differences in the types of batteries and the scopes of the analyses. First and foremost, the silicon anodes compared are not the same, differing in composition, production process, and performance. For example, while this study examined the environmental impacts of a pure amorphous silicon thin film anode with a gravimetric capacity of 1,500 mAh/g that is produced in a PECVD process using silane, Deng *et al.* [65] investigated the impacts of a silicon nanotube anode manufactured via the synthesis of silica with an assumed capacity of 2,000 mAh/g. Li *et al.* [62] and Wu & Kong [66] even assumed a gravimetric capacity of 2,400 mAh/g for the silicon nanowire anode produced via metal-assisted chemical leaching of silicon powder in their studies. In addition, the benchmark anodes containing graphite vary between the studies, of which the majority does not further specify the type of graphite [59, 62, 65–67]. For instance, in contrast to the present analysis, which uses primary data provided by Carrère *et al.* [98] and Engels *et al.* [118] to model the production of both graphite types, Hendrickx *et al.* [63] and Kallitsis *et al.* [64] adapted the corresponding Ecoinvent process, significantly underestimating the impacts of graphite production according to Engels *et al.* [118]. Besides the anodes, the batteries differ in cathode material and scope based on the application assumed in the use phase. While most existing studies model an NMC battery pack that is used in an EV [59, 62, 64, 65, 67, 71], this study analyses an LCO battery cell for consumer electronics. Furthermore, the varying geographical scopes of these studies, concerning the locations of production, use, and EOL phases, significantly influence the results, given the considerable electricity consumption during the production and use phase. Finally, unlike most of the existing LCAs, which employ the ReCiPe characterisation method [59, 63–66, 71, 73], this analysis uses the PEF methodology to calculate the environmental impacts.

Although the present study is the first to use industrial primary data for the silicon anode manufacturing process, the analysis includes some limitations and uncertainties given the early development stage of the technology. Because the most probable production location of silicon anodes is still unclear, this study conducted a location search using indicators that consider the general nature and interests of scale-up businesses. However, a different set of indicators would most likely change the outcomes of the location study, especially since some indicators are based on each other, partially explaining the correlations among them. For instance, the *TBI* includes the *IP protection* indicator, which in turn contains the indicator of *political stability*. Thus, if a country or region has a high *political stability*, there is an increased chance that it scores well in *IP protection* and *TBI*. Nevertheless, a good performance in one indicator does not necessarily imply a good score in another, since all indicators based on datasets are composite indices, consisting of more than one individual sub-indicator. The *TBI* and *IP protection* indicators for example consist of 12 and 24 sub-indicators, respectively. Hence, to perform well in the composite indices, a location needs to perform well in several of its sub-indicators.

Another limitation of the indicator analysis arises from aggregating the countries to regions using

the mean. By comparing the regional averages, positive outliers, meaning countries that score well in poorly performing regions, are excluded. Examples of such countries are Singapore in South Asia and New Zealand in Oceania, which have one of the best scores in *ease of doing business* and *political stability* globally, but were excluded due to the overall poor performance of their regions (see Figure C.1 in the appendix). On the other hand, countries that perform poorly are not excluded if they are in a well-performing region. To mitigate this problem of the outliers, the results of the regional comparison based on the mean were verified by a regional comparison based on the median, which confirmed the previous findings. Nevertheless, since the comparison was still done on the regional level and the median is, like the mean, a measure of central tendency, the problem remains. Moreover, a similar problem occurs during the comparison of the environmental impacts associated with the silicon anode production at a certain location, since the impacts are calculated assuming the regional grid mix for the electricity supply. However, an analysis by Kallitsis *et al.* [48] shows that important battery manufacturing locations in Europe and North America, like Poland and Kentucky, result in comparable or even higher carbon emissions as some Chinese provinces, including Hubei and Qinghai. Thus, producing in a region whose electricity grid mix causes low environmental impacts does not necessarily imply that the country's grid has similarly low impacts, nor the other way around.

Given the relevance of electricity in the production process of the silicon anode, this study performed a sensitivity analysis testing the robustness of the comparative LCA results when the electricity consumption during the silicon anode's production process is varied by $\pm 15\%$. As shown by Figure 4.1, all impact categories are affected by the variations in electricity consumption. The greatest change is observable in ionising radiation, closely followed by climate change, where a 1% increase in electricity consumed results in a 0.92% and 0.89% increase in the impacts of the categories, respectively. On the other hand, the impacts in material resources change the least among all categories, as a 1% increase in electricity consumption implies only a 0.21% increase in material resources. Hence, the categories whose impacts are primarily caused by electricity are more affected, whereas the categories whose impacts are less driven by electricity, like material resources, which is more influenced by the emissions of copper production, change less with a varying electricity consumption. Nevertheless, even with a 15% reduction in the electricity used during the production process, the silicon anode performs worse than the two graphite anodes in the majority of impact categories, as visible in Table C.2, which contains the absolute impact results.

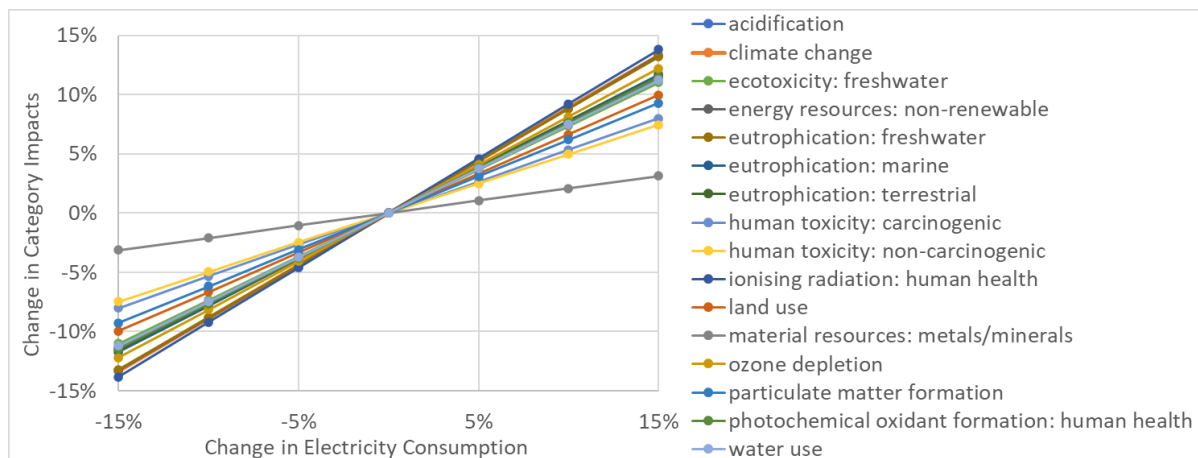


Figure 4.1.: Sensitivity Analysis of Electricity Consumption

Values are scaled relative to the base case results per category. FU: the production of 1 kWh activated silicon anode material.

The trend of graphite anodes being environmentally less impactful than silicon anodes still persists when the allocation method is changed. Following the ISO standards [100, 101], this study conducted a sensitivity analysis on the allocation method using a conservative allocation approach, which as-

4. Discussion

signs all burdens to the reference flows. The absolute impact results are displayed in Table C.1 in the appendix. In the majority of impact categories, the battery with a synthetic graphite anode shows the greatest increase in the environmental impacts, as its product system is the one with the most multi-functionalities. The impacts of the LIBs with a silicon and natural graphite anode on the other hand remain almost identical in all categories except for PM formation, since the impacts caused by the dust created during the mining of natural graphite and the purification of silica are fully allocated to the respective reference flows instead of the graphite fines and silica by-products. Nonetheless, as depicted by Figure 4.2, the choice of allocation method has no influence on the overall outcomes. Hence, the results of the comparative analysis prove to be robust when the allocation method is changed.

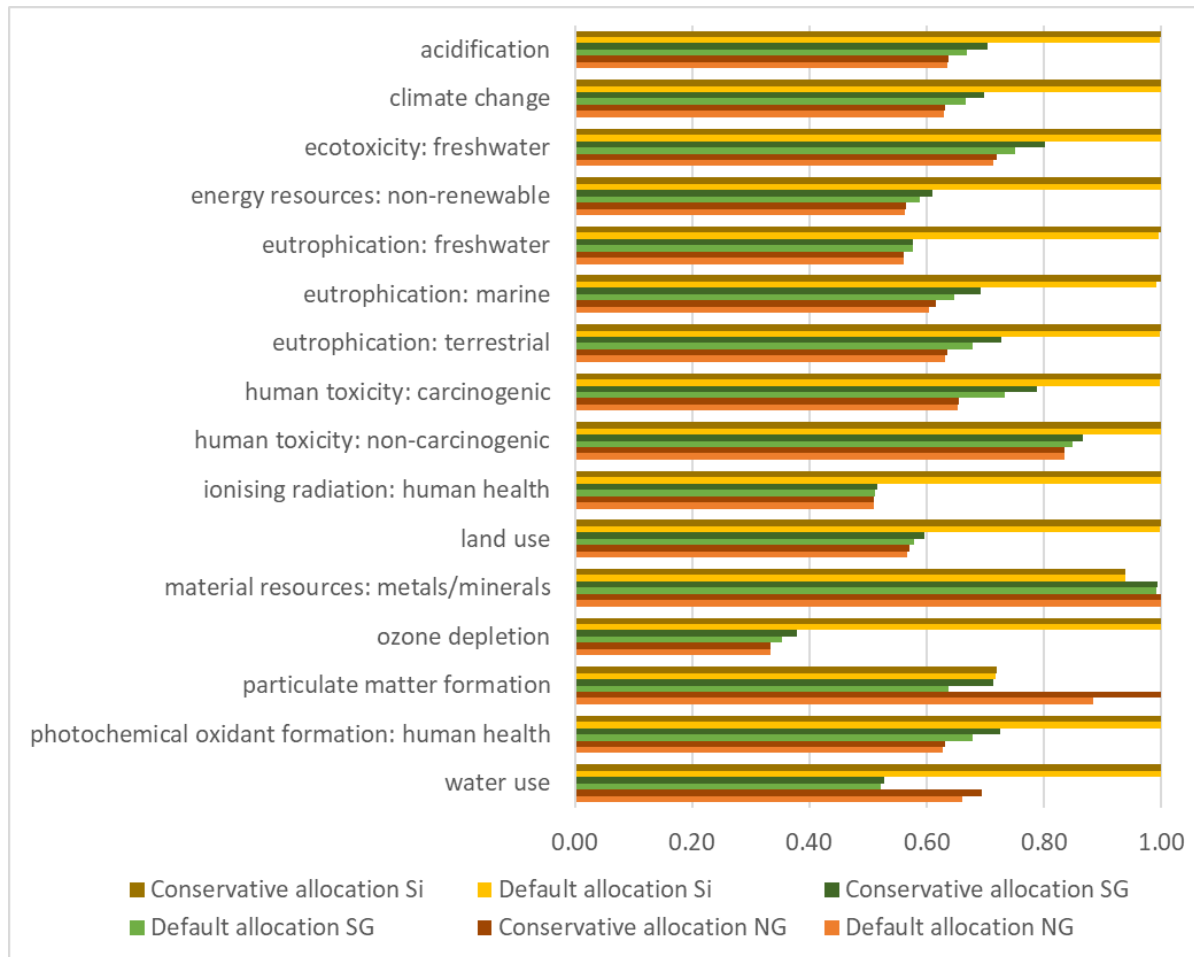


Figure 4.2.: Comparison of Category Impacts Between the Product Systems for two Allocation Methods; Values are scaled relative to the largest impact per category. FU: the delivery of 1 kWh stored energy.

To verify whether the assumptions and data underlying the three models are consistent between each other and with the goal and scope, a consistency check was performed. Given the similarity of the battery assembly, use phase, and EOL management, the consistency check is limited to the production of the anodes. The results, presented in Table C.3 in the appendix, indicate several inconsistencies between the models. Firstly, the technological coverage is not consistent between the three product systems, since natural and synthetic graphite anodes are a mature technology, whereas silicon anodes are emerging. However, as part of the study's objective is to compare the environmental impacts of silicon anodes as an upcoming technology before their commercialisation with the current market standard, this inconsistency between the product systems is still in line with the goal and scope of this study. Nevertheless, when comparing the impacts, it should be acknowledged that natural and synthetic graphite anodes are mass-produced, while the silicon anode production is on the level of

demonstration plants incurring lower production efficiencies. Secondly, there is a difference in the geographical coverage of the three anodes, because this study assumes that the silicon anodes are produced in Europe instead of China, which is the established production location for both graphite anodes. But, similar to the technological coverage, this inconsistency is still in accordance with the goal and scope, since Europe was identified as a suitable production location for silicon anode manufacturers as part of the study's objective. Finally, the inconsistency in data age can be explained by a discrepancy of data availability for the silicon and graphite anodes. Because graphite anodes are the current market standard with an established production route, there are many existing life cycle inventory analyses updating their production data. Conversely, the early development state of silicon anodes leads to a variety in types of the technology, differing in their production processes and precursor materials. As a consequence, there are only few studies about the production process of silane gas, which causes this study to rely on data from 1992 and 1995 [115, 116]. To reduce the discrepancy in data age, this study attempted to update the silane production data by increasing the efficiency of the silica purification to 85 % based on information from Phylipsen & Alsema [115]. Nevertheless, future research should close the gap by updating the data of silane production to improve the anodes' comparability.

Although the outcomes of this study indicate that silicon-based LIBs have a significantly worse environmental life cycle performance than the current market standard of graphite-based LIBs, silicon anodes should not be dismissed as a viable alternative to graphite anodes given their early development stage. First of all, since silicon anodes are an emerging technology with growing research interest [137], significant improvements in the anode's and thus battery's performance can be expected, including the cycle life and energy density [138–140]. In addition, as the existing battery value chain is optimised for graphite anodes, changes in the battery design and components regarding the cathode and electrolyte can further improve the performance, especially with the development of all solid-state LIBs, which solve the issue of continuous SEI formation [137, 141]. Considering the scenario results of the present study, these expectations imply a promising outlook for the environmental performance of silicon-based LIBs. Furthermore, this study excluded the electronic device from the analysis. However, batteries are nowadays often installed in such a way in their devices that they cannot be easily replaced [142]. Due to their higher energy density, silicon anodes have the potential to prolong the lifetime of CE devices by increasing the battery's energy capacity without increasing the size or weight of the battery and device. Hence, future studies should incorporate the electronic device in their analysis to identify the overall contribution of the silicon anode to the environmental impacts of CE devices and assess the effect of a higher energy density on the environmental performance of the whole device. Beyond CE, incorporating the device becomes especially important for applications of silicon-based LIBs in transportation, like EVs, as the higher energy density prolongs the EV's lifetime by increasing its driving range [27, 28]. Together with the anode's property to allow for fast charging [23], silicon-based LIBs can promote the acceptance of EVs and thus possibly reduce emissions directly and indirectly. Finally, since silicon anodes are not commercialised yet, no single-best type has emerged so far, resulting in a broad range of silicon anode technologies with varying production processes, precursor materials, and performance characteristics that are associated with significantly different environmental impacts [cf. 62–67]. Thus, at this point, silicon anodes should not be dismissed as a viable alternative to graphite anodes, as the developments of the anode regarding its preferred variant, technical improvements, and possible efficiency gains in an up-scaling production process are too uncertain. Instead, the author of this study recommends to continue research around silicon anodes and observe which variants can assert themselves on the market. Nevertheless, the development of silicon anodes should be critically monitored regarding their life cycle environmental impacts, taking into account their recyclability at the EOL. These impacts should be considered when selecting the single-best one in order to ensure that the new technology is preferable to the existing one.

5. Conclusions

The goal of this study is to evaluate the life cycle environmental impacts of a pure silicon anode, using industrial primary data, while considering the choice of production location, and to compare those with the life cycle environmental impacts of the current market standards, namely natural and synthetic graphite anodes. Accordingly, this study attempts to answer the following research question: *Depending on the optimal production location, what are the life-cycle environmental impacts of a lithium-ion battery with a pure silicon anode, and how does it compare to the market standard of synthetic and natural graphite-based lithium-ion batteries?*

The research question can be divided into three parts: the search for a suitable production location for pure silicon anodes, the calculation of its environmental footprint, and a comparison of its impacts to the ones of a synthetic and natural graphite anode. To answer the first part, this study adapted the SFA framework to determine the globally optimal location for a silicon anode manufacturer, taking into account the security of company-owned knowledge, ease of factory setup, stability of production and input supply, and the environmental production footprint. Based on the result, this analysis conducted a detailed, ex-ante, cradle-to-grave LCA using the PEF impact categories to answer the second and third part of the research question by calculating the life cycle environmental impacts of an LCO LIB with a silicon, synthetic graphite, and natural graphite anode. Moreover, hot-spot and sensitivity analyses were performed to identify the main contributors and test the robustness of the models.

The outcomes of the location study reveal that North America, Europe, and South Asia are adequate locations for silicon anode producers, as they allow scaling up a stable production under manageable risks. Among these regions, Europe was found to be the most acceptable location to stakeholders, since its electricity grid mix results in the lowest environmental, and especially carbon, footprint of the silicon anode, which influences the public acceptance and chance of success for subsidies and investments. The findings of the subsequent LCA indicate that, despite its higher energy density, the LIB with a silicon anode performs significantly worse than its graphite-based counterparts in almost all impact categories. For instance, although Europe was determined to be the most suitable production location due to its favourable energy mix, the climate change impacts of 1 kWh delivered energy by a LIB with a silicon anode produced in Europe are with 0.80 kg CO₂-eq./kWh still significantly higher than those of a LIB with a synthetic or natural graphite anode produced in China, causing 0.53 kg CO₂-eq./kWh and 0.51 kg CO₂-eq./kWh, respectively. The only exceptions are PM formation, because of the dust caused by the mining of natural graphite, and material resources, as the current collector of the silicon anode contains only recycled copper. Among the graphite-based alternatives, the LIB with a natural graphite anode outperforms the LIB with a synthetic graphite anode in the majority of categories.

The differences between the environmental impacts of the three battery types can mostly be explained by the differences in the anodes' compositions and production processes. Unlike the copper foil in the silicon anode, the current collector of the natural graphite anode consists of 85 % primary copper, resulting in comparably high impacts from copper mining and production. The impacts of the natural graphite anode are closely followed by the ones of the synthetic graphite anode, since the latter contains the same copper foil but has a higher electricity consumption during its production due to the energy-intensive graphitisation of needle coke in the electric Acheson furnace. Although the high energy density of the silicon anode reduces the amount of battery required to deliver a certain amount of energy, its environmental gains are more than offset by the considerable electricity consumption

5. Conclusions

of the anode's production process, which is mainly caused by the plasma generation in the PECVD process, contributing 55 % to the carbon production footprint of the silicon anode. Furthermore, due to the relevance of electricity, the environmental impacts of the three alternatives reflect the emissions associated with the grid mixes of the anodes' production locations. While China's electricity mix depends primarily on hard coal, driving the freshwater ecotoxicity impacts of the graphite anodes, Europe's electricity grid relies more on nuclear power and natural gas, causing the significantly higher impacts of the silicon anode in ozone depletion and ionising radiation. On the basis of the whole life cycle, the emissions and impacts of the three battery types converge, given the similarity of the use and EOL phases across the three product systems. Nevertheless, the ranking in terms of environmental performance remains identical, even in different battery performance and production efficiency scenarios. Moreover, the comparative results prove to be robust with respect to the allocation method and the electricity consumption during the silicon anode production process. Therefore, to answer the main research question, the outcomes of the LCA indicate that, independent of the scope and functional unit of the analysis, a battery with a silicon anode produced in Europe is environmentally more impactful than its graphite based counterparts from China in the majority of impact categories, despite its higher energy density.

However, given the early development stage of silicon anodes, the results of this study must be interpreted with caution. Since silicon anodes are not an established technology, only few studies about their production process and the associated environmental impacts exist. In addition, no single-best type of silicon anode has emerged so far, as the anode is not on the market yet where it could have proven itself, resulting in a variety of types and production processes of silicon anodes. Hence, it is difficult to find recent data on the production of the anode and its precursor materials. As a consequence, this study relies on data from 1995 for the production process of silane gas. Furthermore, as opposed to its graphite-based alternatives, silicon anodes are not on mass-production scale, resulting in lower production efficiencies. However, the findings of the scenario analysis regarding different levels of silane utilisation indicate that small improvements at the beginning can have considerable effects on the environmental impacts caused by the production process, especially when coupled with improvements in the battery performance. Therefore, the author recommends that future research should update the data of both the production processes of the input materials, including especially the preparation of silicon and silane, and the manufacturing process of the silicon anode, after its market entry. Furthermore, based on the results of the scenario analysis, the author encourages silicon anode producers to rather improve several of their production and performance parameters of the anode a little than to focus on one parameter individually.

List of Figures

1.1.	Data network of LCI data for silicon anodes, their sources and their further usage in different publications	8
2.1.	Research Flow Diagram of the Adapted SFA Framework	10
2.2.	World Map Partitioned into Regions	11
2.3.	LCA Framework According to the ISO 14040 [100] and ISO 14044 [101] Standards . . .	13
2.4.	Connecting the Life Cycle Stages of the Three Battery Systems to the Geographical Scope of the Comparative LCA. The icon for graphite (Gr) represents both types, synthetic and natural graphite. The silane gas and silicon (Si) anode are produced in Europe, which is the optimal production location for silicon anode manufacturers according to the outcome of the location study. The purple arrows indicate the transport of products.	14
2.5.	Flowchart LCO Battery with Silicon Anode	18
2.6.	Flowchart LCO Battery with Natural Graphite Anode	19
2.7.	Flowchart LCO Battery with Synthetic Graphite Anode	20
3.1.	The Ease of Doing Business, Political Stability, IP Protection, Trade Barrier Index, and Global Peace Index for All Countries and the Respective Distribution per Region . . .	28
3.2.	Silane Producer Map	29
3.3.	Regional Environmental Footprint of a LIB with a Silicon Anode	30
3.4.	Correlation Between the Carbon Footprint of a Region's Electricity Grid Mix and the Production Footprint of a Silicon Anode. 100 % wind energy is sourced from Switzerland (CH).	31
3.5.	Relative Cradle-to-Grave Impact of the PEF Impact Categories for 1 kWh Delivered Energy of LIBs with a Silicon (Si), Natural Graphite (NG), and Synthetic Graphite (SG) Anode	32
3.6.	Relative Cradle-to-Gate Impact of the PEF Impact Categories for 1 kWh Activated Silicon (Si), Natural Graphite (NG), and Synthetic Graphite (SG) Anode	34
3.7.	Categorised Process Contributions to Cradle-to-grave Environmental Impacts of All Three Product Systems	36
3.8.	Categorised Process Contributions to Cradle-to-gate Environmental Impacts of All Three Product Systems	37
3.9.	Absolute Contribution of Life Cycle Stages to Climate Change Impacts	39
3.10.	Environmental Impacts of 1 kWh Delivered Energy by a Battery Containing a Silicon Anode (blue) with Changing Cycle Life for Three Categories; For reference, the environmental impacts of 1 kWh energy delivered by LIBs with natural (grey) and synthetic (orange) graphite anodes with a fixed cycle life of 1,000 cycles are included.	40
3.11.	Relative Environmental Impacts of 1 kWh Activated Silicon Anode with Changing Mass Loading	41
3.12.	Relative Environmental Impacts of 1 kWh Activated Silicon Anode with Changing Silane Utilisation	42
4.1.	Sensitivity Analysis of Electricity Consumption	45
4.2.	Comparison of Category Impacts Between the Product Systems for two Allocation Methods	46

A.1. 18650 Lithium-Ion Battery Cell with LCO Cathode	61
B.1. Electricity Mix by Region in 2020	69
B.2. Relative Contribution of Life Cycle Stages to Climate Change Impacts	75
B.3. Environmental Impacts of 1 kWh Activated Silicon Anode with Changing Cycle Life per Category	80
B.4. Environmental Impacts of 1 kWh Activated Silicon Anode with Changing Cycle Life per Category – Continued	81
C.1. Ease of Doing Business Score and Political Stability Performance of all Countries In- dividually	82

List of Tables

2.1.	The SFA Strategy Framework by Related Criteria	11
2.2.	Quantitative Indicators from Publicly Available Data Sets	12
2.3.	Technical Properties and Geographical Coverage of the Reference Batteries	15
3.1.	Average Performance of Each Region per Quantitative Indicator	28
A.1.	Bill of Material of Modelled Battery Types	62
A.2.	Details of the Scenario Parameters	63
B.1.	Median Performance of Each Region per Quantitative Indicator	64
B.2.	Silane Supplier	65
B.3.	Environmental Impacts of PEF Impact Categories for Reference Flows of the Location Study	68
B.4.	Cradle-to-Grave Environmental Impact of the PEF Impact Categories for 1 kWh Delivered Energy of LIBs with a Silicon (Si), Natural Graphite (NG), and Synthetic Graphite (SG) Anode	70
B.5.	Cradle-to-Gate Environmental Impact of the PEF Impact Categories for 1 kWh Activated Silicon (Si), Natural Graphite (NG), and Synthetic Graphite (SG) Anode	71
B.6.	Cradle-to-Gate Environmental Impact of the PEF Impact Categories for 1 kg Activated Silicon (Si), Natural Graphite (NG), and Synthetic Graphite (SG) Anode	72
B.7.	Cradle-to-Gate Environmental Impact of the PEF Impact Categories for 1 kWh LCO LIB cell with a Silicon (Si), Natural Graphite (NG), and Synthetic Graphite (SG) Anode	73
B.8.	Cradle-to-Gate Environmental Impact of the PEF Impact Categories for 1 kg LCO LIB cell with a Silicon (Si), Natural Graphite (NG), and Synthetic Graphite (SG) Anode	74
B.9.	Cradle-to-Gate Environmental Impact of the PEF Impact Categories for 1 kWh Activated Silicon (Si) Anode with Different Mass Loading (ML) Scenarios	76
B.10.	Cradle-to-Gate Environmental Impact of the PEF Impact Categories for 1 kWh Activated Silicon (Si) Anode with Different Silicon Utilisation Scenarios	77
B.11.	Cradle-to-Grave Environmental Impact of the PEF Impact Categories for 1 kWh Delivered Energy of a Silicon-based LIB with Different Cycle Life Scenarios	78
B.12.	Cradle-to-Gate Environmental Impact of the PEF Impact Categories for 1 kWh Activated Silicon (Si), Natural Graphite (NG), and Synthetic Graphite (SG) Anode Compared to the Hydrogen Reuse Scenario	79
C.1.	Cradle-to-Grave Impacts of the Three Product Systems with Conservative Allocation	84
C.2.	Cradle-to-Gate Environmental Impact of the PEF Impact Categories for 1 kWh Activated Silicon (Si) Anode with Variations in Electricity Consumption ($\pm 15\%$)	85
C.3.	Results of the Consistency Check Regarding the Anode Production Processes	86

Bibliography

1. United Nations. Paris Agreement. https://unfccc.int/sites/default/files/english_paris_agreement.pdf (2015).
2. Climate Watch. *World Greenhouse Gas Emissions by Sector 2021 (Sunburst chart)* <https://www.wri.org/data/world-greenhouse-gas-emissions-sector-2021-sunburst-chart>. Last visited Dec. 17, 2024. (2024).
3. IEA. *Greenhouse Gas Emissions from Energy* <https://www.iea.org/data-and-statistics/data-product/greenhouse-gas-emissions-from-energy#data-sets>. Last visited Dec. 17, 2024. (2024).
4. Masson-Delmotte, V. *et al. Global Warming of 1.5 C: IPCC special report on impacts of global warming of 1.5 C above pre-industrial levels in context of strengthening response to climate change, sustainable development, and efforts to eradicate poverty* (Cambridge University Press, 2022).
5. Lutsey, N. Global climate change mitigation potential from a transition to electric vehicles. *The International Council on Clean Transportation* **2015**, 5 (2015).
6. Verma, S., Dwivedi, G. & Verma, P. Life cycle assessment of electric vehicles in comparison to combustion engine vehicles: A review. *Materials Today: Proceedings* **49**, 217–222 (2022).
7. Chu, S. & Majumdar, A. Opportunities and challenges for a sustainable energy future. *nature* **488**, 294–303 (2012).
8. Holechek, J. L., Geli, H. M., Sawalhah, M. N. & Valdez, R. A global assessment: can renewable energy replace fossil fuels by 2050? *Sustainability* **14**, 4792 (2022).
9. Nzereogu, P., Omah, A., Ezema, F., Iwuoha, E. & Nwanya, A. Anode materials for lithium-ion batteries: A review. *Applied Surface Science Advances* **9**, 100233 (2022).
10. Leonard, M. D., Michaelides, E. E. & Michaelides, D. N. Energy storage needs for the substitution of fossil fuel power plants with renewables. *Renewable Energy* **145**, 951–962 (2020).
11. Belderbos, A., Virag, A., D’haeseleer, W. & Delarue, E. Considerations on the need for electricity storage requirements: Power versus energy. *Energy Conversion and Management* **143**, 137–149 (2017).
12. Bresser, D., Moretti, A., Varzi, A. & Passerini, S. The role of batteries for the successful transition to renewable energy sources. *Encyclopedia of Electrochemistry: Batteries*, 3–11 (2020).
13. World Economic Forum and Global Battery Alliance. *A vision for a sustainable battery value chain in 2030: Unlocking the full potential to power sustainable development and climate change mitigation* in (Geneva, Switzerland, 2019).
14. IEA. *Batteries and Secure Energy Transitions* <https://www.iea.org/reports/batteries-and-secure-energy-transitions>. Last visited Dec. 18, 2024. (2024).
15. Volta, A. XVII. On the electricity excited by the mere contact of conducting substances of different kinds. In a letter from Mr. Alexander Volta, FRS Professor of Natural Philosophy in the University of Pavia, to the Rt. Hon. Sir Joseph Banks, Bart. KBPR S. *Philosophical transactions of the Royal Society of London*, 403–431 (1800).
16. Planté, G. Note sur la polarisation voltaïque. *Comptes Rendus* **49**, 402–405 (1859).
17. Scrosati, B. History of lithium batteries. *Journal of solid state electrochemistry* **15**, 1623–1630 (2011).
18. Dell, R. Batteries: fifty years of materials development. *Solid State Ionics* **134**, 139–158 (2000).
19. Wulandari, T., Fawcett, D., Majumder, S. B. & Poinern, G. E. Lithium-based batteries, history, current status, challenges, and future perspectives. *Battery Energy* **2**, 20230030 (2023).

Bibliography

20. Ko, M., Chae, S. & Cho, J. Challenges in accommodating volume change of Si anodes for Li-ion batteries. *ChemElectroChem* **2**, 1645–1651 (2015).
21. Wu, F., Maier, J. & Yu, Y. Guidelines and trends for next-generation rechargeable lithium and lithium-ion batteries. *Chemical Society Reviews* **49**, 1569–1614 (2020).
22. Arabkoohsar, A. in *Mechanical Energy Storage Technologies* 1–12 (Academic Press, 2020).
23. Du, C. *et al.* The status of representative anode materials for lithium-ion batteries. *The Chemical Record* **23**, e202300004 (2023).
24. Zhang, H., Yang, Y., Ren, D., Wang, L. & He, X. Graphite as anode materials: Fundamental mechanism, recent progress and advances. *Energy Storage Materials* **36**, 147–170 (2021).
25. European Commission, Joint Research Centre, Tarvydas, D., Tsiropoulos, I. & Lebedeva, N. *Li-ion batteries for mobility and stationary storage applications – Scenarios for costs and market growth* (Publications Office, 2018).
26. Masias, A., Marcicki, J. & Paxton, W. A. Opportunities and challenges of lithium ion batteries in automotive applications. *ACS energy letters* **6**, 621–630 (2021).
27. Xu, J. *et al.* High-energy lithium-ion batteries: recent progress and a promising future in applications. *Energy & Environmental Materials* **6**, e12450 (2023).
28. Feng, K. *et al.* Silicon-based anodes for lithium-ion batteries: from fundamentals to practical applications. *Small* **14**, 1702737 (2018).
29. ADAC. *Elektroautos im Test: So hoch ist die Reichweite wirklich* <https://www.adac.de/rund-ums-fahrzeug/elektromobilitaet/elektroauto/stromverbrauch-elektroautos-adac-test/>. Last visited Dec. 18, 2024. (2024).
30. Schmuch, R., Wagner, R., Hörpel, G., Placke, T. & Winter, M. Performance and cost of materials for lithium-based rechargeable automotive batteries. *Nature energy* **3**, 267–278 (2018).
31. Liang, Y. *et al.* A review of rechargeable batteries for portable electronic devices. *InfoMat* **1**, 6–32 (2019).
32. Glazier, S., Li, J., Louli, A., Allen, J. & Dahn, J. An analysis of artificial and natural graphite in lithium ion pouch cells using ultra-high precision coulometry, isothermal microcalorimetry, gas evolution, long term cycling and pressure measurements. *Journal of The Electrochemical Society* **164**, A3545 (2017).
33. Philippot, M., Alvarez, G., Ayerbe, E., Van Mierlo, J. & Messagie, M. Eco-efficiency of a lithium-ion battery for electric vehicles: Influence of manufacturing country and commodity prices on ghg emissions and costs. *Batteries* **5**, 23 (2019).
34. Andre, D. *et al.* Future generations of cathode materials: an automotive industry perspective. *Journal of Materials Chemistry A* **3**, 6709–6732 (2015).
35. Zuo, X., Zhu, J., Müller-Buschbaum, P. & Cheng, Y.-J. Silicon based lithium-ion battery anodes: A chronicle perspective review. *Nano Energy* **31**, 113–143 (2017).
36. Blomgren, G. E. The development and future of lithium ion batteries. *Journal of The Electrochemical Society* **164**, A5019 (2016).
37. Chae, S., Choi, S.-H., Kim, N., Sung, J. & Cho, J. Integration of graphite and silicon anodes for the commercialization of high-energy lithium-ion batteries. *Angewandte Chemie International Edition* **59**, 110–135 (2020).
38. Zhu, B., Wang, X., Yao, P., Li, J. & Zhu, J. Towards high energy density lithium battery anodes: silicon and lithium. *Chemical science* **10**, 7132–7148 (2019).
39. He, S. *et al.* Considering critical factors of silicon/graphite anode materials for practical high-energy lithium-ion battery applications. *Energy & Fuels* **35**, 944–964 (2020).
40. Chae, S., Choi, S.-H., Kim, N., Sung, J. & Cho, J. Integration of graphite and silicon anodes for the commercialization of high-energy lithium-ion batteries. *Angewandte Chemie International Edition* **59**, 110–135 (2019).
41. Van Mierlo, J. *et al.* Beyond the state of the art of electric vehicles: A fact-based paper of the current and prospective electric vehicle technologies. *World Electric Vehicle Journal* **12**, 20 (2021).

Bibliography

42. Yim, C.-H., Niketic, S., Salem, N., Naboka, O. & Abu-Lebdeh, Y. Towards improving the practical energy density of Li-ion batteries: optimization and evaluation of silicon: graphite composites in full cells. *Journal of The Electrochemical Society* **164**, A6294 (2017).
43. Zhao, H., Yuan, W. & Liu, G. Hierarchical electrode design of high-capacity alloy nanomaterials for lithium-ion batteries. *Nano Today* **10**, 193–212 (2015).
44. Zhang, L. *et al.* The typical structural evolution of silicon anode. *Cell Reports Physical Science* **3** (2022).
45. Zhang, M., Zhang, T., Ma, Y. & Chen, Y. Latest development of nanostructured Si/C materials for lithium anode studies and applications. *Energy Storage Materials* **4**, 1–14 (2016).
46. Cui, Y. Silicon anodes. *Nature Energy* **6**, 995–996 (2021).
47. Duffner, F., Kraetzig, O. & Leker, J. Battery plant location considering the balance between knowledge and cost: A comparative study of the EU-28 countries. *Journal of cleaner production* **264**, 121428 (2020).
48. Kallitsis, E. *et al.* Think global act local: The dependency of global lithium-ion battery emissions on production location and material sources. *Journal of Cleaner Production* **449**, 141725 (2024).
49. Tabrizi, M. K., Bonalumi, D. & Lozza, G. G. Analyzing the global warming potential of the production and utilization of lithium-ion batteries with nickel-manganese-cobalt cathode chemistries in European Gigafactories. *Energy* **288**, 129622 (2024).
50. Degen, F. & Schütte, M. Life cycle assessment of the energy consumption and GHG emissions of state-of-the-art automotive battery cell production. *Journal of Cleaner Production* **330**, 129798 (2022).
51. Signoret, J. & Cieszkowsky, M. *To tackle climate change, governments increasingly turn to green subsidies* <https://blogs.worldbank.org/en/trade/to-tackle-climate-change--governments-increasingly-turn-to-green>. Last visited Dec. 31, 2024. (2024).
52. Nguyen-Tien, V., Dai, Q., Harper, G. D., Anderson, P. A. & Elliott, R. J. Optimising the geospatial configuration of a future lithium ion battery recycling industry in the transition to electric vehicles and a circular economy. *Applied Energy* **321**, 119230 (2022).
53. Sherif, S. U., Asokan, P., Sasikumar, P., Mathiyazhagan, K. & Jerald, J. An integrated decision making approach for the selection of battery recycling plant location under sustainable environment. *Journal of Cleaner Production* **330**, 129784 (2022).
54. Hezam, I. M., Gamal, A., Abdel-Basset, M., Nabeeh, N. A. & Smarandache, F. Optimal selection of battery recycling plant location: strategies, challenges, perspectives, and sustainability. *Soft Computing*, 1–32 (2023).
55. Wang, R., Li, X., Xu, C. & Li, F. Study on location decision framework of electric vehicle battery swapping station: Using a hybrid MCDM method. *Sustainable Cities and Society* **61**, 102149 (2020).
56. Zeng, M., Pan, Y., Zhang, D., Lu, Z. & Li, Y. Data-driven location selection for battery swapping stations. *IEEE Access* **7**, 133760–133771 (2019).
57. Brodd, R. J. & Helou, C. Cost comparison of producing high-performance Li-ion batteries in the US and in China. *Journal of Power Sources* **231**, 293–300 (2013).
58. Asaba, M. C., Duffner, F., Frieden, F., Leker, J. & von Delft, S. Location choice for large-scale battery manufacturing plants: Exploring the role of clean energy, costs, and knowledge on location decisions in Europe. *Journal of Industrial Ecology* **26**, 1514–1527 (2022).
59. Philippot, M. L. *et al.* Life cycle assessment of a lithium-ion battery with a silicon anode for electric vehicles. *Journal of Energy Storage* **60**, 106635 (2023).
60. Lastoskie, C. M. & Dai, Q. Comparative life cycle assessment of laminated and vacuum vapor-deposited thin film solid-state batteries. *Journal of Cleaner Production* **91**, 158–169 (2015).
61. Dunn, J., Ritter, K., Velázquez, J. M. & Kendall, A. Should high-cobalt EV batteries be repurposed? Using LCA to assess the impact of technological innovation on the waste hierarchy. *Journal of Industrial Ecology* **27**, 1277–1290 (2023).

Bibliography

62. Li, B., Gao, X., Li, J. & Yuan, C. Life cycle environmental impact of high-capacity lithium ion battery with silicon nanowires anode for electric vehicles. *Environmental science & technology* **48**, 3047–3055 (2014).
63. Hendrickx, B., Yan, J. & Duflou, J. Life-cycle assessment of the laser sintered-silicon anode for lithium ion battery production. *Procedia CIRP* **116**, 594–599 (2023).
64. Kallitsis, E., Korre, A., Kelsall, G., Kupfersberger, M. & Nie, Z. Environmental life cycle assessment of the production in China of lithium-ion batteries with nickel-cobalt-manganese cathodes utilising novel electrode chemistries. *Journal of Cleaner Production* **254**, 120067 (2020).
65. Deng, Y., Ma, L., Li, T., Li, J. & Yuan, C. Life cycle assessment of silicon-nanotube-based lithium ion battery for electric vehicles. *ACS sustainable chemistry & engineering* **7**, 599–610 (2018).
66. Wu, Z. & Kong, D. Comparative life cycle assessment of lithium-ion batteries with lithium metal, silicon nanowire, and graphite anodes. *Clean Technologies and Environmental Policy* **20**, 1233–1244 (2018).
67. Accardo, A., Garofalo, A., Dotelli, G. & Spessa, E. Prospective LCA of Next-Generation Cells for Electric Vehicle Applications. *IEEE Access* **12**, 19584–19597 (2024).
68. Yan, J., Noguchi, J. & Terashi, Y. Fabrication of single-crystal silicon micro pillars on copper foils by nanosecond pulsed laser irradiation. *CIRP Annals* **66**, 253–256 (2017).
69. Evans, T. & Piper, D. M. *Large-format battery anodes comprising silicon particles* US Patent 17/808 285. July 2022.
70. Li, B., Li, J. & Yuan, C. *Life cycle assessment of lithium ion batteries with silicon nanowire anode for electric vehicles* in *Proceedings of the 2013 International Symposium on Sustainable Systems & Technology, Cincinnati, OH, USA* (2013), 15–17.
71. Oliveira, L. *et al.* in *Emerging nanotechnologies in rechargeable energy storage systems* 231–251 (Elsevier, 2017).
72. Dunn, J. B., Gaines, L., Kelly, J. C., James, C. & Gallagher, K. G. The significance of Li-ion batteries in electric vehicle life-cycle energy and emissions and recycling's role in its reduction. *Energy & Environmental Science* **8**, 158–168 (2014).
73. Wang, F., Deng, Y. & Yuan, C. Comparative life cycle assessment of silicon nanowire and silicon nanotube based lithium ion batteries for electric vehicles. *Procedia CIRP* **80**, 310–315 (2019).
74. Wernet, G. *et al.* The ecoinvent database version 3 (part I): overview and methodology. *The International Journal of Life Cycle Assessment* **21**, pp.1218–1230. <http://link.springer.com/10.1007/s11367-016-1087-8> (9 2016).
75. Benavides, P. T., Dai, Q., Sullivan, J. L., Kelly, J. C. & Dunn, J. B. *Material and energy flows associated with select metals in greet 2. molybdenum, platinum, zinc, nickel, silicon* tech. rep. (Argonne National Lab.(ANL), Argonne, IL (United States), 2015).
76. Frischknecht, R. *et al.* Life cycle inventories and life cycle assessments of photovoltaic systems 2020. *International Energy Agency: Paris, France* (2020).
77. Iyer, R. K. & Kelly, J. C. *Updated Production Inventory for Lithium-Ion Battery Anodes for the GREET® Model, and Review of Advanced Battery Chemistries* tech. rep. (Argonne National Laboratory (ANL), 2022).
78. Piwko, M. *et al.* Hierarchical columnar silicon anode structures for high energy density lithium sulfur batteries. *Journal of Power Sources* **351**, 183–191 (2017).
79. Shi, B. *et al.* Preparation of pure hydrogenated amorphous silicon film via PECVD method as anode materials for high-performance lithium-ion batteries. *Solid State Ionics* **402**, 116366 (2023).
80. Barrio, R., González, N., Portugal, Á., Morant, C. & Gandía, J. J. Hydrogenated Amorphous Silicon-Based Nanomaterials as Alternative Electrodes to Graphite for Lithium-Ion Batteries. *Nanomaterials* **12**, 4400 (2022).
81. González, N., García, T., Morant, C. & Barrio, R. Fine-Tuning Intrinsic and Doped Hydrogenated Amorphous Silicon Thin-Film Anodes Deposited by PECVD to Enhance Capacity and Stability in Lithium-Ion Batteries. *Nanomaterials* **14**, 204 (2024).

Bibliography

82. Zolfani, S. H., Bazrafshan, R., Akaberi, P., Yazdani, M. & Ecer, F. Combining the suitability-feasibility-acceptability (SFA) strategy with the MCDM approach. *Facta Universitatis, Series: Mechanical Engineering* **19**, 579–600 (2021).
83. Hashemkhani Zolfani, S., Bazrafshan, R., Ecer, F. & Karamaşa, Ç. The suitability-feasibility-acceptability strategy integrated with Bayesian BWM-MARCOS methods to determine the optimal lithium battery plant located in South America. *Mathematics* **10**, 2401 (2022).
84. Johnson, J. *et al.* *Exploring strategy* (Pearson UK, 2020).
85. Our World in Data. *World regions according to WB* <https://ourworldindata.org/world-region-map-definitions>. Last visited Jan. 6, 2025. (2023).
86. Montani, D., Gervasio, D., Pulcini, A., *et al.* Startup company valuation: The state of art and future trends. *International Business Research* **13**, 31–45 (2020).
87. Srivastava, S. *IEEFA: Climate change takes investors beyond the balance sheet to ESG* <https://ieefa.org/resources/ieefa-climate-change-takes-investors-beyond-balance-sheet-esg>. Last visited Feb. 16, 2025. (2022).
88. European Commission. *Innovation Fund: Methodology for GHG Emission Avoidance Calculation* https://ec.europa.eu/info/funding-tenders/opportunities/docs/2021-2027/innovfund/guidance/ghg-emission-avoidance-methodology_innovfund_en.pdf. Last visited Feb. 16, 2025. (2024).
89. Federal Transit Administration. *The Infrastructure Investment and Jobs Act* <https://www.transit.dot.gov/IIJA>. Last visited Feb. 16, 2025. (2021).
90. IEA. *Energy Technology Perspectives 2024* <https://www.iea.org/reports/energy-technology-perspectives-2024>. Last visited Feb. 16, 2025. (2024).
91. Li, F., Guo, Y. & Liu, B. Impact of government subsidies and carbon inclusion mechanism on carbon emission reduction and consumption willingness in low-carbon supply chain. *Journal of Cleaner Production* **449**, 141783 (2024).
92. World Bank. *Ease of Doing Business Scores* <https://archive.doingbusiness.org/en/data/doing-business-score>. Last visited Jan. 3, 2025. (2025).
93. World Bank. *Political Stability and Absence of Violence/Terrorism: Estimate* <https://data.worldbank.org/indicator/PV.EST>. Last visited Jan. 3, 2025. (2025).
94. Property Rights Alliance. *International Property Rights Index 2023* <https://internationalpropertyrightsindex.org>. Last visited Jan. 3, 2025. (2023).
95. Tholos Foundation. *International Trade Barrier Index 2023* <https://www.tradebarrierindex.org/>. Last visited Jan. 3, 2025. (2023).
96. Institute for Economics & Peace. *Global Peace Index* <https://www.economicsandpeace.org/global-peace-index/>. Last visited Jan. 3, 2025. (2023).
97. Adham, K. & Francey, S. *A Comparison of Production Routes for Natural Versus Synthetic Graphites Destined for Battery Material* in *Conference of Metallurgists* (2023), 397–403.
98. Carrère, T., Khalid, U., Baumann, M., Bouzidi, M. & Allard, B. Carbon footprint assessment of manufacturing of synthetic graphite battery anode material for electric mobility applications. *Journal of Energy Storage* **94**, 112356 (2024).
99. Chen, S. *et al.* Natural graphite anode for advanced lithium-ion Batteries: Challenges, Progress, and Perspectives. *Chemical Engineering Journal*, 158116 (2024).
100. ISO 14040. *Environmental Management-Life Cycle Assessment-Principles and Framework* tech. rep. (International Organisation for Standardisation, 2006).
101. ISO 14044. *Environmental Management-Life Cycle Assessment-Requirements and Guidelines* tech. rep. (International Organisation for Standardisation, 2018).
102. IEA. *Lithium-ion battery manufacturing capacity, 2022-2030* <https://www.iea.org/data-and-statistics/charts/lithium-ion-battery-manufacturing-capacity-2022-2030>. Last visited Feb. 15, 2025. (2023).

Bibliography

103. Cusenza, M. A., Bobba, S., Ardente, F., Cellura, M. & Di Persio, F. Energy and environmental assessment of a traction lithium-ion battery pack for plug-in hybrid electric vehicles. *Journal of cleaner production* **215**, 634–649 (2019).
104. UMICORE. *Battery Recycling Solutions - Our Recycling Process* <https://brs.umicore.com/en/recycling/>. Last visited Feb. 15, 2025. (2025).
105. Holzer, A., Windisch-Kern, S., Ponak, C. & Raupenstrauch, H. A novel pyrometallurgical recycling process for lithium-ion batteries and its application to the recycling of LCO and LFP. *Metals* **11**, 149 (2021).
106. Baum, Z. J., Bird, R. E., Yu, X. & Ma, J. Lithium-ion battery recycling- overview of techniques and trends. *ACS Energy Letters* **7**, 712–719 (2022).
107. Li, J. *et al.* Toward low-cost, high-energy density, and high-power density lithium-ion batteries. *Jom* **69**, 1484–1496 (2017).
108. USABC. *Electric Vehicle Battery Test Procedures Manual* tech. rep. (U.S. Advanced Battery Consortium, 1996).
109. Mahmood, N., Tang, T. & Hou, Y. Nanostructured anode materials for lithium ion batteries: progress, challenge and perspective. *Advanced Energy Materials* **6**, 1600374 (2016).
110. Baird, S. Review of Technical Criteria for High-Impact Battery Applications with Examples of Industry Performance. *ChemRxiv* (2022).
111. Hellsmark, H., Frishammar, J., Söderholm, P. & Ylinenpää, H. The role of pilot and demonstration plants in technology development and innovation policy. *Research Policy* **45**, 1743–1761 (2016).
112. Romare, M. & Dahllöf, L. *The Life Cycle Energy Consumption and Greenhouse Gas Emissions from Lithium-Ion Batteries: A Study with Focus on Current Technology and Batteries for Light-Duty Vehicles* tech. rep. (IVL Swedish Environmental Research Institute, Stockholm, Sweden, 2017).
113. European Commission. *Product environmental footprint category rules for high specific energy rechargeable batteries for mobile applications* tech. rep. Version 6.3 (The Advanced Rechargeable and Lithium Batteries Association, 2018).
114. Ariemma, G. B., Sorrentino, G., Ragucci, R., de Joannon, M. & Sabia, P. Ammonia/Methane combustion: Stability and NOx emissions. *Combustion and Flame* **241**, 112071 (2022).
115. Philipsen, G. J. M. & Alsema, E. A. *Environmental life-cycle assessment of multicrystalline silicon solar cell modules* (Department of Science, Technology and Society, Utrecht University Utrecht, 1995).
116. Hagedorn, G. & Hellriegel, E. *Band 5: Umweltrelevante Stoffströme bei der Herstellung verschiedener Solarzellen* (Forschungsstelle für Energiewirtschaft, Munich, 1992).
117. Maurits, J. E. in *Treatise on Process Metallurgy* 919–948 (Elsevier, 2014).
118. Engels, P. *et al.* Life cycle assessment of natural graphite production for lithium-ion battery anodes based on industrial primary data. *Journal of Cleaner Production* **336**, 130474 (2022).
119. Peters, J. F., Baumann, M., Binder, J. R. & Weil, M. On the environmental competitiveness of sodium-ion batteries under a full life cycle perspective—a cell-chemistry specific modelling approach. *Sustainable Energy & Fuels* **5**, 6414–6429 (2021).
120. Ellingsen, L. A.-W. *et al.* Life cycle assessment of a lithium-ion battery vehicle pack. *Journal of Industrial Ecology* **18**, 113–124 (2014).
121. Peters, J., Buchholz, D., Passerini, S. & Weil, M. Life cycle assessment of sodium-ion batteries. *Energy & Environmental Science* **9**, 1744–1751 (2016).
122. Edwards, L., Hunt, M., Verma, P., Weyell, P. & Koop, J. *Sustainable CPC Production at the Vizag Calciner* in *Proceedings of the 38th International ICSOBA Conference, Online* (2020), 525–535.
123. Surovtseva, D., Crossin, E., Pell, R. & Stamford, L. Toward a life cycle inventory for graphite production. *Journal of industrial Ecology* **26**, 964–979 (2022).

Bibliography

124. Dunn, J. B. *et al.* *Material and energy flows in the production of cathode and anode materials for lithium ion batteries* tech. rep. (Argonne National Lab.(ANL), Argonne, IL (United States), 2015).
125. Cisco. *Cisco Annual Internet Report, 2018–2023* <https://www.cisco.com/c/en/us/solutions/collateral/executive-perspectives/annual-internet-report/white-paper-c11-741490.pdf>. Last visited Jan. 11, 2025. (2020).
126. Statista. *Consumer Electronics* <https://www.statista.com/outlook/cmo/consumer-electronics/worldwide>. Last visited Jan. 11, 2025. (2024).
127. Kallitsis, E., Korre, A. & Kelsall, G. H. Life cycle assessment of recycling options for automotive Li-ion battery packs. *Journal of cleaner production* **371**, 133636 (2022).
128. Notteboom, T., Pallis, A. & Rodrigue, J.-P. *Port economics, management and policy* 1st ed. (Routledge, London, 2022).
129. Cullinane, K. & Wang, T.-F. Port governance in China. *Research in Transportation Economics* **17**, 331–356 (2006).
130. Bureau of Transportation Statistics. *Value, Tonnage, and Ton-Miles of Freight by Distance Band (2023)* <https://www.bts.gov/browse-statistical-products-and-data/freight-facts-and-figures/value-tonnage-and-ton-miles-freight>. Last visited Feb. 13, 2025. (2017).
131. Eurostat. *Road freight transport by type of goods and type of transport (t, tkm) - annual data* https://ec.europa.eu/eurostat/databrowser/product/page/road_go_ta_tg. Last visited Feb. 13, 2025. (2024).
132. Peters, J. F., Baumann, M., Zimmermann, B., Braun, J. & Weil, M. The environmental impact of Li-Ion batteries and the role of key parameters—A review. *Renewable and Sustainable Energy Reviews* **67**, 491–506 (2017).
133. Gottschalk, L., Strzelczyk, N., Adam, A. & Kwade, A. Influence of different anode active materials and blends on the performance and fast-charging capability of lithium-ion battery cells. *Journal of Energy Storage* **68**, 107706 (2023).
134. Zhao, X. & Lehto, V.-P. Challenges and prospects of nanosized silicon anodes in lithium-ion batteries. *Nanotechnology* **32**, 042002 (2020).
135. European Commission. Commission Recommendation (EU) 2021/2279 of 15 December 2021 on the Use of the Environmental Footprint Methods to Measure and Communicate the Life Cycle Environmental Performance of Products and Organisations. *Official Journal of the European Union* **64** (2021).
136. GreenDelta. *openLCA* version 2.2. 2023. <https://www.openlca.org/> Dec. 17, 2024.
137. Sun, L. *et al.* Recent progress and future perspective on practical silicon anode-based lithium ion batteries. *Energy Storage Materials* **46**, 482–502 (2022).
138. Jin, Y., Zhu, B., Lu, Z., Liu, N. & Zhu, J. Challenges and recent progress in the development of Si anodes for lithium-ion battery. *Advanced Energy Materials* **7**, 1700715 (2017).
139. Sun, L., Liu, Y., Wang, L. & Jin, Z. Advances and Future Prospects of Micro-Silicon Anodes for High-Energy-Density Lithium-Ion Batteries: A Comprehensive Review. *Advanced Functional Materials*, 2403032 (2024).
140. Zhang, C. *et al.* Challenges and recent progress on silicon-based anode materials for next-generation lithium-ion batteries. *Small Structures* **2**, 2100009 (2021).
141. Sun, Z. *et al.* Building better solid-state batteries with silicon-based anodes. *Interdisciplinary Materials* **2**, 635–663 (2023).
142. European Environmental Bureau. *Non-replaceable batteries are bad news for the environment and consumers, new research finds* <https://eeb.org/non-replaceable-batteries-are-bad-news-for-the-environment-and-consumers-new-research-finds/>. Last visited Feb. 16, 2025. (2021).
143. HiMAX. *18650 3.7V 3000mAh Rechargeable Lithium Ion Battery Cells and Packs* <https://himaxelctronics.com/product-item/18650-3-7v-3000mah-li-ion-battery-cell/>. Last visited Jan. 9, 2025. (2024).

Bibliography

144. The Engineering ToolBox. *Specific Heat of common Substances* https://www.engineeringtoolbox.com/specific-heat-capacity-d_391.html. Last visited Nov. 12, 2024. (2003).
145. PermuTrade. *What is Petcoke? And What is it Used For?* <https://www.permutrade.com/what-is-petcoke-and-what-is-it-used-for>. Last visited Nov. 12, 2024. (2024).
146. Shanghai Metals Market (SMM). *SMM Spot Metal Prices* <https://www.metal.com/>. Last visited Nov. 12, 2024. (2024).
147. Business Analytiq. *Metal silicon price index* <https://businessanalytiq.com/procurementanalytics/index/metal-silicon-price-index/>. Last visited Nov. 12, 2024. (2024).
148. IEA. *Electricity supply mix by region, 2020* <https://www.iea.org/data-and-statistics/charts/electricity-supply-mix-by-region-2020>. Last visited Jan. 19, 2025. (2020).
149. IEA. *North America* <https://www.iea.org/regions/north-america/natural-gas>. Last visited Feb. 10, 2025. (2024).
150. Erbach, G. Shale gas and EU energy security (2014).
151. Inman, M. Can fracking power Europe? *Nature* **531**, 22 (2016).

Appendix

A. Method

A.1. Adapted Suitability-Feasibility-Acceptability Framework

The following countries were excluded from the location study due to a lack of data:

- British Virgin Islands
- Channel Islands
- Curacao
- Faroe Islands
- French Polynesia
- Gibraltar
- Isle of Man
- St. Martin (French part)
- Northern Mariana Islands
- New Caledonia
- Sint Maarten (Dutch part)
- Taiwan
- Turks and Caicos Islands
- Western Sahara

A.2. Life Cycle Assessment

The figure below displays a 18650 cylindrical battery cell with an LCO cathode, which is similar to the reference battery modelled in this study.



Figure A.1.: 18650 Lithium-Ion Battery Cell with LCO Cathode [143]

Table A.1 provides the detailed bill of material (BOM) of the three battery systems. Part of this table was removed due to confidentiality reasons.

Table A.1.: Bill of Material of Modelled Battery Types
Graphite refers to both graphite types discussed in this study: natural and synthetic.

Component	Battery Content	Cell part	Graphite		Silicon	
			value [kg]	share	value	share
Lithium Cobalt Oxide		cathode	2.95E-01	30 %	2.94E-01	29 %
Anode			2.54E-01	25 %	–	–
Graphite		anode	1.93E-01	19 %	0.00E+00	0 %
SBR (binder)		anode	1.18E-03	0 %	0.00E+00	0 %
CMC (binder)		anode	2.74E-03	0 %	0.00E+00	0 %
Silicon on Cu		anode	0.00E+00	0 %	–	–
Current collector Cu			5.71E-02	6 %	–	–
Current collector, primary copper		anode	4.86E-02	5 %	0.00E+00	0 %
Current collector, secondary copper		anode	8.57E-03	1 %	–	–
Nickel, 99.5 %		cathode	1.07E-03	0 %	1.07E-03	0 %
carbon black		cathode	1.63E-02	2 %	1.62E-02	2 %
polyethylene, LDPE, granulate		separator	1.74E-02	2 %	1.73E-02	2 %
Chromium steel 18/8		casing	2.15E-01	22 %	2.14E-01	21 %
Ethylene carbonate		electrolyte	1.03E-01	10 %	1.03E-01	10 %
Lithium hexafluorophosphate		electrolyte	1.61E-02	2 %	1.61E-02	2 %
Polyvinylfluoride film		casing	2.82E-02	3 %	2.81E-02	3 %
PET, granulate, bottle grade		casing	1.05E-02	1 %	1.05E-02	1 %
Aluminium, primary		cathode	4.24E-02	4 %	4.23E-02	4 %
Total			1.00E+00	100 %	1.00E+00	100 %

A.2.1. Multi-functionality and Allocation

The following describes the data used to calculate the allocation factors, described in Section 2.2.2.4. The whole list of allocation factors is provided in the Supplementary Material "Multifunctionality_and_Contribution-Analysis" under "Multifunctionality".

Natural graphite spheronisation The economic allocation for the graphite fines co-produced in this process is based on information given by Engels *et al.* [118], who state that "[t]he by-product 'fines' account for approximately 25 % of the economic added value of the process". Thus, this study allocated 25 % of the environmental and economic flows to the graphite fines and 75 % to the spherical graphite.

Calcining petroleum coke The multifunctionality of this process was solved with energy allocation. Thus, the calorific value, also called lower heating value (LHV), of each functional flow was multiplied by the respective amount of product produced. For sulfated lime, the LHV of limestone from The Engineering ToolBox [144] was used as a proxy. Similarly, the LHV of calcined petroleum coke was approximated with the one of green coke taken from PermuTrade [145]. The amount of electricity was converted into kilocalorie given that $1 \text{ kcal} \approx 0.001 \text{ kWh}$. The resulting energy contents were then used for allocation.

Calcined coke milling For the economic allocation of this process, the respective prices in dollar per tonne (\$/t) were extracted from the Shanghai Metals Market (SMM) in November, 2024 [146]. Since the prices of the exact products were not available, the economic values of the coke fines and

the calcined coke powder were estimated with the prices of calcined petroleum coke and graphitised coke powder, respectively. It should be noted that on the SMM two types of graphitised coke powder are traded, namely a light and heavy variant. As it is uncertain which one is the more suitable proxy for the calcined coke powder, this study used the average price of both types.

Acheson powder graphitisation The economic allocation of this process was done in the same manner as the one of the calcined coke milling. Therefore, the graphitised coke powder has the same price as the calcined coke powder in the prior step, where it was used as a proxy. Due to a lack of data, the economic value of the crucible chips was determined based on the price of battery-grade synthetic graphite traded on the SMM [146], given that, according to Carrère *et al.* [98], the value of crucible chips is ca. 20 times lower than that of the synthetic graphite.

Micronisation and spheronisation As neither the price of micronised graphite powder nor synthetic graphite fines was available, this study assumed that the two products have the same value as their natural graphite counterparts. Thus, like in the natural graphite spheronisation process, this study allocated 25 % of the environmental and economic flows to the synthetic graphite fines and 75 % to the micronised synthetic graphite powder.

Purification of silica to metallurgical-grade silicon To solve the multifunctionality of this process, economic allocation was used. The economic value of mg-Si was determined by its European market price in January, 2024, as published by Business Analytiq [147]. The price of the silica was extracted from the SMM [146] in the last quarter of 2024.

A.2.2. Scenario Development

Table A.2 summarises the scenarios analysed in this study regarding the production and performance of the silicon-based LIB. Part of this table was removed due to confidentiality reasons.

Table A.2.: Details of the Scenario Parameters

Parameter	Scenarios			
	Mass Loading	Silane Utilisation	Cycle Life	Hydrogen Reuse
Silicon Mass Loading	1.5–2.5	–	–	–
Utilisation of Silane	–	15 %–30 %	–	–
Charging Cycles	800	800	500–1500	800
H ₂ in off-gas	burned	burned	burned	reused

B. Results

B.1. Location Study

The following table visualises the performance of each region in all indicators by taking, per indicator, the median of each region and comparing it to the global median. Its results support the conclusions drawn from Table 3.1 in the main text, which assessed the mean instead of the median.

Table B.1.: Median Performance of Each Region per Quantitative Indicator

Darkgreen = Outperforms indicator median by more than one standard deviation (σ); Green = Outperforms indicator median within one σ ; Yellow = Within one σ worse than indicator median; Red = More than one σ worse than indicator median.

Index	Median ($\pm \sigma$)	CAS	EAS	EUR	LCN	MEA	NAC	OCE	SAS	SSF
EDB	62.713 (± 13.839)	68.850	81.000	76.222	59.872	63.951	81.819	60.413	62.829	51.902
PS	0.044 (± 0.999)	-0.468	0.577	0.582	0.348	-0.623	0.781	1.050	-0.239	-0.499
IP	5.034 (± 1.42)	4.287	7.067	6.064	4.392	5.233	7.473	7.740	4.807	4.074
TBI	3.880 (± 0.703)	5.105	3.750	3.640	3.590	4.010	3.565	4.055	5.150	4.180
GPI	2.079 (± 0.51)	2.035	1.974	1.675	2.179	2.206	2.035	1.536	2.048	2.339

Table B.2 lists all silane producer shown in the map of Figure 3.2 and provides a bit more detail regarding their product lines, maturity, and production capacity.

Table B.2.: Silane Supplier

Company	Location	Products	Capacity [Mt/y]	Maturity	Distr.	Website
ACE Gases	Malaysia	Industrial, specialty gases and chemicals	NA	Established (2016, subsidiary)	Yes	https://acegases.com/
Argosun (ArgoTech)	China	Special gases and precursors	200	Established (2012)	No	https://www.argosun.com/
American Elements	USA	Materials Science Manufacturer	NA	Established (1997)	Yes	https://www.americanelements.com/
Cangzhou Huayu Special Gas Technology Co., Ltd.	China	Gases	3,000	National plan (2017)	No	http://www.czcip.gov.cn/czcip/c100999/202301/ab3110c90b904f0ab26e13dbac1f26f5.shtml
CG Silane (Jiangsu Chengguang Silane Co., Ltd.)	China	Specialty chemicals	3,000	Established (2001)	No	http://www.cgsilane.com/english/index.aspx
Denal Silane (Denka Group & Air Liquide)	Japan	Monosilane, di- & hexachlorosilane	600	Established (1987)	No	https://www.denka.co.jp/english/#top
Evonik	Germany	Specialty chemicals	NA	Established (2007)	No	https://www.evonik.com/en.html
Fujian Highsun (Hengshen) Electronic Material Technology Co., Ltd. (HSCC)	China	Chemicals and chemical fibres	3,000	National plan (2020)	No	https://www.hsc.com/
Guangdong Huate Gas CO., Ltd.	China	Industrial gases	NA	Established (1999)	NA	https://www.huatehfc.com/
Green14	Sweden	Silane	NA	Start-up (2021)	No	https://www.green14.com/
Haining Indusair Electronics Co., Ltd.	China	Chemicals, fertiliser, pesticides	800	Established (2011)	No	no website
Hanwha	South Korea	energy, ocean, aerospace, finance, and retail & services	NA	Established (1977)	No	https://www.hanwha.com/
Henan Silane Technology Development Co., Ltd. (HST)	China	Silane	8,200	Established (2012)	No	https://www.bloomberg.com/profile/company/2142340D:CH

Continued on next page

Table B.2 – continued from previous page

Company	Location	Products	Capacity [Mt/y]	Maturity	Distr.	Website
Hubei Heyuan New Materials (Hubei Heyuan Gas)	China	Industrial grade chemicals, electric-grade silane	3,000	Established (2003)	No	https://en.hbhy-gas.com/
Jinghong Gas (jh-gas)	China	Gases, Mixture gases, equipment, on-site gas supply	NA	Established (1999)	No	https://www.jh-gas.com/
Linde AG	USA	Industrial gases and welding supplies	NA	Established (1879)	Yes	https://www.lindedirect.com/
Mitsui Chemicals	Japan	Chemicals	200	Established (1997)	No	https://jp.mitsuichemicals.com/en/index.htm
Neimenggu / Inner Mongolia Xingyang Technology	China	Silicones	8,400	Established (2014)	No	https://dataintel.com/report/global-electronic-grade-sih4-silane-gas-market
New Radar Gas	China	Specialty gases	NA	Established (1996)	No	https://newradargas.com/
OCI Company Ltd.	South Korea	Polysilicon	NA	Established (1959)	No	https://www.oci.co.kr/en/company/intro
PCC	Poland	Specialty chemicals and industrial formulations	NA	Established (2003)	No	https://pcc.eu/en/
Polysilicon Technology Development Co., Ltd. (GCL Tech)	China	Granular silicon	4,800	Established (2006)	No	http://www.gcltech.com/en/about/about.html
Praxair	India	Industrial gases	NA	Established	No	https://www.praxair.co.in/
REC Silicon	USA	Silane-based, high-purity silicon materials	30,000	Established (1983)	No	https://recsilicon.com/
ReSi	Netherlands	Polysilicon	13,500	Start-up	No	https://resilicon.eu/
Shaanxi Non-ferrous Tian Hong REC Silicon Materials (trsilicon)	China	Electronic Grade and Granular Polysilicon, High Purity Silane Gas	4,000	Established (2017, subsidiary)	No	http://www.trsilicon.com/en/index
Shihlien Fine Chemicals (SFC)	Taiwan	Electronic specialty gases	600	Established (2006)	No	https://www.shihlienenergy.com/index.aspx

Continued on next page

Table B.2 – continued from previous page

Company	Location	Products	Capacity [Mt/y]	Maturity	Distr.	Website
Sinosico (China Silicon Corporation)	China	Polysilicon	1,000	Established (2003)	No	http://www.sinosico.com/en/
SK Specialty (SK Siltron, SKST)	South Korea	Specialty gases and chemicals	2,000	Established (1983)	No	https://www.sksspecialty.com/new/eng/html/main/
Taiyo Nippon Sanso (NSHC)	Japan	Industrial gases	NA	Established (1918)	Yes	https://www.nipponsanso-hd.co.jp/en/
Tianjin Summit Chemical & Gases Company Ltd.	China	Specialty gases and chemicals	NA	Established (2015)	No	https://www.smtgases.com/
TYHJ	China	Industrial gases	NA	Established (2002)	NA	https://www.tyhjgas.com/
Yongxiang Co., Ltd. (Tongwei Group)	China	Silicon and green energy	1,500	Subsidiary	No	https://www.scyxgf.com/
Zhejiang Zhongning Silicon (cn-silicon)	China	(Nano-) Silicon powder, high-purity silane gas, polysilicon	2,000	Established (2007)	No	http://en.cn-silicon.com.cn/

B. Results

Table B.3 contains the absolute characterisation results of the PEF impact categories for all reference flows of the location study, visualised in Figure 3.3.

Table B.3.: Environmental Impacts of PEF Impact Categories for Reference Flows of the Location Study

Impact category	Si - CN	Si - RNA	Si - RER	Unit
acidification	6.67×10^{-3}	3.69×10^{-3}	3.94×10^{-3}	mol H ⁺ -Eq
climate change	1.30×10^0	9.00×10^{-1}	8.02×10^{-1}	kg CO ₂ -Eq
climate change: biogenic	2.55×10^{-3}	2.81×10^{-3}	3.90×10^{-3}	kg CO ₂ -Eq
climate change: fossil	1.30×10^0	8.94×10^{-1}	7.96×10^{-1}	kg CO ₂ -Eq
climate change: land use and land use change	1.88×10^{-3}	2.66×10^{-3}	2.22×10^{-3}	kg CO ₂ -Eq
ecotoxicity: freshwater	3.87×10^0	2.46×10^0	2.50×10^0	CTUe
ecotoxicity: freshwater, inorganics	3.60×10^0	2.20×10^0	2.23×10^0	CTUe
ecotoxicity: freshwater, organics	2.70×10^{-1}	2.62×10^{-1}	2.64×10^{-1}	CTUe
energy resources: non-renewable	1.80×10^1	1.73×10^1	1.71×10^1	MJ, LHV
eutrophication: freshwater	5.30×10^{-4}	6.10×10^{-4}	6.40×10^{-4}	kg P-Eq
eutrophication: marine	1.32×10^{-3}	6.80×10^{-4}	6.90×10^{-4}	kg N-Eq
eutrophication: terrestrial	1.33×10^{-2}	6.12×10^{-3}	6.19×10^{-3}	mol N-Eq
human toxicity: carcinogenic	4.57×10^{-10}	3.87×10^{-10}	3.94×10^{-10}	CTUh
human toxicity: carcinogenic, inorganics	3.14×10^{-10}	2.37×10^{-10}	2.44×10^{-10}	CTUh
human toxicity: carcinogenic, organics	1.43×10^{-10}	1.50×10^{-10}	1.50×10^{-10}	CTUh
human toxicity: non-carcinogenic	1.75×10^{-8}	1.27×10^{-8}	1.31×10^{-8}	CTUh
human toxicity: non-carcinogenic, inorganics	1.69×10^{-8}	1.22×10^{-8}	1.26×10^{-8}	CTUh
human toxicity: non-carcinogenic, organics	5.97×10^{-10}	4.51×10^{-10}	4.41×10^{-10}	CTUh
ionising radiation: human health	2.72×10^{-1}	3.90×10^{-1}	4.30×10^{-1}	kBq U235-Eq
land use	3.72×10^0	3.36×10^0	3.09×10^0	dimensionless
material resources: metals/minerals	7.32×10^{-6}	7.31×10^{-6}	7.39×10^{-6}	kg Sb-Eq
ozone depletion	5.28×10^{-9}	5.12×10^{-9}	9.34×10^{-9}	kg CFC-11-Eq
particulate matter formation	7.11×10^{-8}	2.00×10^{-8}	1.77×10^{-8}	disease incidence
photochemical oxidant formation: human health	3.88×10^{-3}	2.21×10^{-3}	2.12×10^{-3}	kg NMVOC-Eq
water use	3.74×10^{-1}	4.41×10^{-1}	4.43×10^{-1}	m ³ world eq. deprived

Figure B.1 displays the regional electricity mixes in 2020, which is how they are modelled in Ecoinvent 3.9 [74]. The figure was taken directly from IEA [148]. It should be noted that the significant difference in ozone depletion between Europe and North America, visible in Figure 3.3, is primarily driven by the type of gas used in the regional electricity production. In North America, the majority of gas is produced by the USA using fracking from onshore shale gas resources [149, 150]. In contrast, Europe obtains most of its gas from off- and onshore natural gas reserves in the North Sea, Russia, and Norway [150, 151]. Therefore, the higher levels of ozone depletion in case of Europe as an anode production location (Table B.3), despite the lower share of gas in its electricity grid mix (Figure B.1), can be explained by a considerably larger amount of Chlorofluorocarbons (CFCs) emitted during the extraction of natural gas and its long distance transport in pipelines. All other impacts associated with the two locations are comparable due to the similarity in their grid mixes (Figure B.1).

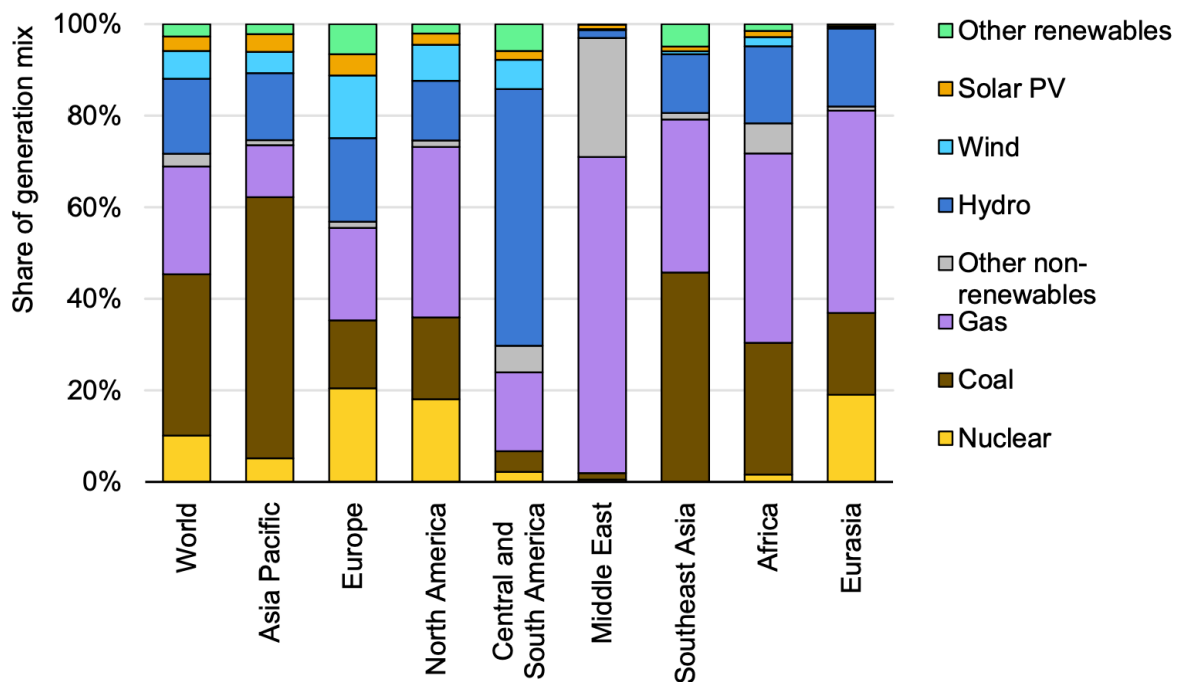


Figure B.1.: Electricity Mix by Region in 2020, source: IEA [148]

B.2. Comparative Analysis

The following tables contain the characterisation results for the three product systems. While Table B.4 encompasses the base case results of *the delivery of 1 kWh stored energy* by a LCO LIB with one of the three anode types, the other tables contain the results of the three product systems with changes in the functional unit and scope compared to the base case. Since the anode alternatives remain the same, the following only lists the adapted functional units.

1. Table B.4: the delivery of 1 kWh stored energy (base case)
2. Table B.5: the production of 1 kWh activated anode material
3. Table B.6: the production of 1 kg activated anode material
4. Table B.7: the production of 1 kWh LCO battery cell
5. Table B.8: the production of 1 kg LCO battery cell

B. Results

Table B.4.: Cradle-to-Grave Environmental Impact of the PEF Impact Categories for 1 kWh Delivered Energy of LIBs with a Silicon (Si), Natural Graphite (NG), and Synthetic Graphite (SG) Anode

Impact category	Si	SG	NG	Unit
acidification	3.94×10^{-3}	2.64×10^{-3}	2.51×10^{-3}	mol H ⁺ -Eq
climate change	8.02×10^{-1}	5.34×10^{-1}	5.05×10^{-1}	kg CO ₂ -Eq
climate change: biogenic	3.90×10^{-3}	1.26×10^{-3}	1.26×10^{-3}	kg CO ₂ -Eq
climate change: fossil	7.96×10^{-1}	5.32×10^{-1}	5.02×10^{-1}	kg CO ₂ -Eq
climate change: land use and land use change	2.22×10^{-3}	1.36×10^{-3}	1.36×10^{-3}	kg CO ₂ -Eq
ecotoxicity: freshwater	2.50×10^0	1.88×10^0	1.78×10^0	CTUe
ecotoxicity: freshwater, inorganics	2.23×10^0	1.72×10^0	1.63×10^0	CTUe
ecotoxicity: freshwater, organics	2.64×10^{-1}	1.51×10^{-1}	1.52×10^{-1}	CTUe
energy resources: non-renewable	1.71×10^1	1.00×10^1	9.64×10^0	MJ, LHV
eutrophication: freshwater	6.40×10^{-4}	3.70×10^{-4}	3.60×10^{-4}	kg P-Eq
eutrophication: marine	6.90×10^{-4}	4.50×10^{-4}	4.20×10^{-4}	kg N-Eq
eutrophication: terrestrial	6.19×10^{-3}	4.21×10^{-3}	3.91×10^{-3}	mol N-Eq
human toxicity: carcinogenic	3.94×10^{-10}	2.89×10^{-10}	2.58×10^{-10}	CTUh
human toxicity: carcinogenic, inorganics	2.44×10^{-10}	1.90×10^{-10}	1.87×10^{-10}	CTUh
human toxicity: carcinogenic, organics	1.50×10^{-10}	9.87×10^{-11}	7.05×10^{-11}	CTUh
human toxicity: non-carcinogenic	1.31×10^{-8}	1.11×10^{-8}	1.09×10^{-8}	CTUh
human toxicity: non-carcinogenic, inorganics	1.26×10^{-8}	1.07×10^{-8}	1.05×10^{-8}	CTUh
human toxicity: non-carcinogenic, organics	4.41×10^{-10}	4.36×10^{-10}	4.29×10^{-10}	CTUh
ionising radiation: human health	4.30×10^{-1}	2.20×10^{-1}	2.19×10^{-1}	kBq U235-Eq
land use	3.09×10^0	1.79×10^0	1.76×10^0	dimensionless
material resources: metals/minerals	7.39×10^{-6}	7.82×10^{-6}	7.88×10^{-6}	kg Sb-Eq
ozone depletion	9.34×10^{-9}	3.30×10^{-9}	3.12×10^{-9}	kg CFC-11-Eq
particulate matter formation	1.77×10^{-8}	1.57×10^{-8}	2.18×10^{-8}	disease incidence
photochemical oxidant formation: human health	2.12×10^{-3}	1.44×10^{-3}	1.33×10^{-3}	kg NMVOC-Eq
water use	4.43×10^{-1}	2.31×10^{-1}	2.93×10^{-1}	m ³ world eq. deprived

B. Results

Table B.5.: Cradle-to-Gate Environmental Impact of the PEF Impact Categories for 1 kWh Activated Silicon (Si), Natural Graphite (NG), and Synthetic Graphite (SG) Anode

Impact category	Si	SG	NG	Unit
acidification	8.25×10^{-1}	2.30×10^{-1}	1.65×10^{-1}	mol H+-Eq
climate change	1.42×10^2	2.28×10^1	8.87×10^0	kg CO2-Eq
climate change: biogenic	1.18×10^0	1.67×10^{-2}	1.70×10^{-2}	kg CO2-Eq
climate change: fossil	1.40×10^2	2.28×10^1	8.84×10^0	kg CO2-Eq
climate change: land use and land use change	3.45×10^{-1}	1.18×10^{-2}	1.03×10^{-2}	kg CO2-Eq
ecotoxicity: freshwater	4.88×10^2	2.26×10^2	1.82×10^2	CTUe
ecotoxicity: freshwater, inorganics	4.35×10^2	2.22×10^2	1.77×10^2	CTUe
ecotoxicity: freshwater, organics	5.25×10^1	4.53×10^0	5.01×10^0	CTUe
energy resources: non-renewable	3.31×10^3	2.90×10^2	9.40×10^1	MJ, LHV
eutrophication: freshwater	1.30×10^{-1}	1.35×10^{-2}	1.11×10^{-2}	kg P-Eq
eutrophication: marine	1.43×10^{-1}	2.91×10^{-2}	1.55×10^{-2}	kg N-Eq
eutrophication: terrestrial	1.28×10^0	3.26×10^{-1}	1.83×10^{-1}	mol N-Eq
human toxicity: carcinogenic	8.05×10^{-8}	3.62×10^{-8}	2.11×10^{-8}	CTUh
human toxicity: carcinogenic, inorganics	4.55×10^{-8}	2.12×10^{-8}	1.95×10^{-8}	CTUh
human toxicity: carcinogenic, organics	3.50×10^{-8}	1.51×10^{-8}	1.61×10^{-9}	CTUh
human toxicity: non-carcinogenic	2.54×10^{-6}	1.79×10^{-6}	1.70×10^{-6}	CTUh
human toxicity: non-carcinogenic, inorganics	2.46×10^{-6}	1.71×10^{-6}	1.62×10^{-6}	CTUh
human toxicity: non-carcinogenic, organics	7.94×10^{-8}	8.38×10^{-8}	8.07×10^{-8}	CTUh
ionising radiation: human health	8.88×10^1	9.91×10^{-1}	4.63×10^{-1}	kBq U235-Eq
land use	6.53×10^2	8.44×10^1	6.79×10^1	dimensionless
material resources: metals/minerals	1.21×10^{-3}	1.57×10^{-3}	1.59×10^{-3}	kg Sb-Eq
ozone depletion	2.76×10^{-6}	2.39×10^{-7}	1.53×10^{-7}	kg CFC-11-Eq
particulate matter formation	3.44×10^{-6}	1.79×10^{-6}	4.70×10^{-6}	disease incidence
photochemical oxidant formation: human health	4.16×10^{-1}	1.02×10^{-1}	5.09×10^{-2}	kg NMVOC-Eq
water use	9.28×10^1	3.84×10^0	3.35×10^1	m3 world eq. deprived

B. Results

Table B.6.: Cradle-to-Gate Environmental Impact of the PEF Impact Categories for 1 kg Activated Silicon (Si), Natural Graphite (NG), and Synthetic Graphite (SG) Anode

Impact category	NG	Si	SG	Unit
acidification	1.63×10^{-1}	9.82×10^{-1}	2.28×10^{-1}	mol H ⁺ -Eq
climate change	8.78×10^0	1.69×10^2	2.25×10^1	kg CO ₂ -Eq
climate change: biogenic	1.68×10^{-2}	1.41×10^0	1.65×10^{-2}	kg CO ₂ -Eq
climate change: fossil	8.75×10^0	1.67×10^2	2.25×10^1	kg CO ₂ -Eq
climate change: land use and land use change	1.02×10^{-2}	4.10×10^{-1}	1.16×10^{-2}	kg CO ₂ -Eq
ecotoxicity: freshwater	1.80×10^2	5.80×10^2	2.24×10^2	CTUe
ecotoxicity: freshwater, inorganics	1.75×10^2	5.18×10^2	2.20×10^2	CTUe
ecotoxicity: freshwater, organics	4.96×10^0	6.25×10^1	4.48×10^0	CTUe
energy resources: non-renewable	9.30×10^1	3.94×10^3	2.87×10^2	MJ, LHV
eutrophication: freshwater	1.10×10^{-2}	1.54×10^{-1}	1.34×10^{-2}	kg P-Eq
eutrophication: marine	1.53×10^{-2}	1.70×10^{-1}	2.88×10^{-2}	kg N-Eq
eutrophication: terrestrial	1.81×10^{-1}	1.52×10^0	3.22×10^{-1}	mol N-Eq
human toxicity: carcinogenic	2.09×10^{-8}	9.58×10^{-8}	3.58×10^{-8}	CTUh
human toxicity: carcinogenic, inorganics	1.93×10^{-8}	5.41×10^{-8}	2.09×10^{-8}	CTUh
human toxicity: carcinogenic, organics	1.60×10^{-9}	4.16×10^{-8}	1.49×10^{-8}	CTUh
human toxicity: non-carcinogenic	1.68×10^{-6}	3.02×10^{-6}	1.77×10^{-6}	CTUh
human toxicity: non-carcinogenic, inorganics	1.60×10^{-6}	2.92×10^{-6}	1.69×10^{-6}	CTUh
human toxicity: non-carcinogenic, organics	7.98×10^{-8}	9.46×10^{-8}	8.30×10^{-8}	CTUh
ionising radiation: human health	4.58×10^{-1}	1.06×10^2	9.81×10^{-1}	kBq U235-Eq
land use	6.72×10^1	7.77×10^2	8.35×10^1	dimensionless
material resources: metals/minerals	1.58×10^{-3}	1.44×10^{-3}	1.55×10^{-3}	kg Sb-Eq
ozone depletion	1.51×10^{-7}	3.28×10^{-6}	2.36×10^{-7}	kg CFC-11-Eq
particulate matter formation	4.65×10^{-6}	4.10×10^{-6}	1.77×10^{-6}	disease incidence
photochemical oxidant formation: human health	5.04×10^{-2}	4.95×10^{-1}	1.01×10^{-1}	kg NMVOC-Eq
water use	3.32×10^1	1.10×10^2	3.80×10^0	m ³ world eq. deprived

B. Results

Table B.7.: Cradle-to-Gate Environmental Impact of the PEF Impact Categories for 1 kWh LCO LIB cell with a Silicon (Si), Natural Graphite (NG), and Synthetic Graphite (SG) Anode

Impact category	Si	SG	NG	Unit
acidification	2.54×10^0	1.33×10^0	1.22×10^0	mol H ⁺ -Eq
climate change	3.82×10^2	1.47×10^2	1.24×10^2	kg CO ₂ -Eq
climate change: biogenic	2.85×10^0	4.21×10^{-1}	4.22×10^{-1}	kg CO ₂ -Eq
climate change: fossil	3.78×10^2	1.46×10^2	1.23×10^2	kg CO ₂ -Eq
climate change: land use and land use change	1.16×10^0	4.32×10^{-1}	4.29×10^{-1}	kg CO ₂ -Eq
ecotoxicity: freshwater	2.23×10^3	1.66×10^3	1.58×10^3	CTUe
ecotoxicity: freshwater, inorganics	2.04×10^3	1.57×10^3	1.49×10^3	CTUe
ecotoxicity: freshwater, organics	1.87×10^2	8.76×10^1	8.84×10^1	CTUe
energy resources: non-renewable	8.46×10^3	2.25×10^3	1.92×10^3	MJ, LHV
eutrophication: freshwater	3.05×10^{-1}	6.17×10^{-2}	5.76×10^{-2}	kg P-Eq
eutrophication: marine	4.13×10^{-1}	1.88×10^{-1}	1.65×10^{-1}	kg N-Eq
eutrophication: terrestrial	3.58×10^0	1.73×10^0	1.49×10^0	mol N-Eq
human toxicity: carcinogenic	3.02×10^{-7}	2.00×10^{-7}	1.75×10^{-7}	CTUh
human toxicity: carcinogenic, inorganics	2.01×10^{-7}	1.47×10^{-7}	1.44×10^{-7}	CTUh
human toxicity: carcinogenic, organics	1.01×10^{-7}	5.37×10^{-8}	3.12×10^{-8}	CTUh
human toxicity: non-carcinogenic	9.21×10^{-6}	7.21×10^{-6}	7.06×10^{-6}	CTUh
human toxicity: non-carcinogenic, inorganics	8.95×10^{-6}	6.97×10^{-6}	6.82×10^{-6}	CTUh
human toxicity: non-carcinogenic, organics	2.57×10^{-7}	2.41×10^{-7}	2.36×10^{-7}	CTUh
ionising radiation: human health	2.17×10^2	3.31×10^1	3.22×10^1	kBq U235-Eq
land use	1.74×10^3	5.71×10^2	5.44×10^2	dimensionless
material resources: metals/minerals	1.59×10^{-2}	1.62×10^{-2}	1.62×10^{-2}	kg Sb-Eq
ozone depletion	9.38×10^{-6}	4.05×10^{-6}	3.91×10^{-6}	kg CFC-11-Eq
particulate matter formation	1.60×10^{-5}	1.37×10^{-5}	1.86×10^{-5}	disease incidence
photochemical oxidant formation: human health	1.22×10^0	5.95×10^{-1}	5.10×10^{-1}	kg NMVOC-Eq
water use	8.19×10^2	6.35×10^2	6.85×10^2	m ³ world eq. deprived

B. Results

Table B.8.: Cradle-to-Gate Environmental Impact of the PEF Impact Categories for 1 kg LCO LIB cell with a Silicon (Si), Natural Graphite (NG), and Synthetic Graphite (SG) Anode

Impact category	Si	SG	NG	Unit
acidification	3.82×10^{-1}	2.00×10^{-1}	1.83×10^{-1}	mol H ⁺ -Eq
climate change	5.73×10^1	2.20×10^1	1.85×10^1	kg CO ₂ -Eq
climate change: biogenic	4.27×10^{-1}	6.32×10^{-2}	6.32×10^{-2}	kg CO ₂ -Eq
climate change: fossil	5.67×10^1	2.19×10^1	1.84×10^1	kg CO ₂ -Eq
climate change: land use and land use change	1.75×10^{-1}	6.48×10^{-2}	6.44×10^{-2}	kg CO ₂ -Eq
ecotoxicity: freshwater	3.34×10^2	2.49×10^2	2.38×10^2	CTUe
ecotoxicity: freshwater, inorganics	3.06×10^2	2.35×10^2	2.24×10^2	CTUe
ecotoxicity: freshwater, organics	2.80×10^1	1.31×10^1	1.33×10^1	CTUe
energy resources: non-renewable	1.27×10^3	3.38×10^2	2.89×10^2	MJ, LHV
eutrophication: freshwater	4.58×10^{-2}	9.25×10^{-3}	8.64×10^{-3}	kg P-Eq
eutrophication: marine	6.19×10^{-2}	2.82×10^{-2}	2.48×10^{-2}	kg N-Eq
eutrophication: terrestrial	5.38×10^{-1}	2.59×10^{-1}	2.23×10^{-1}	mol N-Eq
human toxicity: carcinogenic	4.53×10^{-8}	3.01×10^{-8}	2.63×10^{-8}	CTUh
human toxicity: carcinogenic, inorganics	3.01×10^{-8}	2.20×10^{-8}	2.16×10^{-8}	CTUh
human toxicity: carcinogenic, organics	1.52×10^{-8}	8.06×10^{-9}	4.68×10^{-9}	CTUh
human toxicity: non-carcinogenic	1.38×10^{-6}	1.08×10^{-6}	1.06×10^{-6}	CTUh
human toxicity: non-carcinogenic, inorganics	1.34×10^{-6}	1.05×10^{-6}	1.02×10^{-6}	CTUh
human toxicity: non-carcinogenic, organics	3.86×10^{-8}	3.61×10^{-8}	3.54×10^{-8}	CTUh
ionising radiation: human health	3.25×10^1	4.96×10^0	4.83×10^0	kBq U235-Eq
land use	2.61×10^2	8.57×10^1	8.16×10^1	dimensionless
material resources: metals/minerals	2.39×10^{-3}	2.42×10^{-3}	2.43×10^{-3}	kg Sb-Eq
ozone depletion	1.41×10^{-6}	6.08×10^{-7}	5.86×10^{-7}	kg CFC-11-Eq
particulate matter formation	2.41×10^{-6}	2.06×10^{-6}	2.79×10^{-6}	disease incidence
photochemical oxidant formation: human health	1.83×10^{-1}	8.93×10^{-2}	7.65×10^{-2}	kg NMVOC-Eq
water use	1.23×10^2	9.53×10^1	1.03×10^2	m ³ world eq. deprived

B.2.1. Economic Flow Analysis

Figure B.2 depicts the relative contribution of the lifecycle stages and battery components to the climate change impacts of the three product systems. Analogously to Figure 3.9, the following figure is divided into three parts to increase the level of detail regarding the production process. Each part consists of three columns, one per battery type. Accordingly, the first three columns show the complete lifecycle, whereas the second and third part zoom into the production of the batteries and anodes, respectively.

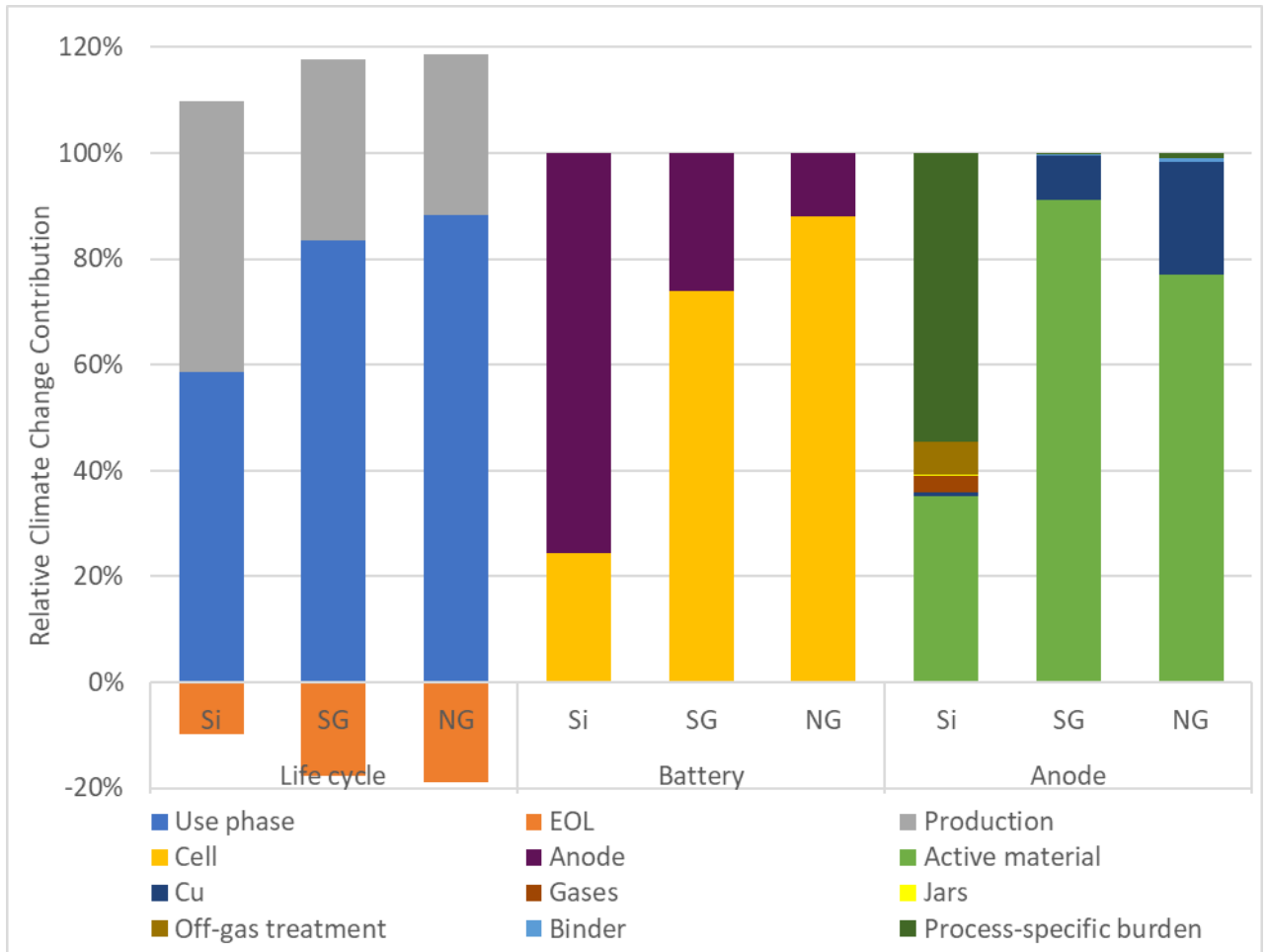


Figure B.2.: Relative Contribution of Life Cycle Stages to Climate Change Impacts

B.2.2. Scenarios

The following tables show the absolute characterisation results of the four scenarios discussed and visualised in Section 3.2.3.

Table B.9.: Cradle-to-Gate Environmental Impact of the PEF Impact Categories for 1 kWh Activated Silicon (Si) Anode with Different Mass Loading (ML) Scenarios

Impact category	1.5ML	1.75ML	2.0ML	2.25ML	2.5ML	Unit
acidification	8.56×10^{-1}	8.41×10^{-1}	8.31×10^{-1}	8.22×10^{-1}	8.16×10^{-1}	mol H ⁺ -Eq
climate change	1.41×10^2	kg CO ₂ -Eq				
climate change: biogenic	1.18×10^0	1.18×10^0	1.17×10^0	1.17×10^0	1.17×10^0	kg CO ₂ -Eq
climate change: fossil	1.40×10^2	1.40×10^2	1.40×10^2	1.39×10^2	1.39×10^2	kg CO ₂ -Eq
climate change: land use and land use change	3.43×10^{-1}	3.43×10^{-1}	3.42×10^{-1}	3.42×10^{-1}	3.42×10^{-1}	kg CO ₂ -Eq
ecotoxicity: freshwater	5.12×10^2	5.01×10^2	4.93×10^2	4.87×10^2	4.82×10^2	CTUe
ecotoxicity: freshwater, inorganics	4.60×10^2	4.49×10^2	4.41×10^2	4.35×10^2	4.30×10^2	CTUe
ecotoxicity: freshwater, organics	5.23×10^1	5.22×10^1	5.22×10^1	5.21×10^1	5.21×10^1	CTUe
energy resources: non-renewable	3.29×10^3	3.29×10^3	3.28×10^3	3.28×10^3	3.28×10^3	MJ, LHV
eutrophication: freshwater	1.30×10^{-1}	1.30×10^{-1}	1.29×10^{-1}	1.29×10^{-1}	1.28×10^{-1}	kg P-Eq
eutrophication: marine	1.43×10^{-1}	1.43×10^{-1}	1.42×10^{-1}	1.42×10^{-1}	1.42×10^{-1}	kg N-Eq
eutrophication: terrestrial	1.29×10^0	1.28×10^0	1.27×10^0	1.27×10^0	1.27×10^0	mol N-Eq
human toxicity: carcinogenic	8.66×10^{-8}	8.40×10^{-8}	8.20×10^{-8}	8.05×10^{-8}	7.93×10^{-8}	CTUh
human toxicity: carcinogenic, inorganics	5.10×10^{-8}	4.88×10^{-8}	4.71×10^{-8}	4.58×10^{-8}	4.47×10^{-8}	CTUh
human toxicity: carcinogenic, organics	3.55×10^{-8}	3.52×10^{-8}	3.50×10^{-8}	3.48×10^{-8}	3.46×10^{-8}	CTUh
human toxicity: non-carcinogenic	3.11×10^{-6}	2.88×10^{-6}	2.71×10^{-6}	2.58×10^{-6}	2.48×10^{-6}	CTUh
human toxicity: non-carcinogenic, inorganics	3.01×10^{-6}	2.79×10^{-6}	2.63×10^{-6}	2.50×10^{-6}	2.40×10^{-6}	CTUh
human toxicity: non-carcinogenic, organics	1.04×10^{-7}	9.43×10^{-8}	8.71×10^{-8}	8.16×10^{-8}	7.71×10^{-8}	CTUh
ionising radiation: human health	8.83×10^1	8.82×10^1	8.82×10^1	8.81×10^1	8.81×10^1	kBq U235-Eq
land use	6.61×10^2	6.56×10^2	6.52×10^2	6.49×10^2	6.47×10^2	dimensionless
material resources: metals/minerals	1.68×10^{-3}	1.50×10^{-3}	1.36×10^{-3}	1.26×10^{-3}	1.17×10^{-3}	kg Sb-Eq
ozone depletion	2.74×10^{-6}	kg CFC-11-Eq				
particulate matter formation	3.50×10^{-6}	3.47×10^{-6}	3.44×10^{-6}	3.42×10^{-6}	3.41×10^{-6}	disease incidence
photochemical oxidant formation: human health	4.19×10^{-1}	4.17×10^{-1}	4.15×10^{-1}	4.13×10^{-1}	4.12×10^{-1}	kg NMVOC-Eq
water use	9.25×10^1	9.23×10^1	9.22×10^1	9.21×10^1	9.20×10^1	m ³ world eq. deprived

Table B.10.: Cradle-to-Gate Environmental Impact of the PEF Impact Categories for 1 kWh Activated Silicon (Si) Anode with Different Silicon Utilisation Scenarios

Impact category	Si - 15 %	Si - 20 %	Si - 25 %	Si - 30 %	SG - base	NG - base	Unit
acidification	1.03×10^0	7.87×10^{-1}	6.42×10^{-1}	5.46×10^{-1}	2.30×10^{-1}	1.65×10^{-1}	mol H+-Eq
climate change	1.80×10^2	1.35×10^2	1.08×10^2	9.03×10^1	2.28×10^1	8.87×10^0	kg CO2-Eq
climate change: biogenic	1.50×10^0	1.12×10^0	9.00×10^{-1}	7.51×10^{-1}	1.67×10^{-2}	1.70×10^{-2}	kg CO2-Eq
climate change: fossil	1.78×10^2	1.33×10^2	1.07×10^2	8.94×10^1	2.28×10^1	8.84×10^0	kg CO2-Eq
climate change: land use and land use change	4.36×10^{-1}	3.28×10^{-1}	2.62×10^{-1}	2.19×10^{-1}	1.18×10^{-2}	1.03×10^{-2}	kg CO2-Eq
ecotoxicity: freshwater	6.05×10^2	4.66×10^2	3.82×10^2	3.26×10^2	2.26×10^2	1.82×10^2	CTUe
ecotoxicity: freshwater, inorganics	5.38×10^2	4.16×10^2	3.42×10^2	2.93×10^2	2.22×10^2	1.77×10^2	CTUe
ecotoxicity: freshwater, organics	6.65×10^1	4.99×10^1	4.00×10^1	3.34×10^1	4.53×10^0	5.01×10^0	CTUe
energy resources: non-renewable	4.19×10^3	3.14×10^3	2.52×10^3	2.10×10^3	2.90×10^2	9.40×10^1	MJ, LHV
eutrophication: freshwater	1.63×10^{-1}	1.23×10^{-1}	9.92×10^{-2}	8.32×10^{-2}	1.35×10^{-2}	1.11×10^{-2}	kg P-Eq
eutrophication: marine	1.80×10^{-1}	1.36×10^{-1}	1.09×10^{-1}	9.16×10^{-2}	2.91×10^{-2}	1.55×10^{-2}	kg N-Eq
eutrophication: terrestrial	1.61×10^0	1.22×10^0	9.80×10^{-1}	8.23×10^{-1}	3.26×10^{-1}	1.83×10^{-1}	mol N-Eq
human toxicity: carcinogenic	9.89×10^{-8}	7.70×10^{-8}	6.39×10^{-8}	5.51×10^{-8}	3.62×10^{-8}	2.11×10^{-8}	CTUh
human toxicity: carcinogenic, inorganics	5.49×10^{-8}	4.37×10^{-8}	3.70×10^{-8}	3.25×10^{-8}	2.12×10^{-8}	1.95×10^{-8}	CTUh
human toxicity: carcinogenic, organics	4.39×10^{-8}	3.33×10^{-8}	2.69×10^{-8}	2.27×10^{-8}	1.51×10^{-8}	1.61×10^{-9}	CTUh
human toxicity: non-carcinogenic	2.95×10^{-6}	2.46×10^{-6}	2.17×10^{-6}	1.97×10^{-6}	1.79×10^{-6}	1.70×10^{-6}	CTUh
human toxicity: non-carcinogenic, inorganics	2.86×10^{-6}	2.38×10^{-6}	2.10×10^{-6}	1.91×10^{-6}	1.71×10^{-6}	1.62×10^{-6}	CTUh
human toxicity: non-carcinogenic, organics	8.94×10^{-8}	7.76×10^{-8}	7.05×10^{-8}	6.57×10^{-8}	8.38×10^{-8}	8.07×10^{-8}	CTUh
ionising radiation: human health	1.12×10^2	8.44×10^1	6.76×10^1	5.64×10^1	9.91×10^{-1}	4.63×10^{-1}	kBq U235-Eq
land use	8.21×10^2	6.22×10^2	5.02×10^2	4.22×10^2	8.44×10^1	6.79×10^1	dimensionless
material resources: metals/minerals	1.32×10^{-3}	1.19×10^{-3}	1.11×10^{-3}	1.06×10^{-3}	1.57×10^{-3}	1.59×10^{-3}	kg Sb-Eq
ozone depletion	3.49×10^{-6}	2.62×10^{-6}	2.10×10^{-6}	1.75×10^{-6}	2.39×10^{-7}	1.53×10^{-7}	kg CFC-11-Eq
particulate matter formation	4.32×10^{-6}	3.28×10^{-6}	2.65×10^{-6}	2.23×10^{-6}	1.79×10^{-6}	4.70×10^{-6}	disease incidence
photochemical oxidant formation: human health	5.24×10^{-1}	3.96×10^{-1}	3.19×10^{-1}	2.68×10^{-1}	1.02×10^{-1}	5.09×10^{-2}	kg NMVOC-Eq
water use	1.17×10^2	8.82×10^1	7.07×10^1	5.90×10^1	3.84×10^0	3.35×10^1	m3 world eq. deprived

Table B.11.: Cradle-to-Grave Environmental Impact of the PEF Impact Categories for 1 kWh Delivered Energy of a Silicon-based LIB with Different Cycle Life Scenarios

Impact category	500 LC	600 LC	700 LC	800 LC	900 LC	1000 LC	1500 LC	Unit
acidification	5.18×10^{-3}	4.63×10^{-3}	4.24×10^{-3}	3.94×10^{-3}	3.71×10^{-3}	3.53×10^{-3}	2.98×10^{-3}	mol H+-Eq
climate change	1.00×10^0	9.14×10^{-1}	8.50×10^{-1}	8.02×10^{-1}	7.65×10^{-1}	7.35×10^{-1}	6.45×10^{-1}	kg CO2-Eq
climate change: biogenic	5.61×10^{-3}	4.85×10^{-3}	4.30×10^{-3}	3.90×10^{-3}	3.58×10^{-3}	3.33×10^{-3}	2.57×10^{-3}	kg CO2-Eq
climate change: fossil	9.95×10^{-1}	9.06×10^{-1}	8.43×10^{-1}	7.96×10^{-1}	7.59×10^{-1}	7.29×10^{-1}	6.41×10^{-1}	kg CO2-Eq
climate change: land use and land use change	2.73×10^{-3}	2.51×10^{-3}	2.34×10^{-3}	2.22×10^{-3}	2.13×10^{-3}	2.05×10^{-3}	1.83×10^{-3}	kg CO2-Eq
ecotoxicity: freshwater	3.16×10^0	2.86×10^0	2.65×10^0	2.50×10^0	2.37×10^0	2.28×10^0	1.98×10^0	CTUe
ecotoxicity: freshwater, inorganics	2.82×10^0	2.56×10^0	2.37×10^0	2.23×10^0	2.12×10^0	2.04×10^0	1.77×10^0	CTUe
ecotoxicity: freshwater, organics	3.36×10^{-1}	3.04×10^{-1}	2.81×10^{-1}	2.64×10^{-1}	2.51×10^{-1}	2.40×10^{-1}	2.08×10^{-1}	CTUe
energy resources: non-renewable	2.18×10^1	1.97×10^1	1.82×10^1	1.71×10^1	1.62×10^1	1.55×10^1	1.34×10^1	MJ, LHV
eutrophication: freshwater	8.20×10^{-4}	7.40×10^{-4}	6.80×10^{-4}	6.40×10^{-4}	6.10×10^{-4}	5.80×10^{-4}	5.00×10^{-4}	kg P-Eq
eutrophication: marine	9.20×10^{-4}	8.20×10^{-4}	7.50×10^{-4}	6.90×10^{-4}	6.50×10^{-4}	6.20×10^{-4}	5.20×10^{-4}	kg N-Eq
eutrophication: terrestrial	8.16×10^{-3}	7.28×10^{-3}	6.66×10^{-3}	6.19×10^{-3}	5.83×10^{-3}	5.54×10^{-3}	4.66×10^{-3}	mol N-Eq
human toxicity: carcinogenic	5.19×10^{-10}	4.63×10^{-10}	4.23×10^{-10}	3.94×10^{-10}	3.70×10^{-10}	3.52×10^{-10}	2.96×10^{-10}	CTUh
human toxicity: carcinogenic, inorganics	3.22×10^{-10}	2.87×10^{-10}	2.62×10^{-10}	2.44×10^{-10}	2.29×10^{-10}	2.17×10^{-10}	1.82×10^{-10}	CTUh
human toxicity: carcinogenic, organics	1.97×10^{-10}	1.76×10^{-10}	1.61×10^{-10}	1.50×10^{-10}	1.41×10^{-10}	1.34×10^{-10}	1.14×10^{-10}	CTUh
human toxicity: non-carcinogenic	1.66×10^{-8}	1.50×10^{-8}	1.39×10^{-8}	1.31×10^{-8}	1.24×10^{-8}	1.19×10^{-8}	1.03×10^{-8}	CTUh
human toxicity: non-carcinogenic, inorganics	1.61×10^{-8}	1.45×10^{-8}	1.34×10^{-8}	1.26×10^{-8}	1.20×10^{-8}	1.15×10^{-8}	9.94×10^{-9}	CTUh
human toxicity: non-carcinogenic, organics	5.52×10^{-10}	5.03×10^{-10}	4.68×10^{-10}	4.41×10^{-10}	4.21×10^{-10}	4.04×10^{-10}	3.55×10^{-10}	CTUh
ionising radiation: human health	5.51×10^{-1}	4.97×10^{-1}	4.59×10^{-1}	4.30×10^{-1}	4.07×10^{-1}	3.89×10^{-1}	3.35×10^{-1}	kBq U235-Eq
land use	4.02×10^0	3.61×10^0	3.31×10^0	3.09×10^0	2.92×10^0	2.78×10^0	2.36×10^0	dimensionless
material resources: metals/minerals	9.17×10^{-6}	8.38×10^{-6}	7.82×10^{-6}	7.39×10^{-6}	7.07×10^{-6}	6.80×10^{-6}	6.01×10^{-6}	kg Sb-Eq
ozone depletion	1.26×10^{-8}	1.11×10^{-8}	1.01×10^{-8}	9.34×10^{-9}	8.74×10^{-9}	8.26×10^{-9}	6.83×10^{-9}	kg CFC-11-Eq
particulate matter formation	2.33×10^{-8}	2.08×10^{-8}	1.91×10^{-8}	1.77×10^{-8}	1.67×10^{-8}	1.58×10^{-8}	1.34×10^{-8}	disease incidence
photochemical oxidant formation: human health	2.75×10^{-3}	2.47×10^{-3}	2.27×10^{-3}	2.12×10^{-3}	2.00×10^{-3}	1.91×10^{-3}	1.62×10^{-3}	kg NMVOC-Eq
water use	5.74×10^{-1}	5.15×10^{-1}	4.74×10^{-1}	4.43×10^{-1}	4.18×10^{-1}	3.99×10^{-1}	3.41×10^{-1}	m3 world eq. deprived

Table B.12.: Cradle-to-Gate Environmental Impact of the PEF Impact Categories for 1 kWh Activated Silicon (Si), Natural Graphite (NG), and Synthetic Graphite (SG) Anode Compared to the Hydrogen Reuse Scenario

Impact category	Si-H2 reuse	Si - base	SG - base	NG - base	Unit
acidification	8.24×10^{-1}	8.25×10^{-1}	2.30×10^{-1}	1.65×10^{-1}	mol H+-Eq
climate change	1.42×10^2	1.42×10^2	2.28×10^1	8.87×10^0	kg CO2-Eq
climate change: biogenic	1.18×10^0	1.18×10^0	1.67×10^{-2}	1.70×10^{-2}	kg CO2-Eq
climate change: fossil	1.40×10^2	1.40×10^2	2.28×10^1	8.84×10^0	kg CO2-Eq
climate change: land use and land use change	3.45×10^{-1}	3.45×10^{-1}	1.18×10^{-2}	1.03×10^{-2}	kg CO2-Eq
ecotoxicity: freshwater	4.84×10^2	4.88×10^2	2.26×10^2	1.82×10^2	CTUe
ecotoxicity: freshwater, inorganics	4.31×10^2	4.35×10^2	2.22×10^2	1.77×10^2	CTUe
ecotoxicity: freshwater, organics	5.24×10^1	5.25×10^1	4.53×10^0	5.01×10^0	CTUe
energy resources: non-renewable	3.30×10^3	3.31×10^3	2.90×10^2	9.40×10^1	MJ, LHV
eutrophication: freshwater	1.30×10^{-1}	1.30×10^{-1}	1.35×10^{-2}	1.11×10^{-2}	kg P-Eq
eutrophication: marine	1.43×10^{-1}	1.43×10^{-1}	2.91×10^{-2}	1.55×10^{-2}	kg N-Eq
eutrophication: terrestrial	1.28×10^0	1.28×10^0	3.26×10^{-1}	1.83×10^{-1}	mol N-Eq
human toxicity: carcinogenic	8.04×10^{-8}	8.05×10^{-8}	3.62×10^{-8}	2.11×10^{-8}	CTUh
human toxicity: carcinogenic, inorganics	4.54×10^{-8}	4.55×10^{-8}	2.12×10^{-8}	1.95×10^{-8}	CTUh
human toxicity: carcinogenic, organics	3.50×10^{-8}	3.50×10^{-8}	1.51×10^{-8}	1.61×10^{-9}	CTUh
human toxicity: non-carcinogenic	2.54×10^{-6}	2.54×10^{-6}	1.79×10^{-6}	1.70×10^{-6}	CTUh
human toxicity: non-carcinogenic, inorganics	2.46×10^{-6}	2.46×10^{-6}	1.71×10^{-6}	1.62×10^{-6}	CTUh
human toxicity: non-carcinogenic, organics	7.94×10^{-8}	7.94×10^{-8}	8.38×10^{-8}	8.07×10^{-8}	CTUh
ionising radiation: human health	8.88×10^1	8.88×10^1	9.91×10^{-1}	4.63×10^{-1}	kBq U235-Eq
land use	6.53×10^2	6.53×10^2	8.44×10^1	6.79×10^1	dimensionless
material resources: metals/minerals	1.21×10^{-3}	1.21×10^{-3}	1.57×10^{-3}	1.59×10^{-3}	kg Sb-Eq
ozone depletion	2.75×10^{-6}	2.76×10^{-6}	2.39×10^{-7}	1.53×10^{-7}	kg CFC-11-Eq
particulate matter formation	3.43×10^{-6}	3.44×10^{-6}	1.79×10^{-6}	4.70×10^{-6}	disease incidence
photochemical oxidant formation: human health	4.15×10^{-1}	4.16×10^{-1}	1.02×10^{-1}	5.09×10^{-2}	kg NMVOC-Eq
water use	9.28×10^1	9.28×10^1	3.84×10^0	3.35×10^1	m3 world eq. deprived

B. Results

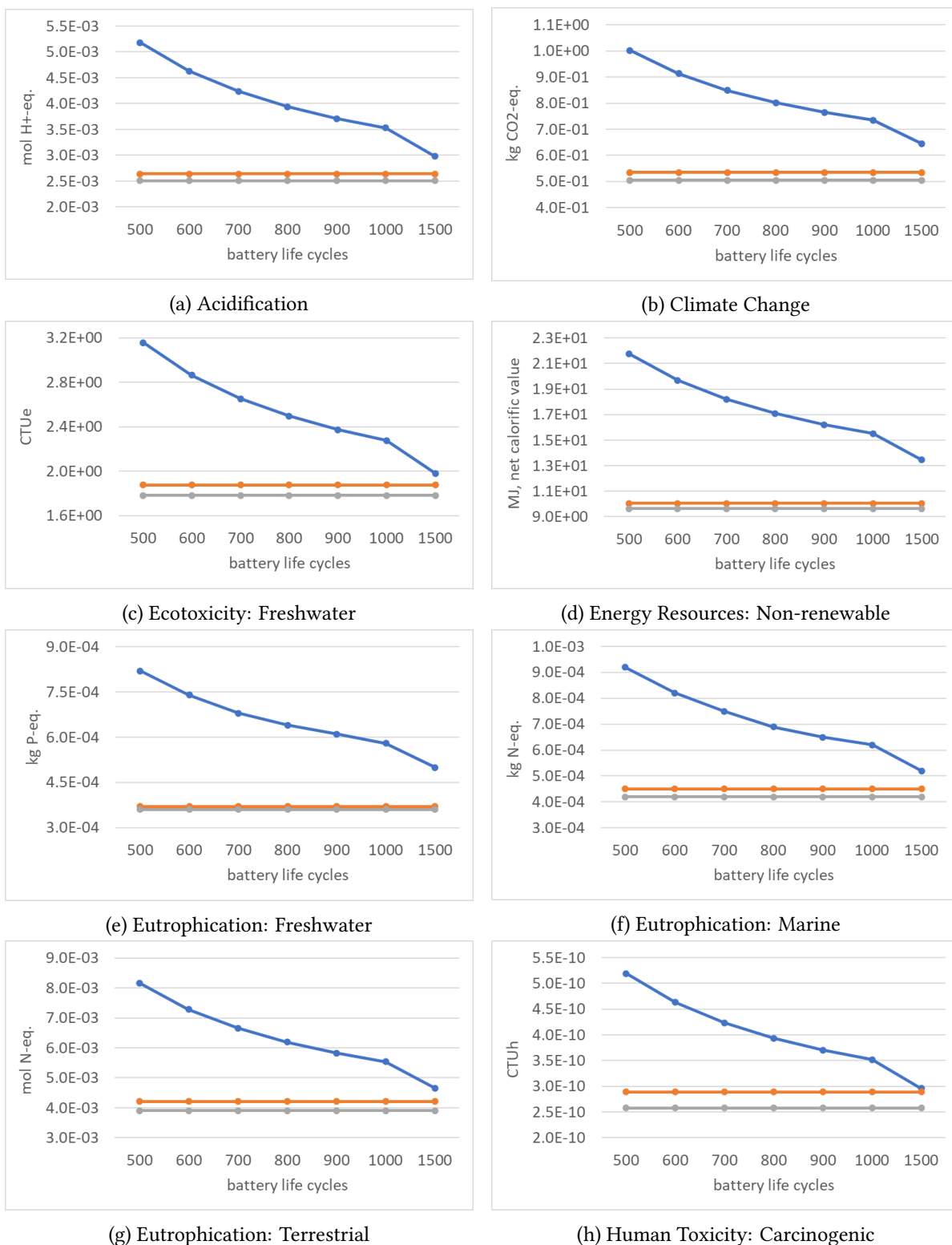


Figure B.3.: Environmental Impacts of 1 kWh Activated Silicon Anode (blue) with Changing Cycle Life per Category; For reference, the environmental impacts of 1 kWh activated natural (grey) and synthetic (orange) graphite anodes with a fixed cycle life of 1,000 cycles are included.

B. Results

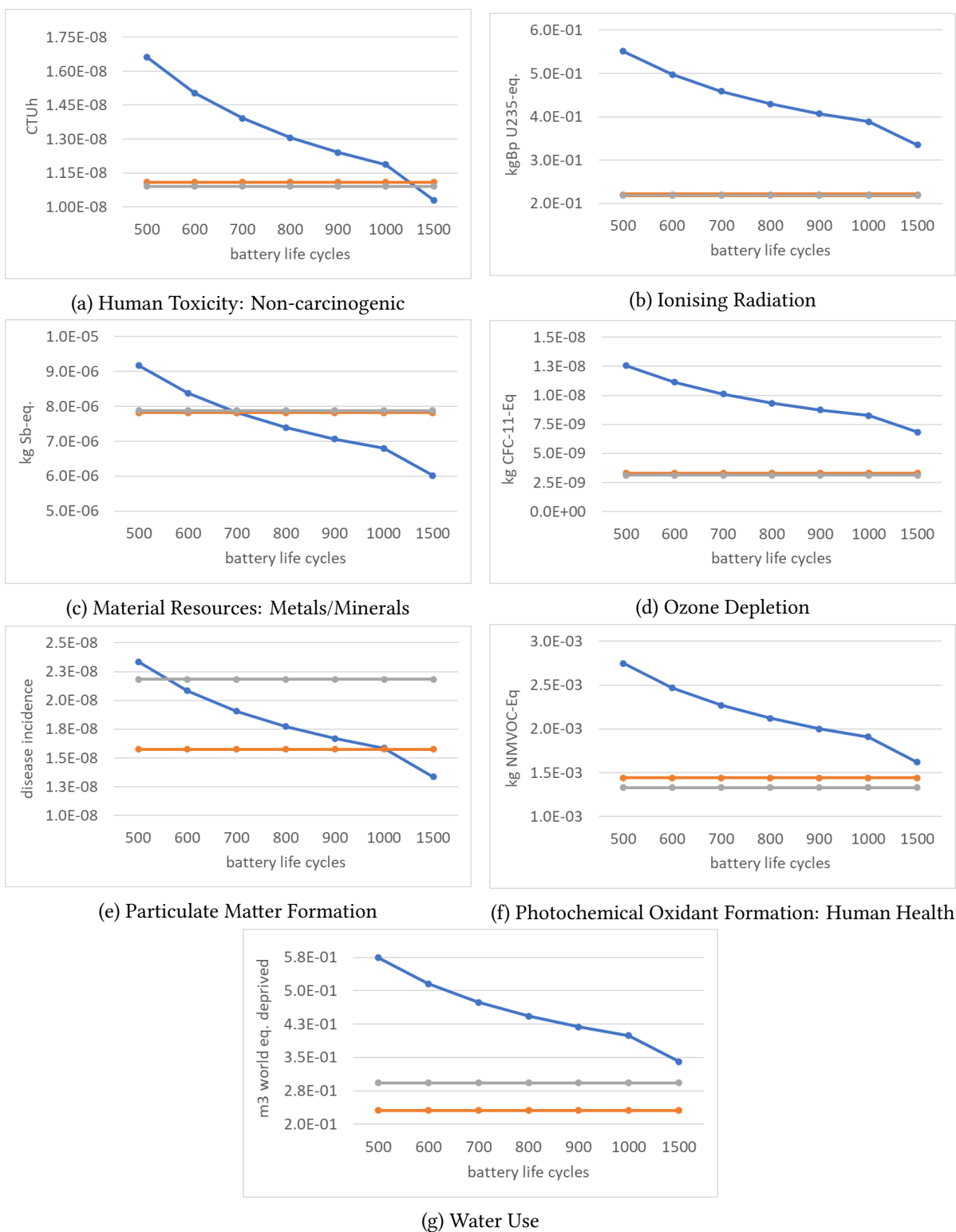


Figure B.4.: Environmental Impacts of 1 kWh Activated Silicon Anode (blue) with Changing Cycle Life per Category – Continued; For reference, the environmental impacts of 1 kWh activated natural (grey) and synthetic (orange) graphite anodes with a fixed cycle life of 1,000 cycles are included.

C. Discussion

Figure C.1 plots the *ease of doing business* and *political stability* score of all countries. The colour of the data points indicate the respective region of the country, as defined in Section 2.1. The plots on the second x- and y-axis on the top and right of the figure show the univariate distribution per region for both indicators.

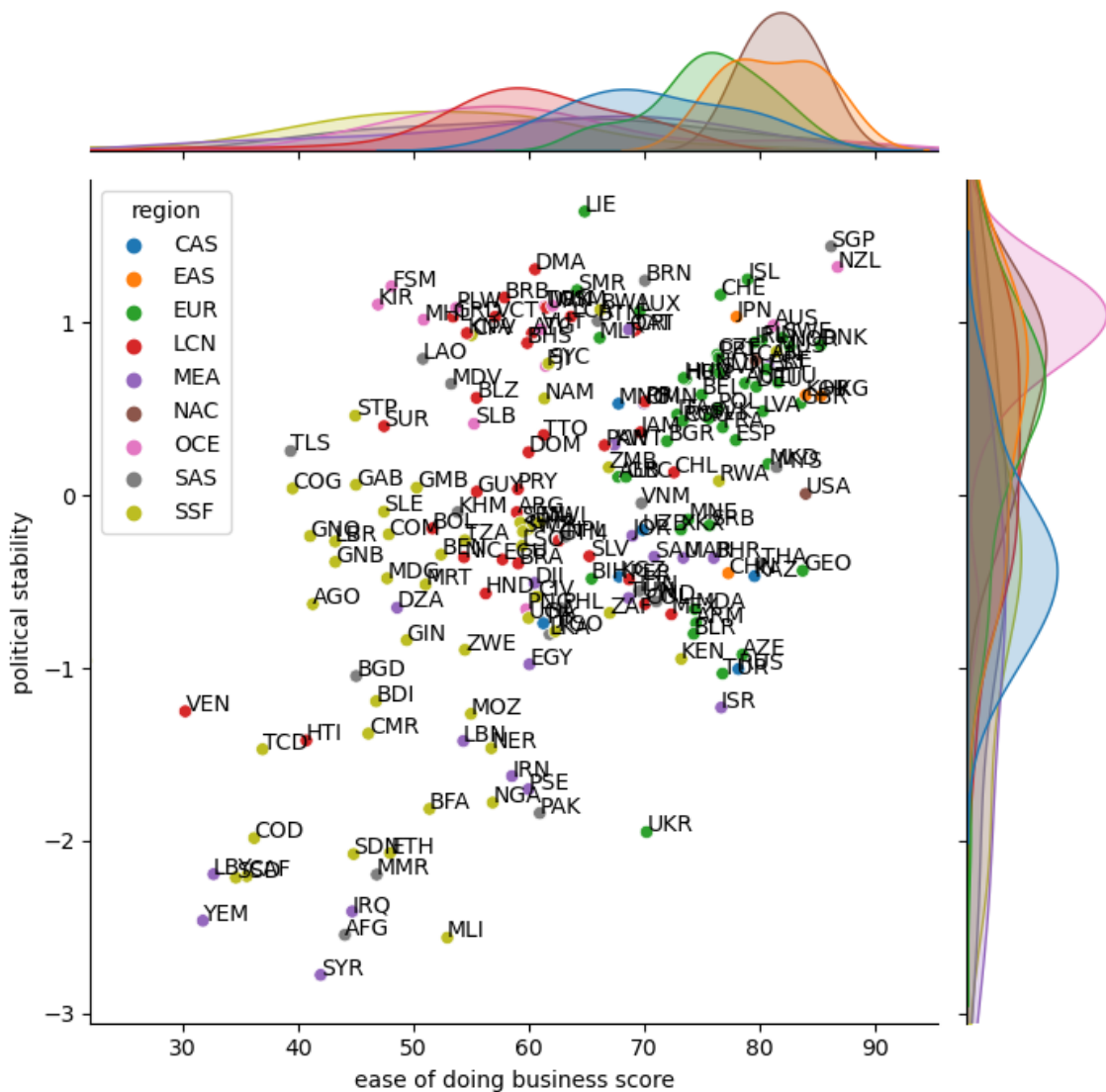


Figure C.1.: Ease of Doing Business Score and Political Stability Performance of all Countries Individually

Data points are labelled with the country abbreviation and coloured by region. The second x- and y-axis contain the univariate distribution per region and indicator.

As discussed in Section 3.1, the two indicators seem to be positively correlated, suggesting that a better performance in *ease of doing business* is associated with a better performance in *political stability* and vice versa, since for both indicators a higher value is preferable. The univariate distributions of the *ease of doing business* score indicate that East Asia and North America perform notably better than the remaining regions, followed by Europe and Central Asia. The *political stability* indicator shows a more mixed picture, with Oceania seemingly performing better than all other regions. On the level of the individual countries, Singapore (SGP) and New Zealand (NZL) achieve one of the highest scores in both indicators. However, this observation is only in line with the results on the regional level in case of New Zealand in *political stability*, as its whole region, namely Oceania, performs well in this indicator. On the other hand, in the case of the *ease of doing business* indicator, all other countries in Oceania score considerably worse, resulting in an overall lower score of the region as compared to the global average. Singapore even outperforms its corresponding region in both indicators significantly, since South Asia scores in both of them below the global average. Thus, despite their high rating in the two indicators, New Zealand and Singapore are excluded from the further location search in this study, pointing at the problematic associated with the aggregating of the countries.

C.1. Sensitivity Analysis

The following tables show the absolute characterisation results of the two sensitivity analyses examined and visualised in the Discussion. Table C.1 contains the environmental impacts of all three product systems when applying a conservative allocation method that assigns all life cycle environmental impacts to the reference flows of the product systems, namely the delivery of 1 kWh stored energy by the three types of LIBs, respectively. Table C.2 includes the results of the sensitivity analysis regarding the electricity consumed during the production of the silicon anode. Therefore, the table entails the change in environmental impacts associated with the production of the silicon anode only.

Table C.1.: Cradle-to-Grave Impacts of the Three Product Systems with Conservative Allocation

Impact category	NG	Si	SG	Unit
acidification	2.52×10^{-3}	3.94×10^{-3}	2.78×10^{-3}	mol H ⁺ -Eq
climate change	5.07×10^{-1}	8.02×10^{-1}	5.60×10^{-1}	kg CO ₂ -Eq
climate change: biogenic	1.27×10^{-3}	3.92×10^{-3}	1.27×10^{-3}	kg CO ₂ -Eq
climate change: fossil	5.04×10^{-1}	7.96×10^{-1}	5.58×10^{-1}	kg CO ₂ -Eq
climate change: land use and land use change	1.36×10^{-3}	2.22×10^{-3}	1.37×10^{-3}	kg CO ₂ -Eq
ecotoxicity: freshwater	1.80×10^0	2.50×10^0	2.00×10^0	CTUe
ecotoxicity: freshwater, inorganics	1.64×10^0	2.23×10^0	1.85×10^0	CTUe
ecotoxicity: freshwater, organics	1.55×10^{-1}	2.64×10^{-1}	1.57×10^{-1}	CTUe
energy resources: non-renewable	9.66×10^0	1.71×10^1	1.04×10^1	MJ, LHV
eutrophication: freshwater	3.61×10^{-4}	6.43×10^{-4}	3.71×10^{-4}	kg P-Eq
eutrophication: marine	4.28×10^{-4}	6.95×10^{-4}	4.82×10^{-4}	kg N-Eq
eutrophication: terrestrial	3.94×10^{-3}	6.20×10^{-3}	4.52×10^{-3}	mol N-Eq
human toxicity: carcinogenic	2.58×10^{-10}	3.94×10^{-10}	3.10×10^{-10}	CTUh
human toxicity: carcinogenic, inorganics	1.87×10^{-10}	2.44×10^{-10}	1.95×10^{-10}	CTUh
human toxicity: carcinogenic, organics	7.07×10^{-11}	1.50×10^{-10}	1.16×10^{-10}	CTUh
human toxicity: non-carcinogenic	1.09×10^{-8}	1.31×10^{-8}	1.13×10^{-8}	CTUh
human toxicity: non-carcinogenic, inorganics	1.05×10^{-8}	1.26×10^{-8}	1.09×10^{-8}	CTUh
human toxicity: non-carcinogenic, organics	4.30×10^{-10}	4.42×10^{-10}	4.44×10^{-10}	CTUh
ionising radiation: human health	2.19×10^{-1}	4.30×10^{-1}	2.21×10^{-1}	kBq U235-Eq
land use	1.77×10^0	3.10×10^0	1.84×10^0	dimensionless
material resources: metals/minerals	7.88×10^{-6}	7.39×10^{-6}	7.84×10^{-6}	kg Sb-Eq
ozone depletion	3.13×10^{-9}	9.34×10^{-9}	3.54×10^{-9}	kg CFC-11-Eq
particulate matter formation	2.47×10^{-8}	1.78×10^{-8}	1.76×10^{-8}	disease incidence
photochemical oxidant formation: human health	1.34×10^{-3}	2.12×10^{-3}	1.54×10^{-3}	kg NMVOC-Eq
water use	3.07×10^{-1}	4.43×10^{-1}	2.34×10^{-1}	m ³ world eq. deprived

Table C.2.: Cradle-to-Gate Environmental Impact of the PEF Impact Categories for 1 kWh Activated Silicon (Si) Anode with Variations in Electricity Consumption ($\pm 15\%$)

Impact category	-15 %	-10 %	-5 %	0 %	+5 %	+10 %	+15 %	Unit
acidification	7.31×10^{-1}	7.62×10^{-1}	7.93×10^{-1}	8.25×10^{-1}	8.56×10^{-1}	8.88×10^{-1}	9.19×10^{-1}	mol H+-Eq
climate change	1.23×10^2	1.29×10^2	1.36×10^2	1.42×10^2	1.48×10^2	1.55×10^2	1.61×10^2	kg CO2-Eq
climate change: biogenic	1.09×10^0	1.12×10^0	1.15×10^0	1.18×10^0	1.22×10^0	1.25×10^0	1.28×10^0	kg CO2-Eq
climate change: fossil	1.22×10^2	1.28×10^2	1.34×10^2	1.40×10^2	1.47×10^2	1.53×10^2	1.59×10^2	kg CO2-Eq
climate change: land use and land use change	2.98×10^{-1}	3.14×10^{-1}	3.29×10^{-1}	3.45×10^{-1}	3.60×10^{-1}	3.76×10^{-1}	3.92×10^{-1}	kg CO2-Eq
ecotoxicity: freshwater	4.34×10^2	4.52×10^2	4.70×10^2	4.88×10^2	5.05×10^2	5.23×10^2	5.41×10^2	CTUe
ecotoxicity: freshwater, inorganics	3.88×10^2	4.04×10^2	4.19×10^2	4.35×10^2	4.51×10^2	4.66×10^2	4.82×10^2	CTUe
ecotoxicity: freshwater, organics	4.55×10^1	4.78×10^1	5.02×10^1	5.25×10^1	5.49×10^1	5.72×10^1	5.96×10^1	CTUe
energy resources: non-renewable	2.87×10^3	3.01×10^3	3.16×10^3	3.31×10^3	3.45×10^3	3.60×10^3	3.75×10^3	MJ, LHV
eutrophication: freshwater	1.12×10^{-1}	1.18×10^{-1}	1.24×10^{-1}	1.30×10^{-1}	1.35×10^{-1}	1.41×10^{-1}	1.47×10^{-1}	kg P-Eq
eutrophication: marine	1.26×10^{-1}	1.32×10^{-1}	1.37×10^{-1}	1.43×10^{-1}	1.48×10^{-1}	1.54×10^{-1}	1.60×10^{-1}	kg N-Eq
eutrophication: terrestrial	1.13×10^0	1.18×10^0	1.23×10^0	1.28×10^0	1.33×10^0	1.38×10^0	1.43×10^0	mol N-Eq
human toxicity: carcinogenic	7.40×10^{-8}	7.62×10^{-8}	7.83×10^{-8}	8.05×10^{-8}	8.26×10^{-8}	8.47×10^{-8}	8.69×10^{-8}	CTUh
human toxicity: carcinogenic, inorganics	4.17×10^{-8}	4.30×10^{-8}	4.42×10^{-8}	4.55×10^{-8}	4.67×10^{-8}	4.80×10^{-8}	4.92×10^{-8}	CTUh
human toxicity: carcinogenic, organics	3.23×10^{-8}	3.32×10^{-8}	3.41×10^{-8}	3.50×10^{-8}	3.59×10^{-8}	3.68×10^{-8}	3.77×10^{-8}	CTUh
human toxicity: non-carcinogenic	2.35×10^{-6}	2.41×10^{-6}	2.47×10^{-6}	2.54×10^{-6}	2.60×10^{-6}	2.66×10^{-6}	2.73×10^{-6}	CTUh
human toxicity: non-carcinogenic, inorganics	2.27×10^{-6}	2.33×10^{-6}	2.40×10^{-6}	2.46×10^{-6}	2.52×10^{-6}	2.58×10^{-6}	2.64×10^{-6}	CTUh
human toxicity: non-carcinogenic, organics	7.54×10^{-8}	7.67×10^{-8}	7.81×10^{-8}	7.94×10^{-8}	8.08×10^{-8}	8.22×10^{-8}	8.35×10^{-8}	CTUh
ionising radiation: human health	7.66×10^1	8.07×10^1	8.48×10^1	8.88×10^1	9.29×10^1	9.70×10^1	1.01×10^2	kBq U235-Eq
land use	5.88×10^2	6.10×10^2	6.31×10^2	6.53×10^2	6.75×10^2	6.96×10^2	7.18×10^2	dimensionless
material resources: metals/minerals	1.17×10^{-3}	1.19×10^{-3}	1.20×10^{-3}	1.21×10^{-3}	1.23×10^{-3}	1.24×10^{-3}	1.25×10^{-3}	kg Sb-Eq
ozone depletion	2.42×10^{-6}	2.53×10^{-6}	2.65×10^{-6}	2.76×10^{-6}	2.87×10^{-6}	2.98×10^{-6}	3.10×10^{-6}	kg CFC-11-Eq
particulate matter formation	3.12×10^{-6}	3.23×10^{-6}	3.33×10^{-6}	3.44×10^{-6}	3.55×10^{-6}	3.65×10^{-6}	3.76×10^{-6}	disease incidence
photochemical oxidant formation: human health	3.68×10^{-1}	3.84×10^{-1}	4.00×10^{-1}	4.16×10^{-1}	4.32×10^{-1}	4.48×10^{-1}	4.63×10^{-1}	kg NMVOC-Eq
water use	8.24×10^1	8.59×10^1	8.93×10^1	9.28×10^1	9.63×10^1	9.97×10^1	1.03×10^2	m3 world eq. deprived

C.2. Consistency Check

Table C.3 summarises the results of the consistency check. It should be noted that this assessment was conducted by the author themselves and not an independent external party. Furthermore, the analysis is limited to the production of the anodes given the similarity of the battery assembly, use phase, and EOL management across the three product systems. The results of the consistency check are further discussed in Chapter 4.

Table C.3.: Results of the Consistency Check Regarding the Anode Production Processes

Check	Si Anode		SG Anode		NG Anode		Comparison	Action
Technology coverage	Emerging	OK	Mature	OK	Mature	OK	Not consistent	No action, since study goal
Time-related coverage	Actual	OK	Actual	OK	Actual	OK	Consistent	No action
Geographical coverage	EUR	OK	CN	OK	CN	OK	Not consistent	No action, since study goal
Data source	Ecoinvent, Literature, Primary	OK	Ecoinvent, Literature	OK	Ecoinvent, Literature	OK	Consistent	No action
Data accuracy	Good	OK	Good	OK	Good	OK	Consistent	No action
Data age	1992-2024	Goal & Scope not met	2014-2024	OK	2014-2022	OK	Not consistent	Update silane production data

D. Supplementary Material

The Excel files contain the following information:

1. Unit_process_tables:
 - Unit Process Tables
 - Background Calculations for Use, Transport, and Recycling
 - Assumptions and Limitations of the LCA
 - All References used in the LCA
2. Multifunctionality_and_Contribution-Analysis:
 - Allocations
 - Contribution Analysis